UNIVERSITY OF CALIFORNIA
RIVERSIDE

Innate Immune Responses to Mucosal Infection are Regulated by RELMα

A Dissertation submitted in partial satisfaction
of the requirements for the degree of

Doctor of Philosophy

in

Microbiology

by

Sang Yong Kim

December 2022

Dissertation Committee:
Dr. Meera G. Nair, Chairperson
Dr. Adler Dillman
Dr. Juliet Morrison

The Dissertation of Sang Yong Kim is approved:

Committee Chairperson

University of California, Riverside

ACKNOWLEDGEMENTS

First, I would like to sincerely thank my advisor, Dr. Meera Nair. Without her help, I would not have successfully completed my PhD at UCR. Thank you for letting me work in your lab and always leading me the right way. I'm looking forward to working as a postdoctoral researcher in your lab.

I would also like to express my gratitude to the dissertation committees, Dr. Adler Dillman and Dr. Juliet Morrison. Thank you very much for your advice and guidance that is always helpful.

I would also like to express my gratitude to my past and present lab members and collaborators. It was a great honor to be able to do research with you all.

Lastly, I want to express my sincere gratitude to my family and friends for always supporting me no matter what I do. Without your help, I would not be able to accomplish these.

The text of this dissertation, in part or in full, is a reprint of the material as it appears in "Macrophages in wound healing: activation and plasticity" in Immunology & Cell Biology, 2019. Sang Yong Kim wrote this article and Meera G. Nair listed in that

publication wrote, directed and supervised the research which forms the basis for this dissertation.

The text of this dissertation, in part or in full, is a reprint of the material as it appears in "CX3CR1-Expressing Myeloid Cells Regulate Host–Helminth Interaction and Lung Inflammation." in Advanced Biology, 2022. Sang Yong Kim, Mark A. Barnes, Suhas Sureshchandra, Andrea R. Menicucci, and Jay J. Patel performed the investigation, formal analysis and visualization. Ilhem Messaoudi, and Meera G. Nair listed in that publication directed and supervised the research which forms the basis for this dissertation.

DEDICATION

I dedicate this dissertation to my dad, mom, Dami, Soyul, Soeun, my beloved wife, and my upcoming baby Pampam.

ABSTRACT OF THE DISSERTATION

Innate Immune Responses to Mucosal Infection are Regulated by RELMα

by

Sang Yong Kim

Doctor of Philosophy, Graduate Program in Microbiology
University of California, Riverside, December 2022
Dr. Meera G. Nair, Chairperson

Preclinical models of infection, such as murine infection models and transgenic mice, provide critical knowledge for the treatment and diagnosis of infections of significant public health concern. In particular, the mucosal barrier, such as the lung and intestine are susceptible to multiple infectious pathogens given their exposure to the external environment. The goal of this dissertation was to investigate the function of RELMα and CX3CR1 in mucosal infections with parasitic helminths and influenza virus, as these are pathogens of significant health concern worldwide.

RELMα is a mouse protein, which has orthologs in humans such as resistin and RELMβ. First, we tested the function of RELMα and investigated factors that may regulate its expression in infection. RELMα accelerated resolution of inflammation and tissue repair in infection with mouse intestinal helminth *Heligmosomoides polygyrus*. We also discovered that choline kinase signaling was critical for optimal RELMα expression: when mice were infected with *H. polygyrus* and injected with choline kinase alpha inhibitor, RSM-932A, alternative activation of macrophages and RELMα expression was downregulated in RSM-932A-injected mice.

Previous studies have reported RELMα expression in type 2 cytokine inflammation, however, the functional relevance of RELMα in other infectious contexts, such as viral infections, is unclear. RELMα was induced by IAV infection in the BALF and airway epithelial cells. RELMα induced influenza infections in mouse lung epithelial cells *in vitro* and *in vivo*, suggesting that RELMα expressed in lung epithelial cells promotes influenza infection of neighboring cells.

In the last chapter of this thesis, we broadened our research scope to investigate the function of myeloid-derived cells in helminth infection by targeting CX3CR1, a critical chemokine receptor for monocyte recruitment from the blood vessel to the site of infection. CX3CR1 deficiency induced a more inflammatory response but lower parasite burden in the lung. CX3CR1-deficient monocytes were more cytotoxic and active than WT monocytes, demonstrating the regulatory function of CX3CR1 in monocytes.

Collectively, these studies demonstrate diverse functions of RELMα and CX3CR1 in different infectious diseases and identify putative downstream targets by which RELMα and CX3CR1 modulate the immune response and tissue repair.

TABLE OF CONTENTS

LIST OF FIGURES

CHAPTER ONE – Introduction: Resolution of Inflammation and Wound Healing After Mucosal Infection are Mediated by Macrophages and RELMα

Sang Yong Kim[1], Meera G. Nair[2]

[1]Department of Microbiology, University of California, Riverside, Riverside, CA, USA

[2]Division of Biomedical Sciences, School of Medicine, University of California, Riverside, Riverside, CA, USA

A version of this chapter was published in *Immunology & Cell Biology*, 2019

Soil-transmitted helminth (STH) infections

STH infection is a public health concern because more than 1.5 billion people or 24% of the entire human population are infected with STH [1]. Infections are predominant in tropical and subtropical areas where sanitation is poor. The roundworm (*Ascaris lumbricoides*), whipworm (*Trichuris trichiura)*, and hookworm (*Necator americanus* and *Ancylostoma duodenale)* are the main species that infect people. In humans, the roundworm and whipworm are transmitted by ingestion of eggs, and the hookworm infection is mediated by larvae penetrating the skin [2-4]. After ingestion, the roundworm and whipworm larvae hatch in the small and large intestine, respectively, and develop into adults to produce eggs and pass them with feces. After the penetration of the skin, the hookworm larvae are carried through the blood vessels to the heart and then to the lung. They penetrate the pulmonary alveoli, migrate to the pharynx along the bronchial tree, and are swallowed. Once, they reach to the small intestine, they have a similar life cycle to the roundworm and whipworm. In addition, the threadworm *Strongyloides stercoralis* causes severe morbidity but is the most neglected tropical disease [5]. Unlike other worms, *Strongyloides* larvae hatch and mature in the intestine. Most larvae are passed with feces, but some of the larvae mature and reinfect the host [6].

The distribution of STH infection is concentrated in the endemic region as having heavily infected people harboring most worms [7-9], and these people suffer from various symptoms. Most worm infections cause a type-1 hypersensitivity [9], which involves IgE-mediated release of antibodies against the soluble antigen [10]. Especially in children, adult *Ascaris* can lead to small bowel obstruction, volvulus, or

intussusception, and it can also cause appendicitis, cholecystitis, pancreatitis, and gastric ascariasis in severe cases [9]. Malnutrition and anemia might be resulted from *A lumbricodies* [11, 12], worsening nutritional status of people in developing countries. *T trichuria* causes petechial lesion, blotchy mucosal hemorrhage, oozing, and colonic mucosal inflammation [9, 13-16]. Adult *A duodenale* and *N americanus* burrow their teeth into the mucosa in the small intestine causing blood loss [9], and hookworm infection is a major cause of anemia in children and pregnant women in the world [17, 18]. Commonly, type 2 immunity mediated by Th2 cytokines is required for protection against helminth infections and the maintenance of tissue homeostasis [19]. Moreover, alternatively activated macrophages (AAMs/M2) and proteins secreted from them play a crucial role in the immune response to helminth and tissue repair. In chapter 2 and 3, we will demonstrate the function of AAM-derived protein, RELMα, in tissue repair and how it is regulated by choline metabolism in soil-transmitted helminth infections.

Influenza A Virus (IAV) infections

According to the CDC, flu resulted in 82,000 to 170,000 hospitalizations and 5,000 to 14,000 deaths from 2021 to 2022 in the United States. Among the flu-causing influenza viruses, IAV has a wide range of hosts, which are causing enormous damage to the livestock and medical industries [20]. Influenza virus infection usually causes a mild respiratory disease in the upper respiratory tract with fever, sore throat, runny nose, cough, headache, muscle pain, and fatigue, but pneumonia or secondary viral bacterial infection of the lower respiratory tract in immune-compromised people. Alveolar

epithelial injury and following gas exchange failure are caused by the lower respiratory tract infection [21, 22], leading to acute respiratory syndrome (ARDS) and even death [23-25]. IAV belongs to the *Orthomyxoviridae* family, and its genome is composed of 8 RNA segments, which encode RNA polymerase subunits and other viral proteins [26]. IAV subtype can be decided based on viral glycoprotein, haemagglutinin (HA), and neuraminidase (NA). Variations and reassortment of these proteins between different subtypes result in more virulent subtypes and a new outbreak of flu [26-28]. Due to these frequent variations, vaccines for new subtypes must be developed every year, and the cost and manpower waste are enormous. For these reasons, it is deserving to investigate a host factor regulating the immune response to IAV and targeting strategy for this factor.

IAV binds to a host cell through the interaction of HA and sialic acid linked to galactose on plasma membrane glycoproteins or glycolipids [29, 30]. Epithelial cells in the respiratory system are the main place where IAV replication takes place [26] and modulate the immune response against IAV [31]. Viral entry induces apoptosis and necroptosis of infected epithelial cells, which causes damage to the epithelium [32-34]. Influenza-infected alveolar epithelial cells recognize IAV by a variety of pattern recognition receptors and secret chemokines to turn on a strong inflammatory response to the infection [31, 32, 35-38]. C-C motif ligand (CCL) 2, CCL5, and CCL7 released by infected epithelial cells recruit monocytes to the lung, which develop into macrophages [39]. In addition to chemokines, airway epithelial cells also express interferons, lactoferrin, β-defensins, and nitric oxide, which play an important role in antiviral responses [32]. Recruited monocytes and macrophages heavily produce cytokines and

further increase the cell death of airway epithelial cells, exacerbating the inflammatory response in the lung [31, 40]. Unlike helminth infection, IAV infections induce a Th1 immune response. Dendritic cells from the lung migrate to the draining lymph node and activate CD4 T cells during the IAV infection [41, 42]. Proinflammatory cytokines such as IFN-γ, TNF, and IL-2 are expressed by Th1 cells [43], which activate classically activated macrophages (M1/CAMs) [44]. Th1 cells also induce CD8 T cell differentiation by secreting IL-2 and IFN-γ to clear the viral infection [45, 46]. These inflammatory responses are required for the clearance of viruses but dysregulated hyperinflammation results in irreversible tissue damage. RELMα was recently identified as a marker for monocyte-derived macrophage tissue engraftment and was also reported to be expressed by intestinal epithelium in bacterial infection [47, 48]. However, it has not been studied in which cells RELMα is expressed and what function it has in IAV infection. In the chapter 4, the induction of RELMα and novel function of RELMα in IAV infection will be addressed.

The effect of helminth infection on microparasite infection

In the endemic area where people harbor significant helminth burden, co-infection with microparasites can exacerbate disease. Microparasites are intracellular parasites such as viruses, some bacteria, and protozoa. While helminth infection induces Th2 immune response, the activation of Th2 immune response inhibits Th1 immune response activated by microparasites at the same time [49]. IL-10 and regulatory T (T_{reg}) cells induced by helminth-secreted immunomodulatory protein inhibit the secretion of pro-inflammatory

chemokines [50]. This negative regulation downregulates both Th1 and Th2 immune responses, exacerbating the outcome of both helminth and microparasite infection [51]. In particular, helminth-microparasite coinfection is emerging as a problem especially in light of the COVID-19 pandemic.

In an in vivo coinfection model, peritoneal M2 macrophages activated by *H. polygyrus* infection were able to change to antimicrobial nitric oxide-producing M1 macrophages capable of killing an attenuated *Salmonella* strain when challenged intraperitoneally [52]. In contrast, *Salmonella*-induced M1 macrophages could not be repolarized by IL-4 treatment, indicating that M1 macrophage activation has a more restrictive effect on plasticity than M2 macrophage activation [52]. These studies show that M2 macrophages have some ability to alter their phenotype in response to different stimuli. It can be inferred from these studies that wound healing M2 macrophage subsets may be equally plastic; however, further mechanistic investigation in wound healing models is needed.

When mice were co-infected with *H. polygyrus* and West Nile Virus (WNV), the mortality of mice was significantly increased [53]. The coinfected mice changed in morphology and delayed transit in the gut, commensal bacterial translocation, and impaired T cell response against WNV, leading to increased viral burden because of skewed type 2 immune response by *H. polygyrus* infection. Tuft cells play an important role in initiating type 2 immunity in the small intestine and secret IL-25 by employing a chemosensing pathway to recognize helminths [54-56]. Tuft cell-derived IL-25

aggravated WNV infection, indicating that IL-25 is a key regulator of viral coinfection with helminths [53].

The direct correlation between helminth and influenza infections has never been revealed, but there is a report that parasitic infections negatively affect the efficacy of influenza vaccines [57]. Mice infected with *Litomosoides sigmodontis* exhibited decreased quantity and quality of antibody responses to vaccination against seasonal influenza. Specifically, vaccination could not protect against challenge infections with the H1N1 influenza A virus, which was mediated by IL-10 produced by T_{reg} cells [57]. IL-10 production by T_{reg} is the main feature of Th2 immune response, and the Nair lab found that RELMα expressed by large peritoneal macrophages regulates T_{reg} cell proliferation in IL-4-induced peritoneal inflammation [58]. Therefore, RELMα upregulated by helminth infection may be a key factor in determining the outcome of other pathogen infections.

Macrophages and RELMα in wound healing

Numerous soluble and cellular signals instruct macrophage activation for the final stages of wound healing: tissue remodeling and resolution of inflammation. These include: Th2 cytokines that mediate a tissue remodeling "M2" program, and apoptotic cells that induce an anti-inflammatory macrophage phenotype.

Th2 cytokines

M2 macrophages are important players in tissue repair [59]. M2 macrophages are activated by Th2 cytokines, such as IL-4 and IL-13, that are highly produced in allergic

inflammation and helminth infection. For this reason, significant functional information on M2 macrophages has been acquired from helminth infection and allergy studies [60]. These studies have provided insight into the M2-mediated effector pathways for wound healing. Indeed, helminths are macroscopic organisms that cause tissue injury, and the tissue remodeling that occurs in allergic responses shares similarities with the tissue repair stage in wound healing. In these models of tissue injury and inflammation, the Th2 cytokine response is mediated in a two-step process, as summarized in Figure 1. First, an insult to the barrier causes epithelial cells to release alarmins, including thymic stromal lymphopoietin, IL-25 and IL-33 [60]. These in turn activate Th2 cytokine-producing innate cells, such as group 2 innate lymphoid cells, mast cells, basophils, and eosinophils. The critical importance of M2 macrophages in mediating wound healing is demonstrated in numerous in vitro and in vivo studies. For instance, IL-4/IL-13-activated human THP-1 cells induced proliferation, collagen synthesis and a-smooth muscle actin (a-SMA) expression by human dermal fibroblasts, in a co-culture assay [61]. These M2-differentiated THP-1 cells also increased dermal fibroblast expression of a-SMA, a feature of myofibroblasts, indicating that fibroblasts were differentiated into myofibroblasts [61]. Furthermore, abrogation of IL-4Ra signaling in macrophages impaired wound repair in in vivo models of wound healing by skin punch biopsy, chemical-induced injury, or invasive helminth infection-induced injury [62-64]. Mechanistically, M2 macrophages initiate wound repair through numerous pathways including growth factors and matrix metalloproteinases, summarized in Figure 2 and in recent reviews [59]. In addition, M2 macrophage-derived arginase 1 (Arg1) is a

downstream effector of wound healing in the skin and following helminth infection [60, 65]. The mechanism by which macrophage-derived arginase promotes skin wound healing is likely twofold: dampening inflammation and promoting matrix deposition through its metabolism of L-arginine.

IL-4Ra signaling also stimulates tissue-resident macrophage proliferation, which can have the beneficial outcome of expanding and activating the effector macrophage population for wound healing [63, 66]. Here, additional signals from the tissue environment promoted the IL-4-induced wound-healing capacity of M2 macrophages. Specifically, the surfactant protein A (SP-A) produced in the lung acted through the receptor myosin 18A (Myo18A) to enhance M2 macrophage activation and lung wound healing following *N. brasiliensis* infection-induced injury. Interestingly, in the peritoneal cavity, resident macrophages did not respond to SP-A, but instead were activated by the complement protein C1q, which is structurally homologous to SP-A. The stimulatory effect of C1q on M2 macrophages, likely through Myo18a, was observed in several tissues including the peritoneal cavity, liver, spleen, and adipose tissue. Functionally, C1q promoted M2 macrophage-mediated liver repair following infection with *Listeria monocytogenes*. Whether C1q affects resident tissue macrophage populations, or instead activates monocytes or macrophages recruited to the injury site from the blood or peritoneal cavity is unclear. Another study utilizing carbon tetrachloride (CCL4) treatment as a model of liver injury demonstrated that peritoneal macrophages could cross the mesothelium and penetrate into the injured liver tissue. These macrophages,

originating from the peritoneal cavity, expressed M2 markers Arginase and RELMα, and exhibited a reparative function when recruited to the liver [67]. While tissue-resident macrophages are likely more rapid responders to injury, monocytes recruited from the blood can also differentiate into M2 macrophages and contribute to tissue repair following *Schistosoma mansoni* infection-induced liver injury [68]. This process was impaired in vitamin A-deficient mice suggesting that dietary components are important for optimal M2 macrophage activation.

M2 macrophage-mediated killing of large extracellular helminths exhibits common features of tissue repair. In *Heligmosomoides polygyrus* (*H. polygyrus*) infection, M2 macrophages are recruited to the helminth, and produce factors to trap and kill the pathogen [69]. The contributing factors that immobilize the worm include wound healing factors such as Arginase 1. Understanding the activation pathway and effector molecules of M2 macrophages that kill *H. polygyrus* infection may therefore provide insight into new wound-healing mechanisms. Mechanistically, recruitment and killing of *H. polygyrus* by M2 macrophages involved recognition of helminth antigen-antibody immune complexes and the production of CXCR2 ligands [70]. Mice-deficient in FcγR signaling and activation-induced cytidine deaminase, which contributes to antibody maturation and class switching, exhibited impaired worm killing but also increased intestinal lesions suggesting defective wound repair. Furthermore, at later timepoints, *Fcrg*$^{-/-}$ and *Aid*$^{-/-}$ mice showed severe peritonitis that might be attributed to defective lesion repair resulting in increased bacterial translocation. Investigation of the mechanism of wound repair in this helminth infection model also revealed the importance of an

additional cell type: the myofibroblast, which was activated CXCL2 and CXCL3, via CXCR2, and helminth antigens via dectin-2, to mediate wound closure potentially through expression of a-SMA. Of translational significance, CXCL3 from human monocyte-derived macrophages induced by *Ascaris suum*, the pig helminth closely related to the human parasite *Ascaris lumbricoides*, upregulated wound healing by human myofibroblasts. These data indicate that crosstalk between M2 macrophages and other cell types is necessary for effective wound healing.

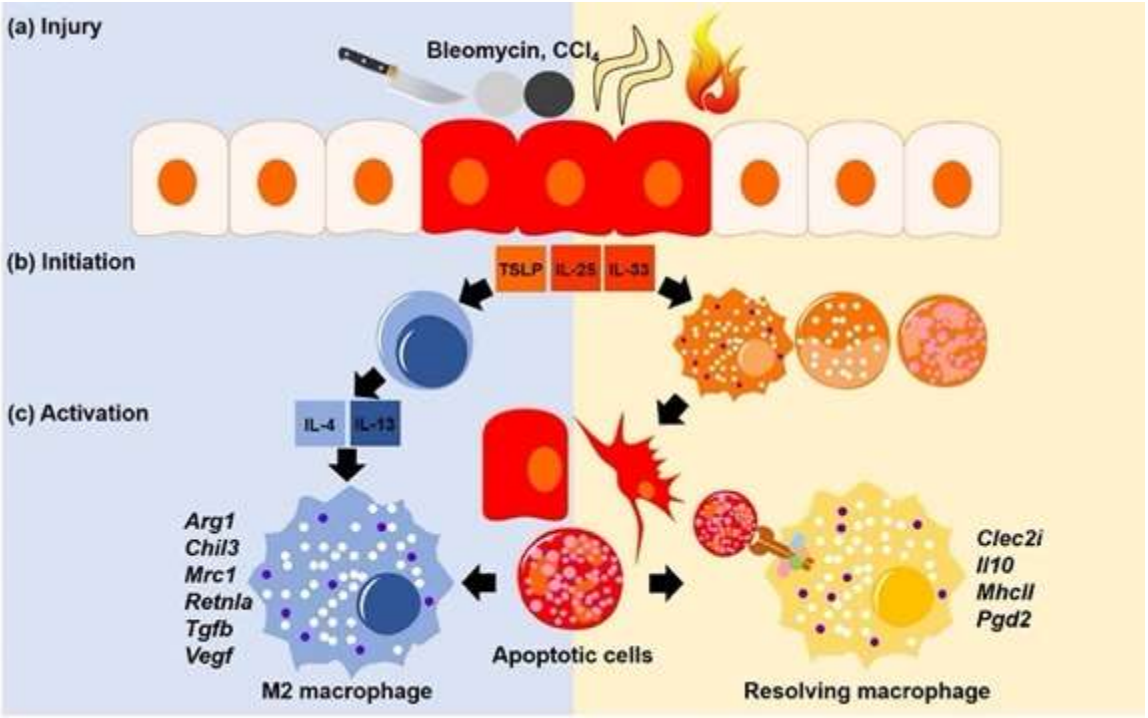

Figure 1. Wound-healing macrophage activation. (a) Injury by cuts, chemicals (CCl4 and bleomycin), helminths or burn injury causes a breach in barrier. (b) The wound-healing response is initiated by dying cells which release cytokines (TSLP, IL-25 and IL-33) that activate Th2 cytokine (IL-4/IL-13)-producing cells. Innate cells such as neutrophils are also recruited to kill invading pathogens, and apoptosed once the challenge is resolved. (c) M2 macrophages (left) are activated by the Th2 cytokines. Equally important is the activation of resolving macrophages (right) which are activated by phagocytosis of the apoptotic cells resulting from the inflammation. Rather than distinct subsets, both M2 and resolving macrophages represent a continuum of macrophage activation that are influenced by both Th2 cytokines and apoptotic cells.

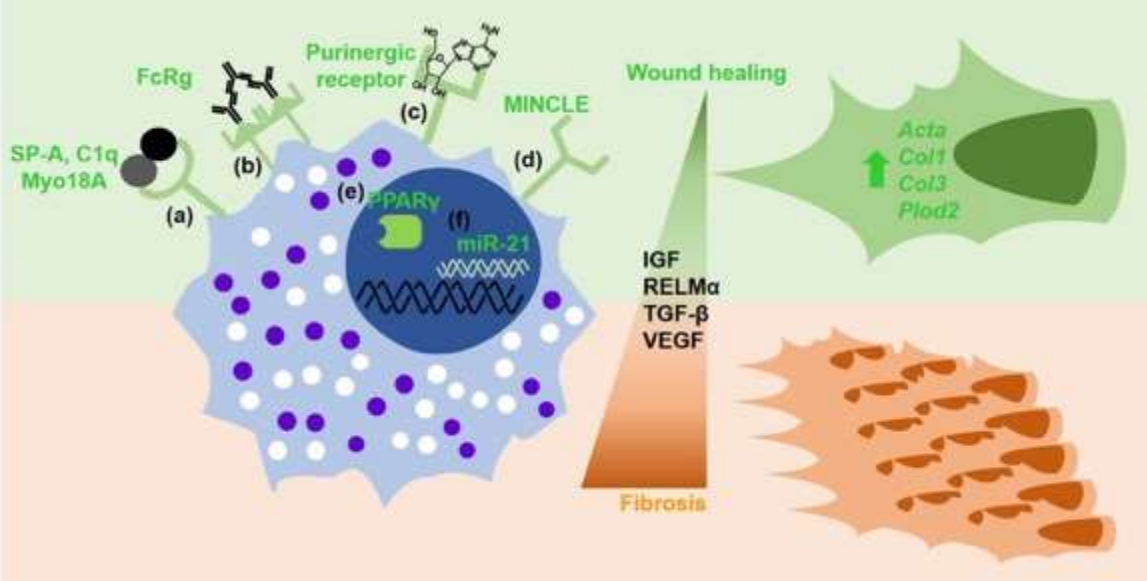

Figure 2. Macrophage enhancers and effectors in wound healing and fibrosis.

Wound-healing macrophage activation is enhanced by the following surface markers: (a) signaling through the Myo18A receptor; (b) FcγR-mediated signaling by immune complexes; (c) ATP or adenosine binding to purinergic receptors; (d) Mincle surface expression; and intracellular factor; (e) nuclear receptor PPARγ; (f) micro-RNA 21. These enhance macrophage effector function to promote wound healing, but if excessive, can lead to fibrosis. ATP, adenosine triphosphate.

Apoptotic cells

A critical step to wound healing is the clearance of apoptotic cells resulting from the inflammatory environment. This process is mediated by resolving, or resolution, macrophages. Resolving macrophages sense and phagocytose phostaphatidylserine (PtdSer)-exposed apoptotic cells in a process called efferocytosis [71]. Effective efferocytosis is dependent on the receptor tyrosine kinases AXL and MERTK. In addition to clearing dead cells, resolving macrophages contribute to wound healing and tissue homeostasis by producing anti-inflammatory molecules such as IL-10, and tissue remodeling growth factors such as TGF-b. Th2 cytokines and apoptotic cell engulfment were originally considered distinct signals, which activated M2 or resolving macrophages, respectively; however, recent studies have uncovered synergism of these signals for optimal wound healing. Indeed, co-treatment of bone marrow-derived macrophages with apoptotic neutrophils and Th2 cytokines induced maximal expression of wound healing genes *Retnla* (RELMa), *Chil3* (Ym1), *Ear2* (Eosinophil-associated, ribonuclease A family, member 2) and *Fn1* (Fibronectin 1) [71]. The essential function of apoptotic cell recognition for optimal M2 activation was demonstrated utilizing macrophages deficient in AXL and MERTK in *N. brasiliensis* infection as an in vivo model of M2 macrophage-dependent wound healing [71]. Critically, AXL and MERTK functional effects on tissue repair were not restricted to the lung, as these proteins were required for upregulation of the anti-inflammatory and wound healing genes in macrophages in the damaged intestine and peritoneal cavity. It has previously been shown that SP-A induces efferocytosis while C1q activates tyrosine-protein kinase Mer

expression [72]. Thus, in addition to M2 activation, SP-A and C1q might promote apoptotic cell sensing [73]. Together, these studies implicate an interdependent, positive feedback loop whereby apoptotic cells and Th2 cytokines act together to promote macrophage-mediated wound healing.

Resistin-Like Molecule Alpha (RELMα)

RELMα is a 10 kDa small-secreted protein, which has a cysteine-rich domain in C-terminal. RELMα was discovered in bronchoalveolar lavage fluid from mice with experimentally induced allergic pulmonary inflammation [74]. The following study showed that RELMα expression is high in the pulmonary vasculature, bronchial epithelial cells, and type 2 pneumocytes in hypoxia conditions [75]. However, RELMα was also shown to be strongly induced in type 2 immune response and expressed by alternatively activated macrophages (AAMs/M2) [66, 76-78]. While an immunomodulatory function of hematopoietic cell-derived RELMα in Th2 immune response has been well studied, there is a still lack of understanding in Th1 immune response. RELMα downregulates the Th2 immune response activated by *N. brasiliensis* in the lung to avoid severe tissue damage, increasing the parasite burden in the host [79, 80]. In addition to AAMs, *N. brasiliensis* infection induces RELMα expression by B cells in the lung, which decreases IL-17A expression to limit lung emphysema [81]. RELMα was also induced by bacterial infection, increasing inflammation in *Citrobacter*-induced colitis by activating IL-23/Th17 axis [48]. On the other hand, RELMα has a protective function in skin bacterial infection [68]. RELMα expression was upregulated by dietary vitamin A and microbiota

colonization in the mouse skin, which has a bactericidal function. Another function of RELMα is the activation of wound healing. RELMα has mitotic and chemotactic functions on bone marrow cells and mesenchymal stem cells [82-85]. RELMα triggers tissue remodeling by recruiting these cells and activating proliferation in the lung. RELMα also regulates genes involved in tissue remodeling. RELMα activates the enzyme lysyl hydrolase 2 (*Plod2*), which mediates optimal collagen cross-linking [62]. In *N. brasiliensis*-infected mice, gene expression analysis of RELMα-treated lung macrophages revealed that RELMα promoted the expression of genes involved in extracellular matrix remodeling: matrix metalloproteinase 9 (*Mmp9*), integrin beta 1 (*Itgb1*) and junctional adhesion molecule A (*F11r*) [80]. However, the exact downstream signaling that controls tissue repair by RELMα has not been fully studied yet, and genes controlled by RELMα in the lesion after the resolution of inflammatory response was investigated in Chapter 2 in chronic intestinal infection with *Heligmosomoides polygyrus*, where granulomas form around the worms as they encyst in the tissue, analogous to a wound being repaired at a site of tissue injury.

C-X3-C motif chemokine receptor 1 (CX3CR1)

CX3CR1 is a G-protein coupled receptor that binds the chemokine CX3CL1/fractalkine. CX3CR1 is expressed on monocytes, where it is critical for effective monocyte adhesion and transmigration through the endothelium into the tissues. Within the tissue, and dependent on the inflammatory environment, CX3CR1-expressing monocytes differentiate into dendritic cells and macrophages, with essential protective

functions against many pathogens, including bacteria and viruses [86, 87]. CX3CR1 signaling also occurs in response to injury and fibrosis. In murine models of spinal cord injury and stroke, CX3CR1-deficient mice have ameliorated neural outcomes associated with a reparative phenotype in CX3CR1-expressing microglia and macrophages [88, 89]. In pulmonary and peritoneal fibrosis models, CX3CR1 signaling is also detrimental, exacerbating fibrosis. Further, in infection with Schistosoma japonicum, acute hepatic granuloma formation, and liver pathology is increased by CX3CR1 signaling, with little effect on parasite burdens [90]. Together, these studies suggest that CX3CR1 signaling is important for optimal effector responses to multiple pathogens but needs to be tightly regulated to reduce inflammatory outcomes and tissue pathology. However, CX3CR1 signaling in pulmonary helminth infection has not previously been examined and will be discussed in the chapter 5.

Conclusion

STH infections are a global public health problem and an effective vaccine has yet to be developed. These macroparasite infection cause damage to the tissue as they migrate through tissues. Exploring the function of macrophages in tissue repair can reveal new pathways to improve responses to injury beyond helminth infection. Upon helminth infections, RELMα is expressed by M2 macrophages in the lungs, which regulate the immune response and induce tissue repair. In chapter 2, we will address how RELMα regulates granuloma produced by *H. polygyrus* infections in the intestine. In chapter 3, we will investigate new factors that promote RELMα expression, specifically the effect of choline, a dietary nutrient.

RELMα is also a marker for monocyte-derived tissue-resident macrophages in non-homeostatic conditions. This means that RELMα is not just a protein that is upregulated and functions in the Th2 immune response but may have different functions in other types of immune response. RELMα was beneficial for the host in helminth infections, but we will demonstrate that RELMα is harmful to the host in influenza infections in chapter 4.

Lastly, the cell-intrinsic function of CX3CR1 was identified. CX3CR1 is a chemokine receptor required for the recruitment and differentiation of monocytes in the inflammatory condition. We validated that CX3CR1 regulates proinflammatory cytokine and cytotoxic molecule production in monocytes in the chapter 5. Collectively, this dissertation will investigate the function of host proteins, RELMα and CX3CR1 in

mucosal infection, and further the mechanism by which they regulate immune responses against pathogens.

References

1. WHO, *Investing to overcome the global impact of neglected tropical diseases: third WHO report on neglected diseases 2015*. 2015, *World Heal Organ*. p. 191.

2. CDC. *Parasites - Ascariasis*. 2019; Available from: https://www.cdc.gov/parasites/ascariasis/biology.html#:~:text=Life%20Cycle%3A&text=Upon%20reaching%20the%20small%20intestine,live%201%20to%202%20years.

3. CDC. *Parasites - Trichuriasis (also known as Whipworm Infection)*. 2013; Available from: https://www.cdc.gov/parasites/whipworm/biology.html.

4. CDC. *Parasites - Hookworm*. 2019; Available from: https://www.cdc.gov/parasites/hookworm/biology.html.

5. Schär, F., et al., *Strongyloides stercoralis: Global Distribution and Risk Factors.* PLoS Negl Trop Dis, 2013. **7**(7): p. e2288.

6. CDC. *Parasites - Strongyloides*. 2020; Available from: https://www.cdc.gov/parasites/strongyloides/gen_info/faqs.html.

7. Bundy, D.A., et al., *Population distribution of Trichuris trichiura in a community of Jamaican children.* Trans R Soc Trop Med Hyg, 1985. **79**(2): p. 232-7.

8. Schad, G.A. and R.M. Anderson, *Predisposition to hookworm infection in humans.* Science, 1985. **228**(4707): p. 1537-40.

9. Jourdan, P.M., et al., *Soil-transmitted helminth infections.* Lancet, 2018. **391**(10117): p. 252-265.

10. Abbas, M., M. Moussa, and H. Akel, *Type I Hypersensitivity Reaction*. 2022, StatPearls [Internet]: Treasure Island (FL).

11. Strunz, E.C., P.S. Suchdev, and D.G. Addiss, *Soil-Transmitted Helminthiasis and Vitamin A Deficiency: Two Problems, One Policy.* Trends Parasitol, 2016. **32**(1): p. 10-18.

12. Wang, P., et al., *[Report on 16 cases of small intestine ascariasis diagnosed by capsule endoscopy].* Zhongguo Ji Sheng Chong Xue Yu Ji Sheng Chong Bing Za Zhi, 2013. **31**(3): p. 242-3.

13. Khuroo, M.S. and N.S. Khuroo, *Trichuris dysentery syndrome: a common cause of chronic iron deficiency anemia in adults in an endemic area (with videos).* Gastrointest Endosc, 2010. **71**(1): p. 200-4.

14. Bartsch, S.M., et al., *The Global Economic and Health Burden of Human Hookworm Infection.* PLoS Negl Trop Dis, 2016. **10**(9): p. e0004922.

15. Cooper, E.S., et al., *Immediate hypersensitivity in colon of children with chronic Trichuris trichiura dysentery.* Lancet, 1991. **338**(8775): p. 1104-7.

16. Dige, A., et al., *Mucosal and systemic immune modulation by Trichuris trichiura in a self-infected individual.* Parasite Immunol, 2017. **39**(1).

17. Brooker, S., P.J. Hotez, and D.A. Bundy, *Hookworm-related anaemia among pregnant women: a systematic review.* PLoS Negl Trop Dis, 2008. **2**(9): p. e291.

18. Hotez, P.J., et al., *Hookworm infection.* N Engl J Med, 2004. **351**(8): p. 799-807.

19. Gause, W.C., C. Rothlin, and P. Loke, *Heterogeneity in the initiation, development and function of type 2 immunity.* Nat Rev Immunol, 2020. **20**(10): p. 603-614.

20. Wahlgren, J., *Influenza A viruses: an ecology review.* Infect Ecol Epidemiol, 2011. **1**.

21. van Riel, D., et al., *Seasonal and pandemic human influenza viruses attach better to human upper respiratory tract epithelium than avian influenza viruses.* Am J Pathol, 2010. **176**(4): p. 1614-8.

22. Shinya, K., et al., *Avian flu: influenza virus receptors in the human airway.* Nature, 2006. **440**(7083): p. 435-6.

23. Chen, X., et al., *Host Immune Response to Influenza A Virus Infection.* Front Immunol, 2018. **9**: p. 320.

24. Herold, S., et al., *Influenza virus-induced lung injury: pathogenesis and implications for treatment.* Eur Respir J, 2015. **45**(5): p. 1463-78.

25. Hogan, B.L., et al., *Repair and regeneration of the respiratory system: complexity, plasticity, and mechanisms of lung stem cell function.* Cell Stem Cell, 2014. **15**(2): p. 123-38.

26. Krammer, F., et al., *Influenza.* Nat Rev Dis Primers, 2018. **4**(1): p. 3.

27. Zeng, L.Y., J. Yang, and S. Liu, *Investigational hemagglutinin-targeted influenza virus inhibitors.* Expert Opin Investig Drugs, 2017. **26**(1): p. 63-73.

28. Hensley, S.E., et al., *Influenza A virus hemagglutinin antibody escape promotes neuraminidase antigenic variation and drug resistance.* PLoS One, 2011. **6**(2): p. e15190.

29. Gottschalk, A., *Chemistry of virus receptors*, in *The viruses: biochemical, biological and biophysical properties* F. Burnet and W. Stanley, Editors. 1959, Academic Press: New York, NY.

30. Palese, P. and M.L. SHAW, *Orthomyxoviridae: the viruses and their replication*, in *Fields virology*, D.M. Knipe and P.M. Howley, Editors. 2007, Lippincott Williams and Wilkins: Philadelphia, PA.

31. Klomp, M., et al., *From virus to inflammation, how influenza promotes lung damage.* J Leukoc Biol, 2021. **110**(1): p. 115-122.

32. Vareille, M., et al., *The airway epithelium: soldier in the fight against respiratory viruses.* Clin Microbiol Rev, 2011. **24**(1): p. 210-29.

33. White, S.R., *Apoptosis and the airway epithelium.* J Allergy (Cairo), 2011. **2011**: p. 948406.

34. Gregory, D.J. and L. Kobzik, *Influenza lung injury: mechanisms and therapeutic opportunities.* Am J Physiol Lung Cell Mol Physiol, 2015. **309**(10): p. L1041-6.

35. Pleschka, S., *Overview of influenza viruses.* Curr Top Microbiol Immunol, 2013. **370**: p. 1-20.

36. Crystal, R.G., et al., *Airway epithelial cells: current concepts and challenges.* Proc Am Thorac Soc, 2008. **5**(7): p. 772-7.

37. Grigg, J., *The platelet activating factor receptor: a new anti-infective target in respiratory disease?* Thorax, 2012. **67**(9): p. 840-1.

38. Lamichhane, P.P. and A.E. Samarasinghe, *The Role of Innate Leukocytes during Influenza Virus Infection.* J Immunol Res, 2019. **2019**: p. 8028725.

39. Lin, K.L., et al., *CCR2+ monocyte-derived dendritic cells and exudate macrophages produce influenza-induced pulmonary immune pathology and mortality.* J Immunol, 2008. **180**(4): p. 2562-72.

40. Vangeti, S., M. Yu, and A. Smed-Sörensen, *Respiratory Mononuclear Phagocytes in Human Influenza A Virus Infection: Their Role in Immune Protection and As Targets of the Virus.* Front Immunol, 2018. **9**: p. 1521.

41. Ingulli, E., et al., *In vivo detection of dendritic cell antigen presentation to CD4(+) T cells.* J Exp Med, 1997. **185**(12): p. 2133-41.

42. Lukens, M.V., et al., *Respiratory syncytial virus-induced activation and migration of respiratory dendritic cells and subsequent antigen presentation in the lung-draining lymph node.* J Virol, 2009. **83**(14): p. 7235-43.

43. Szabo, S.J., et al., *A novel transcription factor, T-bet, directs Th1 lineage commitment.* Cell, 2000. **100**(6): p. 655-69.

44. Liu, S.Y., et al., *Systematic identification of type I and type II interferon-induced antiviral factors.* Proc Natl Acad Sci U S A, 2012. **109**(11): p. 4239-44.

45. Shu, U., et al., *Activated T cells induce interleukin-12 production by monocytes via CD40-CD40 ligand interaction.* Eur J Immunol, 1995. **25**(4): p. 1125-8.

46. Stuber, E., W. Strober, and M. Neurath, *Blocking the CD40L-CD40 interaction in vivo specifically prevents the priming of T helper 1 cells through the inhibition of interleukin 12 secretion.* J Exp Med, 1996. **183**(2): p. 693-8.

47. Sanin, D.E., et al., *A common framework of monocyte-derived macrophage activation.* Sci Immunol, 2022. **7**(70): p. eabl7482.

48. Osborne, L.C., et al., *Resistin-like molecule α promotes pathogenic Th17 cell responses and bacterial-induced intestinal inflammation.* J Immunol, 2013. **190**(5): p. 2292-300.

49. Mosmann, T.R. and S. Sad, *The expanding universe of T-cell subsets: Th1, Th2 and more.* Immunol Today, 1996. **17**(3): p. 138-46.

50. Rolot, M., et al., *Helminth-induced IL-4 expands bystander memory CD8.* Nat Commun, 2018. **9**(1): p. 4516.

51. Ezenwa, V.O. and A.E. Jolles, *From host immunity to pathogen invasion: the effects of helminth coinfection on the dynamics of microparasites.* Integr Comp Biol, 2011. **51**(4): p. 540-51.

52. Rückerl, D., et al., *Macrophage origin limits functional plasticity in helminth-bacterial co-infection.* PLoS Pathog, 2017. **13**(3): p. e1006233.

53. Desai, P., et al., *Enteric helminth coinfection enhances host susceptibility to neurotropic flaviviruses via a tuft cell-IL-4 receptor signaling axis.* Cell, 2021. **184**(5): p. 1214-1231.e16.

54. Gerbe, F., et al., *Intestinal epithelial tuft cells initiate type 2 mucosal immunity to helminth parasites.* Nature, 2016. **529**(7585): p. 226-30.

55. Howitt, M.R., et al., *Tuft cells, taste-chemosensory cells, orchestrate parasite type 2 immunity in the gut.* Science, 2016. **351**(6279): p. 1329-33.

56. von Moltke, J., et al., *Tuft-cell-derived IL-25 regulates an intestinal ILC2-epithelial response circuit.* Nature, 2016. **529**(7585): p. 221-5.

57. Hartmann, W., et al., *Helminth Infections Suppress the Efficacy of Vaccination against Seasonal Influenza.* Cell Rep, 2019. **29**(8): p. 2243-2256.e4.

58. Li, J., et al., *Macrophage-Regulatory T Cell Interactions Promote Type 2 Immune Homeostasis Through Resistin-Like Molecule α.* Front Immunol, 2021. **12**: p. 710406.

59. Minutti, C.M., et al., *Tissue-specific contribution of macrophages to wound healing.* Semin Cell Dev Biol, 2017. **61**: p. 3-11.

60. Gause, W.C., T.A. Wynn, and J.E. Allen, *Type 2 immunity and wound healing: evolutionary refinement of adaptive immunity by helminths.* Nat Rev Immunol, 2013. **13**(8): p. 607-14.

61. Zhu, Z., et al., *Alternatively activated macrophages derived from THP-1 cells promote the fibrogenic activities of human dermal fibroblasts.* Wound Repair Regen, 2017. **25**(3): p. 377-388.

62. Knipper, J.A., et al., *Interleukin-4 Receptor α Signaling in Myeloid Cells Controls Collagen Fibril Assembly in Skin Repair.* Immunity, 2015. **43**(4): p. 803-16.

63. Minutti, C.M., et al., *Local amplifiers of IL-4Rα-mediated macrophage activation promote repair in lung and liver.* Science, 2017. **356**(6342): p. 1076-1080.

64. Weng, S.Y., et al., *IL-4 Receptor Alpha Signaling through Macrophages Differentially Regulates Liver Fibrosis Progression and Reversal.* EBioMedicine, 2018. **29**: p. 92-103.

65. Campbell, L., et al., *Local arginase 1 activity is required for cutaneous wound healing.* J Invest Dermatol, 2013. **133**(10): p. 2461-2470.

66. Jenkins, S.J., et al., *Local macrophage proliferation, rather than recruitment from the blood, is a signature of TH2 inflammation.* Science, 2011. **332**(6035): p. 1284-8.

67. Wang, J. and P. Kubes, *A Reservoir of Mature Cavity Macrophages that Can Rapidly Invade Visceral Organs to Affect Tissue Repair.* Cell, 2016. **165**(3): p. 668-78.

68. Gundra, U.M., et al., *Vitamin A mediates conversion of monocyte-derived macrophages into tissue-resident macrophages during alternative activation.* Nat Immunol, 2017. **18**(6): p. 642-653.

69. Esser-von Bieren, J., et al., *Antibodies trap tissue migrating helminth larvae and prevent tissue damage by driving IL-4Rα-independent alternative differentiation of macrophages.* PLoS Pathog, 2013. **9**(11): p. e1003771.

70. Esser-von Bieren, J., et al., *Immune antibodies and helminth products drive CXCR2-dependent macrophage-myofibroblast crosstalk to promote intestinal repair.* PLoS Pathog, 2015. **11**(3): p. e1004778.

71. Bosurgi, L., et al., *Macrophage function in tissue repair and remodeling requires IL-4 or IL-13 with apoptotic cells.* Science, 2017. **356**(6342): p. 1072-1076.

72. Greenlee-Wacker, M.C., *Clearance of apoptotic neutrophils and resolution of inflammation.* Immunol Rev, 2016. **273**(1): p. 357-70.

73. Bouchery, T. and N.L. Harris, *Specific repair by discerning macrophages.* Science, 2017. **356**(6342): p. 1014.

74. Holcomb, I.N., et al., *FIZZ1, a novel cysteine-rich secreted protein associated with pulmonary inflammation, defines a new gene family.* EMBO J, 2000. **19**(15): p. 4046-55.

75. Teng, X., et al., *FIZZ1/RELMalpha, a novel hypoxia-induced mitogenic factor in lung with vasoconstrictive and angiogenic properties.* Circ Res, 2003. **92**(10): p. 1065-7.

76. Loke, P., et al., *IL-4 dependent alternatively-activated macrophages have a distinctive in vivo gene expression phenotype.* BMC Immunol, 2002. **3**: p. 7.

77. Nair, M.G., et al., *Chitinase and Fizz family members are a generalized feature of nematode infection with selective upregulation of Ym1 and Fizz1 by antigen-presenting cells.* Infect Immun, 2005. **73**(1): p. 385-94.

78. Raes, G., et al., *Differential expression of FIZZ1 and Ym1 in alternatively versus classically activated macrophages.* J Leukoc Biol, 2002. **71**(4): p. 597-602.

79. Krljanac, B., et al., *RELMα-expressing macrophages protect against fatal lung damage and reduce parasite burden during helminth infection.* Sci Immunol, 2019. **4**(35).

80. Batugedara, H.M., et al., *Hematopoietic cell-derived RELMα regulates hookworm immunity through effects on macrophages.* J Leukoc Biol, 2018.

81. Chen, F., et al., *B Cells Produce the Tissue-Protective Protein RELMα during Helminth Infection, which Inhibits IL-17 Expression and Limits Emphysema.* Cell Rep, 2018. **25**(10): p. 2775-2783.e3.

82. Lin, Q., et al., *RELMα Licenses Macrophages for Damage-Associated Molecular Pattern Activation to Instigate Pulmonary Vascular Remodeling.* J Immunol, 2019. **203**(11): p. 2862-2871.

83. Angelini, D.J., et al., *Hypoxia-induced mitogenic factor (HIMF/FIZZ1/RELM alpha) recruits bone marrow-derived cells to the murine pulmonary vasculature.* PLoS One, 2010. **5**(6): p. e11251.

84. Su, Q., Y. Zhou, and R.A. Johns, *Bruton's tyrosine kinase (BTK) is a binding partner for hypoxia induced mitogenic factor (HIMF/FIZZ1) and mediates myeloid cell chemotaxis.* FASEB J, 2007. **21**(7): p. 1376-82.

85. Kolosova, I.A., et al., *Resistin-like molecule α stimulates proliferation of mesenchymal stem cells while maintaining their multipotency.* Stem Cells Dev, 2013. **22**(2): p. 239-47.

86. Manta, C., et al., *CX(3)CR1(+) macrophages support IL-22 production by innate lymphoid cells during infection with Citrobacter rodentium.* Mucosal Immunol, 2013. **6**(1): p. 177-88.

87. Choi, J.Y., et al., *Indispensable Role of CX3CR1+ Dendritic Cells in Regulation of Virus-Induced Neuroinflammation Through Rapid Development of Antiviral Immunity in Peripheral Lymphoid Tissues.* Front Immunol, 2019. **10**: p. 1467.

88. Freria, C.M., et al., *Deletion of the Fractalkine Receptor, CX3CR1, Improves Endogenous Repair, Axon Sprouting, and Synaptogenesis after Spinal Cord Injury in Mice.* J Neurosci, 2017. **37**(13): p. 3568-3587.

89. Faustino, J., et al., *CX3CR1-CCR2-dependent monocyte-microglial signaling modulates neurovascular leakage and acute injury in a mouse model of childhood stroke.* J Cereb Blood Flow Metab, 2019. **39**(10): p. 1919-1935.

90. Ran, L., et al., *Cx3cr1 deficiency in mice attenuates hepatic granuloma formation during acute schistosomiasis by enhancing the M2-type polarization of macrophages.* Dis Model Mech, 2015. **8**(7): p. 691-700.

CHAPTER Two – Resistin-Like Molecule Alpha Induces Tissue Repair in *Heligmosomoides Polygyrus* Infection-Induced Granuloma by Regulating *Serpine1*

Sang Yong Kim[1], Anupama De Silva Ariyaratne[2], Jiang Li[3], Daniel Woo[3], Constance A.M. Finney[2], Meera G. Nair[3]

[1]Department of Microbiology, University of California, Riverside, Riverside, CA, USA

[2] Department of Biological Sciences, Faculty of Science, University of Calgary, Calgary, Alberta, Canada

[3]Division of Biomedical Sciences, School of Medicine, University of California, Riverside, Riverside, CA, USA

Abstract

T helper type 2 cytokine-induced granulomas in helminth infection are critical to trap and eliminate the parasite. However, excessive granuloma formation, or the inability to resolve the granuloma once the helminth has been cleared, causes pathogenic fibrosis. Understanding granuloma formation and resolution could provide insight into balancing helminth trapping, while limiting pathologic outcomes and promoting tissue healing. Th2 cytokine-induced 'M2' macrophages are dominant cell-types in the helminth-induced granuloma and perform dual functions in helminth killing and host healing. M2 macrophages secrete Resistin-like molecule (RELMα), a protein with pleiotropic functions. In the lung and skin, RELMα limits Th2 cytokine responses and promotes tissue healing. However, whether RELMα regulates immune and inflammatory outcomes in chronic intestinal helminth infection is unknown.

Employing *Retnla* knock-out/tdTomato reporter knock-in mice, we investigated RELMα's function in infection with *Heligmosomoides polygyrus* (*H. polygyrus*), a helminth that chronically infects mice and induces macrophage-rich intestinal granulomas. RELMα was highly expressed in granulomas, and *Retnla*$^{tdT/tdT}$ mice had significantly increased granulomas of larger size at day 21 post-infection, suggesting an inability to resolve granulomatous inflammation. Myeloid gene expression analysis revealed significantly elevated ECM-remodeling gene *Serpine1* and monocyte-derived peritoneal macrophages in *Retnla*$^{tdT/tdT}$ granulomas. Serpine1 protein was intensely expressed in the center of *Retnla*$^{tdT/tdT}$ granuloma where many immune cells were still remained. Together, our findings suggest that RELMα constrains the helminth-induced

inflammatory response to the site of infection and injury and promotes granuloma resolution by regulating *Serpine1* expression. Promoting RELMα responses in macrophages may therefore provide an avenue to limit granulomatous inflammation and enhance intestinal tissue healing in chronic helminth infection.

Introduction

Helminths are macroparasites that infect an estimated two billion individuals worldwide and can cause severe morbidities such as growth retardation and organ failure, with no effective vaccine to-date. Remarkably, despite their size and the tissue migratory ability of many of these, the majority of helminth infections are chronic with limited tissue pathology or inflammation [1]. This host disease tolerance, which limits host pathology while at the same time allowing helminth persistence, is mediated by both host immune-regulatory and tissue healing mechanisms and helminth-derived anti-inflammatory molecules [2]. Identifying factors that affect this dynamic balance between helminth killing and host tissue preservation would provide specific mechanisms to promote anti-helminth immunity while limiting tissue pathology. These factors could also identify new anti-inflammatory and tissue healing treatments of relevance beyond helminth infection.

Heligmosomoides polygyrus [3, 4], a natural helminth parasite of mice, offers a useful model for chronic intestinal infection, tissue injury and granuloma formation [5]. The ingested larvae migrate from the intestinal lumen through the tissue to develop into adults in the muscularis externa, then return back to the lumen to establish chronic infections. *H.polygyrus*-induced T helper type 2 (Th2) immune responses promote parasite killing through trapping the parasites in granulomas, and also contribute to tissue healing of the *H.polygyrus*-induced intestinal lesions. Both parasite killing and tissue healing processes have overlapping immune mediators, including alternatively activated, or M2 macrophages. M2 macrophages are dominant cell subsets within the granuloma,

and if depleted by clodronate liposomes or cell-specific IL-4R deletion, mice are impaired in their ability to kill the helminth [6]. The M2 nomenclature may not adequately grasp the expansive heterogeneity of macrophage activation in helminth infection, and the contribution of both Th2 cytokine-dependent and independent macrophage-derived molecules to helminth killing and tissue repair have been reported [7]. Macrophages promoted *H.polygyrus* intestinal lesion healing by activating myofibroblast wound closure [8, 9] through antibody and chemokine signaling-dependent mechanisms, while Arginase1, which is highly expressed by the M2 macrophages within the *H.polygyrus* granuloma, mediates parasite immobilization [10].

RELMα, also known as FIZZ1 and HIMF, was originally identified as a highly secreted protein in the lung during allergic airway inflammation [11], however, it is now well-recognized that RELMα is pleiotropically expressed throughout the body, and a signature gene expressed by macrophages in response to infection by multiple helminth infections [12, 13]. Studies in pulmonary inflammation, hypertension and fibrosis pointed to an inflammatory function for RELMα by promoting immune cell recruitment and fibroblast activation and proliferation associated with pathogenic fibrosis [14, 15]. In the intestine, RELMα promotes Th17 responses and both bacterial and chemical-induced colitis [16, 17]. On the other hand, in response to tissue migratory helminth parasites, RELMα critically prevents fatal lung tissue damage, granulomatous inflammation, and promotes tissue repair [18-21]. RELMα downstream regulatory mechanisms include limiting $CD4^+$ Th2 cytokine and anti-inflammatory responses, as well as promoting collagen cross-linking associated with tissue healing [22-25]. RELMα's downregulation

of CD4 Th2 effector cells also promotes helminth persistence as a disease tolerance mechanism to limit immunopathology at the expense of impaired helminth elimination [18, 23].

H.polygyrus infection induces macrophage expression of Resistin-like molecule (RELM) α in the granuloma, however, RELMα's role in *H.polygyrus* parasite elimination, granuloma formation or intestinal wound healing is unknown [4, 26, 27]. To investigate this, we utilized RELMα-knockout/tDTomato reporter knock-in (*Retnla*$^{tdT/tdT}$) mice and infected them with *H.polygyrus*. Compared to *Retnla*$^{+/+}$ mice (WT), *Retnla*$^{tdT/tdT}$ (KO) mice exhibited increased local immune responses, which was associated with enlarged parasite-induced granulomas with more remaining immune cells in the center. Gene expression analysis of granulomas identified a dysregulated gene, *Serpine1*, in the absence of RELMα. Immunofluorescence staining of granulomas showed that Serpine1 protein expression was significantly higher in *Retnla*$^{tdT/tdT}$ granulomas. Together, our findings demonstrate that RELMα limits *H. polygyrus* immune responses and promotes granuloma healing. Furthermore, a RELMα downstream effector mechanism that involve ECM remodeling was identified. Understanding RELMα and its downstream effector mechanisms may therefore help mitigate helminth infection-induced tissue damage and granulomatous inflammation in the intestine.

Materials and Methods

Mice

Retnla^{tDT} transgenic mice were generated by genOway (Lyon, France) by targeting *Retnla* Exon 2-4 using cre recombinase and Flp-mediated excision and replacement with the tDT reporter gene. Briefly, mice were bred with a genOway proprietary Cre deleter C57BL/6 mouse line to generate constitutive *Retnla*$^{tDT/+}$ mice. *Retnla*$^{tDT/+}$ heterozygote mice were crossed with C57BL/6J mice to generate littermate homozygote (tdT/tdT) and WT (+/+) mice after two generations, then bred in-house. Mice were genotyped by PCR and RELMα serum ELISA. Mice were age matched (6 to 14 weeks old), sex-matched for experiments, and housed five per cage under an ambient temperature with a 12 hours light/12 hours dark cycle. For *H. polygyrus* infection, mice were injected through oral route with water (naive) or *H. polygyrus* L3 following the Bolus (200 L3 at d0) or trickle infection protocol (~30 L3 at d0, 2 ,4, 6, 8, 10 post-infection for a total of 200 L3).

Histology and Immunofluorescence staining

Intestinal tissue was stored overnight in 4% PFA at 4°C. After 24 hours, tissue was removed from 4% PFA and incubated for 24 hours in 30% sucrose. Intestines were blocked in OCT, sectioned at 10µm, and stained by H&E. Area of granulomas and opened lesions were quantified by an ImageJ software. For immunofluorescent staining, sections were incubated with rabbit anti-RELMα (Peprotech, Rock Hill, NJ), APC-conjugated Rat anti-RELMα (eBioscience, San Diego, CA), and rabbit anti-PAI1

(Invitrogen, Waltham, MA) overnight at 4°C. Sections were incubated with anti-Rabbit fluorochrome-conjugated antibody for 2 hours at RT then counterstained with DAPI.

Cytokine quantification

Blood was collected by cutting the renal artery and spun down at 14000g and at 4°C for 10 min to collect serum. The intestinal homogenates were collected by scraping mucus from the small intestine and homogenizing it in 500ul of ice-cold PBS. The homogenized intestinal tissue was spun down at 14000g and 4°C for 1hr and supernatant was collected. For sandwich ELISA, capture and biotinylated detection antibodies were used according to previously described protocols: RELMα (eBioscience) [21].

Nanostring gene expression analysis

Intestinal tissue from naïve mice or dissected granulomas from infected mice were snap-frozen in liquid nitrogen, then RNA isolation performed with TRIZOL (Sigma-Aldrich, St. Louis, MO). RNA was processed and quantified by the Myeloid Innate Immunity v2 panel according to manufacturer's instructions (Nanostring, Seattle, WA). Gene expression analysis was conducted using the Advanced Analysis Nanostring software. Raw counts were normalized to internal controls, then normalized transcripts with $n > 20$ counts were included for analysis (a total of 734 genes). The Nanostring Advanced Analysis algorithm generated biological pathway scores by extracting pathway-level information from a group of genes using the first principal component (PC) of their expression data [28]. Differentially expressed (DE) genes (Adj $p \leq 0.05$, log2Fold≥ 1.5) in each pathway were

graphed as a volcano plot and heatmap. Digital cell quantification was conducted by analyzing log2 gene counts with an Immquant software [29].

Statistical analysis

Data are presented as mean ± SEM and statistical analysis was performed by GraphPad Prism 9 software. Data was assessed by one-way ANOVA followed by post-hoc Tukey's test for multiple comparison, or the unpaired t-test for 2-group comparisons. For data collected over several timepoints, two-way ANOVA with post-Sidak multiple test was performed. *, $p \leq 0.05$; **, $p \leq 0.01$; ***, $p \leq 0.001$, ****, $p \leq 0.001$. Experiments were repeated 2-4 times with n=3-5 per group for each experiment, apart from Nanostring gene expression analysis, which was performed once (n=2 for naive and n=4 for infected per group).

ETHICS STATEMENT

All protocols for animal use and euthanasia were approved by the University of California Riverside Institutional Animal Care and Use Committee (https://or.ucr.edu/ori/committees/iacuc.aspx; protocol A-20180023 and 20210017), and were in accordance with National Institutes of Health guidelines. Animal studies are in accordance with the provisions established by the Animal Welfare Act and the Public Health Services (PHS) Policy on the Humane Care and Use of Laboratory Animals.

Results

H. polygyrus infection induces RELMα expression in granulomas in the small intestine but has no effect on the parasite burden.

We previously investigated *Retnla*$^{-/-}$ mice in infection with rat hookworm *Nippostrongylus brasiliensis* and demonstrated that RELMα-expressing macrophages limit infection-induced lung inflammatory responses [18, 21]. However, caveats exist for this transgenic mouse and infection model, which restrict the ability to determine RELMα function in intestinal helminth infection. Impaired *Retnlb* gene expression could be due to disruption of certain *Retnlb* regulatory motifs by the genetic insertion of the LacZ gene and the antibiotic selection cassette in these transgenic mice. For these reasons, *Retnla*$^{tdt/tdT}$ mice, where the selection cassette was excised and replaced with a tdTomato reporter gene to enable tracking of RELMα-expressing cells, were used in this study. *Retnla*$^{tdt/tdT}$ mice had an equivalent level of RELMβ in the serum of *Retnla*$^{+/+}$ mice, validating that the *Retlna* deletion was specific (Fig 3A). Second, while *N.brasiliensis* provides a useful model to investigate lung tissue migratory parasites, it is a rat parasite and cannot establish chronic intestinal infections in mice. Thus, *Retnla*$^{tdT/tdT}$ and *Retnla*$^{+/+}$ mice were infected with *H. polygyrus*, which establishes chronic infections in BL/6 mice [4, 30]. For *H. polygyrus* infection, we chose both physiologic trickle infection regime [31] and single bolus infection. RELMα ELISA quantification of intestinal tissue and serum from naïve or day 21-infected mice showed that *H. polygyrus* infection induced significant local RELMα in WT mice (Figure 3B and C). Immunofluorescent staining of granulomas for RELMα revealed RELMα-positive cells in the outer areas of granulomas, with less staining in the

necrotic center (Figure 3D). However, there was no difference in egg and adult worm burden in the intestine between WT and KO mice (Figure 3E-G). These data suggest that RELMα is robustly expressed in granulomas in the infection site but has no effect on the parasite burden.

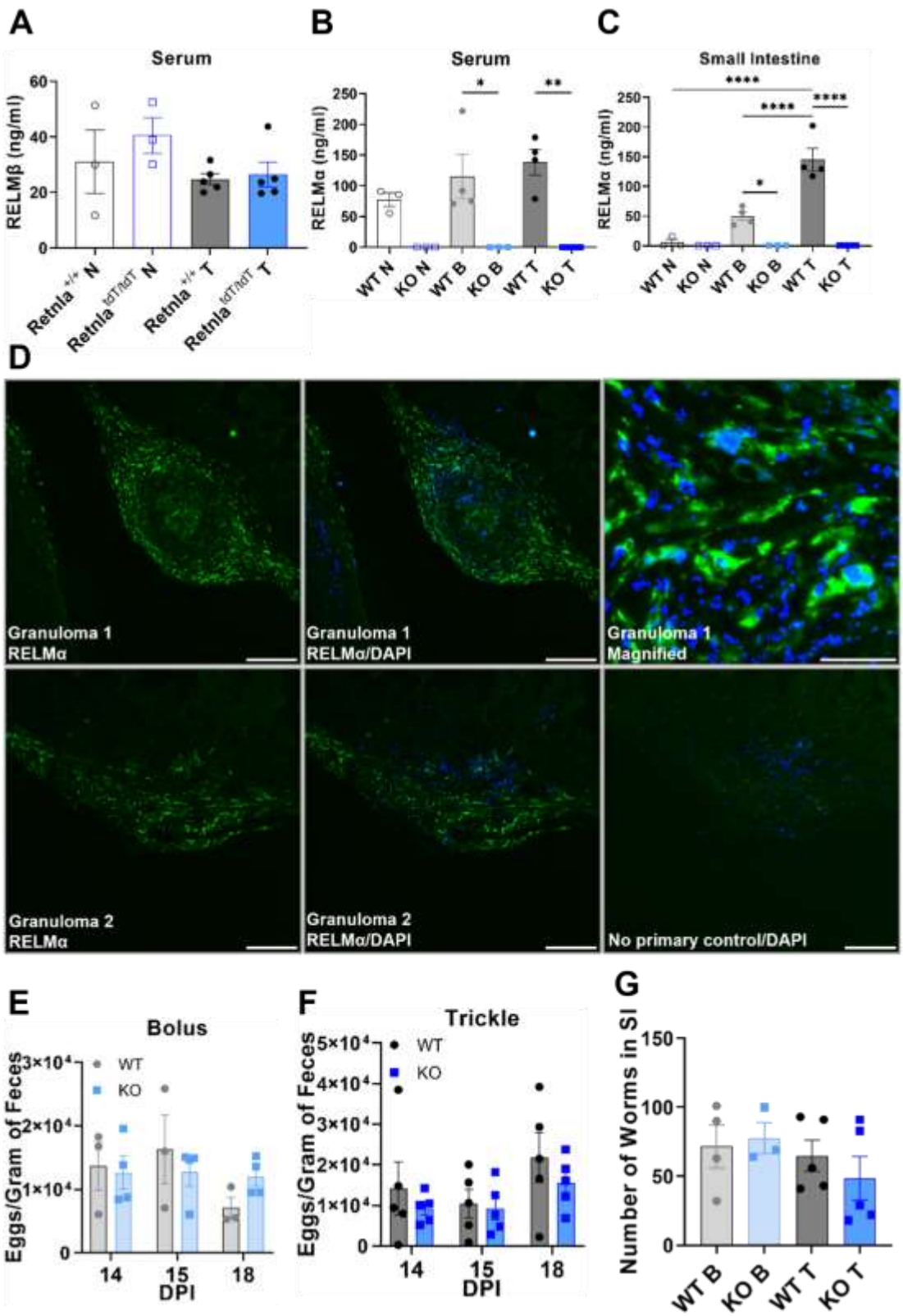
A
Serum
RELMβ (ng/ml)
Retnla +/+ N
Retnla tdT/tdT N
Retnla +/+ T
Retnla tdT/tdT T
B
Serum
RELMα (ng/ml)
WT N
KO N
WT B
KO B
WT T
KO T
C
Small Intestine
RELMα (ng/ml)
D
Granuloma 1 RELMα
Granuloma 1 RELMα/DAPI
Granuloma 1 Magnified
Granuloma 2 RELMα
Granuloma 2 RELMα/DAPI
No primary control/DAPI
E
Bolus
Eggs/Gram of Feces
WT
KO
DPI
F
Trickle
Eggs/Gram of Feces
G
Number of Worms in SI

Figure 3. *H. polygyrus* infection induces RELMα expression in granulomas in the small intestine but has no effect on the parasite burden. *Retnla*$^{+/+}$ (WT), *Retnla*$^{-/-}$, and *Retnla*$^{tdT/tdT}$ (KO) mice were injected with water (naive) or bolus or trickle-infected with *H. polygyrus* L3 (infected) and sacrificed at day 21 post-infection (DPI). (A) RELMβ in the serum was quantified by ELISA. (B and C) RELMα was measured by ELISA in the serum and small intestine (SI) homogenate. (D) RELMα in two representative granulomas from *H. polygyrus*-infected *Retnla*$^{+/tDT}$ mice at day 21 was imaged by immunofluorescence staining. (green: RELMα, blue: DAPI); Scale bar, 200μm; Magnified: 40μm. (E-G) Parasite burdens were quantified by egg counts in the feces, and adult worms in the small intestine. Representative data from 2-3 independent experiment (n = 3-5 per group) were presented as mean ± SEM.

RELMα promotes resolution of inflammation and tissue repair in H. polygyrus-induced granuloma.

When *H. polygyrus* L3 larvae reach to the small intestine, they migrate to the submucosal layer of the small intestine forming Th2-dependent granulomas [3]. Th2-induced granulomas are inflamed tissue where immune cells are accumulated around parasitic larvae or eggs, and they are collagen-rich [5]. In the previous study, RELMα expressed by macrophages polarized by IL-4 induces lysyl hydroxylase 2 (LH2), which plays an important role in pro-fibrotic collagen crosslinks [24]. Since granulomas are pathologic outcome of *H. polygyrus* infection, they were imaged by sectioning the small intestine and H&E staining. While trickle-infected WT and KO mice had similar size of granulomas, bolus-infected KO mice had bigger granulomas compared to WT mice (Figure 4A and B). At day 21 post-infection, inflammation was not completely resolved, and there were still opened lesion and remaining immune cells in the center of granulomas. Both trickle-infected WT and KO mice had wide open lesions because they were lastly infected at day 10 post-infection. Therefore, granuloma formed by larvae at day 10 post-infection had not enough time to resolve inflammation and repair damage. On the other hand, bolus-infected WT mice had smaller and denser granulomas compared to granulomas in KO mice that was more similar to granulomas in trickle-infected mice (Figure 4A and C). These data suggest that RELMα is required for resolving inflammation and wound healing in granulomas formed by *H. polygyrus* infection.

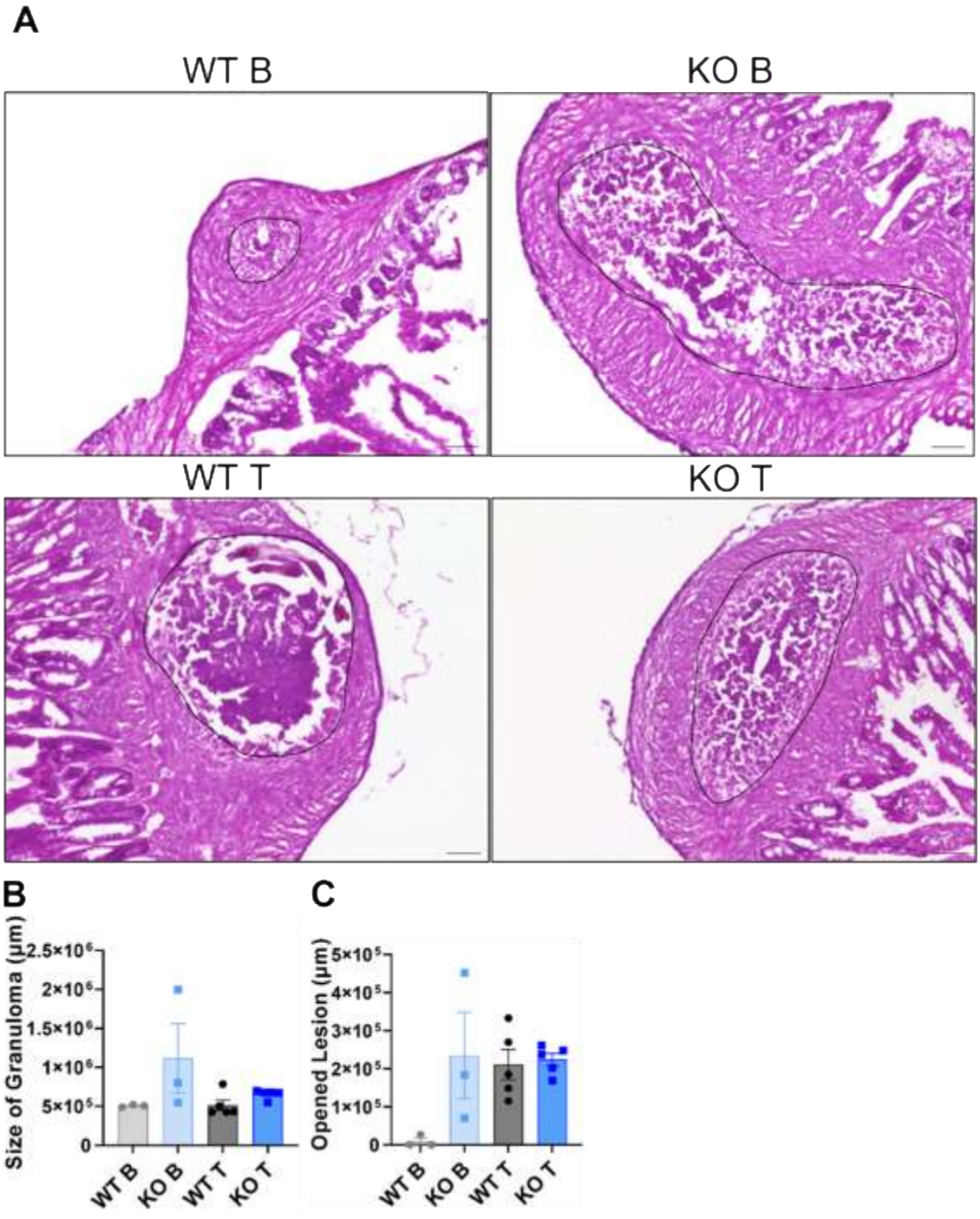
A
WT B
KO B
WT T
KO T
B
Size of Granuloma (µm)
2.5×10⁶
2×10⁶
1.5×10⁶
1×10⁶
5×10⁵
0
WT B
KO B
WT T
KO T
C
Opened Lesion (µm)
5×10⁵
4×10⁵
3×10⁵
2×10⁵
1×10⁵
0
WT B
KO B
WT T
KO T

Figure 4. RELMα promotes resolution of inflammation and tissue repair in *H. polygyrus*-induced granuloma. *Retnla*$^{+/+}$ (WT) *and Retnla*$^{tdT/tdT}$ (KO) mice were gavaged with water (naive) or bolus or trickle-infected with *H. polygyrus* L3 (infected) and sacrificed at day 21 post-infection (DPI). (A) Frozen small intestines were sectioned at 10μm and stained with H&E. (B and C) The entire granuloma size and opened lesion in the center of granuloma were measured by ImageJ. (Scale bar = 100μm) Representative data from 2-3 independent experiment (n = 3-5 per group) were presented as mean ± SEM.

RELMα upregulates migration of monocyte-derived macrophages and downregulates many DE genes in bolus granulomas.

The increased size and opened lesion of granulomas in bolus-infected KO mice suggest that RELMα regulates pathways involved in tissue healing and remodeling, therefore differential expression of genes associated with these pathways were investigated. There were 50 differentially expressed (DE) genes between bolus WT and KO granulomas whereas there was no DE gene between trickle WT and KO granulomas (Figure 5A and trickle data is not shown). In pathway analysis, cell migration and adhesion pathway were significantly more activated in WT granulomas compared to KO granulomas (Figure 5B). Interestingly, $MHCII^{+}F4/80^{lo}$ monocyte-derived peritoneal macrophage ontogeny, which is known to expressing RELMα robustly, were significantly lower in bolus KO granulomas compared to WT granulomas in digital cell quantification (Figure 5C). *Ldlr*, *Eif4ebp2*, *Lrp5*, and *Timp3*, which are important for regulation of inflammation, were upregulated in *H. polygyrus*-induced granulomas compared to naive tissue (Figure 5D). There was increased metabolism gene expression such as *Gk5*, *Sgpp1*, and *Hpgds* in KO naive tissue and granulomas than WT tissues, pointing to more active metabolism in KO mice. In KO granulomas, important genes for differentiation and maintenance of myeloid cells such as *Hnf1b* and *Gadd45b* were upregulated, indicating ongoing myeloid cell activation in KO granulomas. There were some DE genes with increased expression only in KO granulomas compared to naive tissue; Among these genes, *Enc1* is involved in lymphocyte activation, and *Arhgef28*, *Ptgdr*, and *CD276* are related to cell migration and adhesion. Interestingly, *Serpine1*,

which is known to inhibit wound healing and induce fibrosis [32-34], was more expressed in KO granulomas compared to WT granulomas. These data demonstrate that RELMα plays a key role in migration of monocyte-derived macrophages and regulation of many genes including an anti-wound healing gene, *Serpine1*.

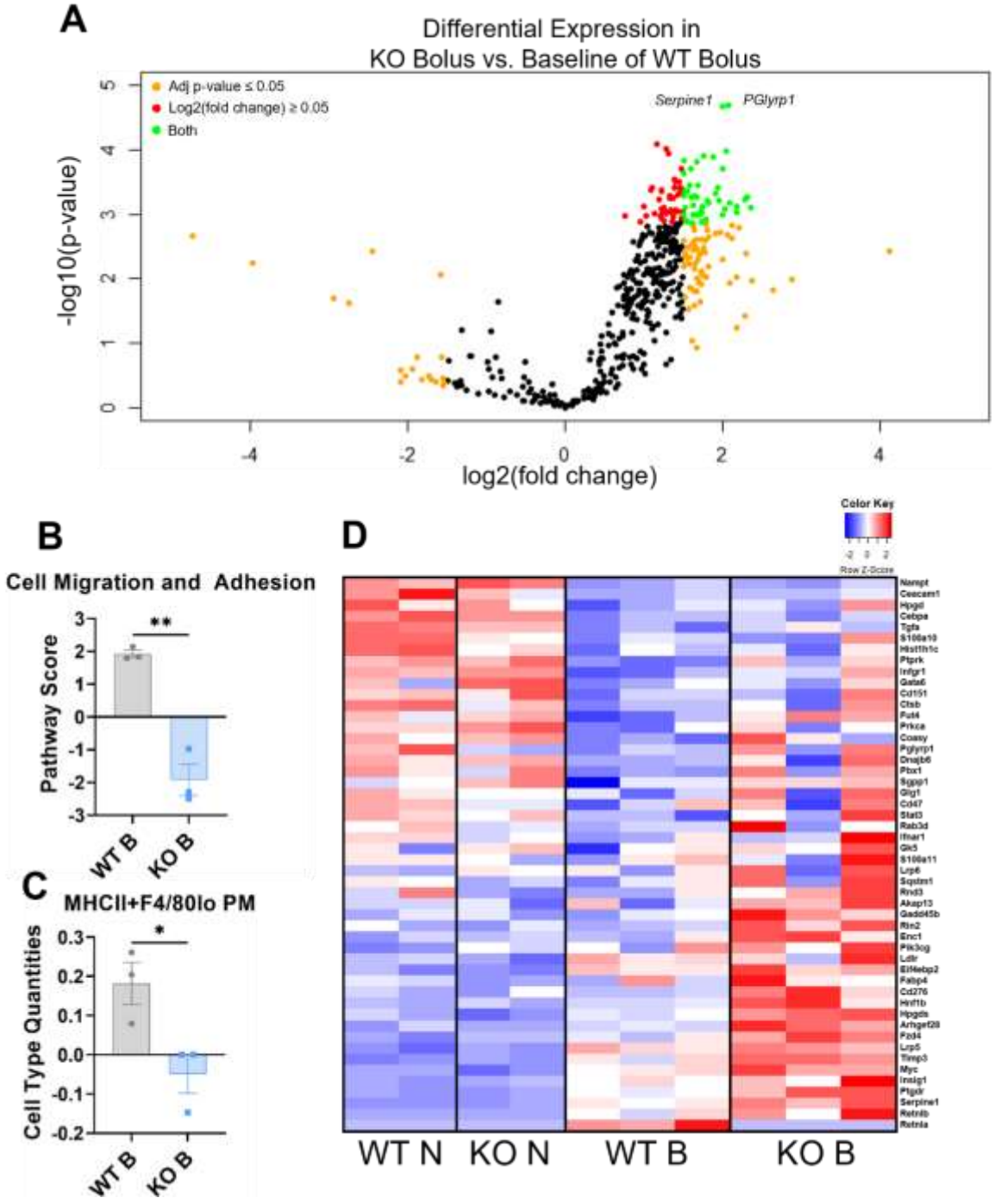
A
Differential Expression in
KO Bolus vs. Baseline of WT Bolus
Adj p-value ≤ 0.05
Log2(fold change) ≥ 0.05
Both
Serpine1
PGlyrp1
-log10(p-value)
log2(fold change)
B
Cell Migration and Adhesion
Pathway Score
**
WT B
KO B
C
MHCII+F4/80lo PM
Cell Type Quantities
*
WT B
KO B
D
Color Key
Row Z-Score
WT N
KO N
WT B
KO B

Figure 5. RELMα upregulates migration of monocyte-derived macrophages and downregulates many DE genes in bolus granulomas. *Retnla*$^{+/+}$ (WT) *and Retnla*$^{tdT/tdT}$ (KO) mice were injected with water (naive) or bolus or trickle-infected with *H. polygyrus* L3 (infected) and sacrificed at day 21 post-infection (DPI). RNA was extracted from isolated granulomas and used for Nanostring. (A) DE genes in KO granulomas with baseline of WT granulomas were shown on the volcano plot. (B) Cell migration and adhesion pathway score was calculated based on expression of genes in the pathway. (C) Immune cells in granuloma were quantified by Immquant (digital cell quantification). (D) DE genes (Adj $p \leq 0.05$, log2Fold≥ 1.5) were shown as a heatmap. Data (n = 2-4 per group) were presented as mean ± SEM.

RELMα expressed in the outer part regulates Serpine1 expression in opened lesion of granulomas.

After trapping and killing larvae, granulomatous tissue should be repaired and turned back to normal tissue to function properly. RELMα regulates a variety of genes involved in tissue repair such as *Plod2*, *Mmp9*, *Itgb1*, and *F11r*. Moreover, the most regulated gene, *Serpine1*, was shown to elevate inflammation and collagen-producing cells, delaying wound healing and inducing fibrosis in various inflammatory conditions [32-34]. Thus, Serpine1 expression was investigated in granulomas. While RELMα was expressed in the outer part of granulomas, Serpine1e was expressed in the center of granulomas where immune cells largely remained (Figure 6A). Interestingly, Serpine1 expression was more intense in the opened lesion in KO granulomas than in WT granulomas, suggesting that RELMα expressed in the outer granulomas regulates Serpine1 in the center and accelerate wound healing.

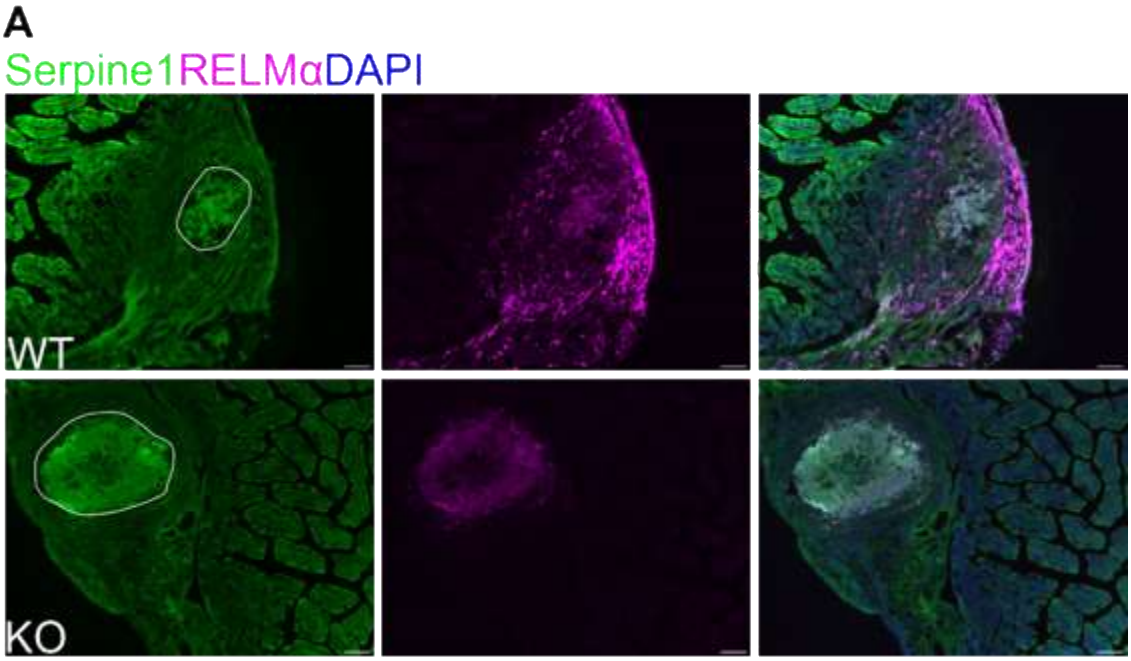

Figure 6. RELMα expressed in the outer part regulates Serpine1 expression in opened lesion of granulomas. *Retnla*$^{+/+}$ (WT) *and Retnla*$^{tdT/tdT}$ (KO) mice were injected with water (Naïve) or bolus or trickle-infected with *H. polygyrus* L3 (Inf) and sacrificed at day 21 post-infection (DPI). (A) Frozen small intestines were sectioned and incubated with fluorochrome-conjugated antibodies followed by imaging by a fluorescence microscope.

DISCUSSION

In this study, we identify a critical function for RELMα in limiting granulomatous immune responses in chronic intestinal helminth infection. In the absence of RELMα, mice were unable to limit infection-induced granuloma expansion or resolution. Helminth-induced granulomas are recognized as important host-protective structures to contain the parasite, but also contribute to the healing of the parasite-caused intestinal lesions (5). In *Retnla*$^{tdT/tdT}$ mice, there were granulomas larger than *Retnla*$^{+/+}$ granulomas. However, there was no significant difference in intestinal egg and worm burdens, suggesting that RELMα function is more focused on tissue repair rather than anti-helminthic immunity in the small intestine.

In Nanostring analysis, cell migration and adhesion pathway were more activated in KO granulomas than WT granulomas. Also, digital cell quantification of the granulomas from *Retnla*$^{+/+}$ or *Retnla*$^{tdT/tdT}$ mice suggested that *Retnla*$^{tdT/tdT}$ granulomas had more monocyte-derived peritoneal macrophage ontogeny, which is a heavy producer of RELMα. These data are in line with recently published paper that suggested RELMα as a marker for tissue-resident macrophages contributed by monocytes [35]. RELMα was shown to protect host by downregulating the Th2 immune response and activating tissue repair in another helminth infection, *Nippostrongylus brasiliensis* [18-20], which support tissue repair function of RELMα expressed in granulomas in this study. Moreover, RELMα functions as a chemotactic factor itself. RELMα recruits bone marrow-derived cells to the pulmonary vasculature and human mesenchymal stem cells [36-38]. Thus, it

is possible that RELMα expressed in granulomas recruited bone marrow-derived macrophages, but also stromal cells to repair damaged tissue.

Controversy on RELMα's function exists including reported pro-fibrotic versus tissue healing properties. Although RELMα's role in exacerbating fibrosis versus promoting tissue healing may appear counterintuitive, the processes of tissue repair and tissue fibrosis share overlapping mechanisms (37). It is likely that RELMα's effects on these protective and pathogenic processes are context-dependent and dictated by the tissue environment. Nanostring and immunofluorescence staining data suggests that RELMα inhibits fibrotic granuloma formation through regulating *Serpine1*. Serpine1 is highly expressed in keloid fibroblasts which is collagen-rich [32], and previous studies showed that Serpine1 delays wound healing and induces fibrosis in the skin and lung [33, 39]. RELMα-deficient mice exhibited both an impaired ability to resolve granulomas over time and increased granuloma size, which implicates a role for RELMα in regulating pro-fibrotic gene *Serpine1* for proper tissue healing to clear the chronic granuloma. In conclusion, a regulatory function of RELMα in the granulomatous intestinal tissue is demonstrated in this study. Here, RELMα performed functions to promote tissue healing and granuloma resolution by limiting pro-fibrotic gene *Serpine1*. Further investigation of this pathway could uncover wound healing pathways that could be exploited to improve tissue repair.

References

1. Gause, W.C., T.A. Wynn, and J.E. Allen, *Type 2 immunity and wound healing: evolutionary refinement of adaptive immunity by helminths.* Nat Rev Immunol, 2013. **13**(8): p. 607-14.

2. Yap, G.S. and W.C. Gause, *Helminth Infections Induce Tissue Tolerance Mitigating Immunopathology but Enhancing Microbial Pathogen Susceptibility.* Front Immunol, 2018. **9**: p. 2135.

3. Reynolds, L.A., K.J. Filbey, and R.M. Maizels, *Immunity to the model intestinal helminth parasite Heligmosomoides polygyrus.* Semin Immunopathol, 2012. **34**(6): p. 829-46.

4. Filbey, K.J., et al., *Innate and adaptive type 2 immune cell responses in genetically controlled resistance to intestinal helminth infection.* Immunol Cell Biol, 2014. **92**(5): p. 436-48.

5. Ariyaratne, A. and C.A.M. Finney, *Eosinophils and Macrophages within the Th2-Induced Granuloma: Balancing Killing and Healing in a Tight Space.* Infect Immun, 2019. **87**(10).

6. Anthony, R.M., et al., *Memory T(H)2 cells induce alternatively activated macrophages to mediate protection against nematode parasites.* Nat Med, 2006. **12**(8): p. 955-60.

7. Kim, S.Y. and M.G. Nair, *Macrophages in wound healing: activation and plasticity.* Immunol Cell Biol, 2019. **97**(3): p. 258-267.

8. Esser-von Bieren, J., et al., *Immune antibodies and helminth products drive CXCR2-dependent macrophage-myofibroblast crosstalk to promote intestinal repair.* PLoS Pathog, 2015. **11**(3): p. e1004778.

9. Esser-von Bieren, J., et al., *Antibody-mediated trapping of helminth larvae requires CD11b and Fcγ receptor I.* J Immunol, 2015. **194**(3): p. 1154-63.

10. Esser-von Bieren, J., et al., *Antibodies trap tissue migrating helminth larvae and prevent tissue damage by driving IL-4Rα-independent alternative differentiation of macrophages.* PLoS Pathog, 2013. **9**(11): p. e1003771.

11. Holcomb, I.N., et al., *FIZZ1, a novel cysteine-rich secreted protein associated with pulmonary inflammation, defines a new gene family.* EMBO J, 2000. **19**(15): p. 4046-55.

12. Pine, G.M., H.M. Batugedara, and M.G. Nair, *Here, there and everywhere: Resistin-like molecules in infection, inflammation, and metabolic disorders.* Cytokine, 2018. **110**: p. 442-451.

13. Jenkins, S.J., et al., *Local macrophage proliferation, rather than recruitment from the blood, is a signature of TH2 inflammation.* Science, 2011. **332**(6035): p. 1284-8.

14. Liu, T., et al., *The in vivo fibrotic role of FIZZ1 in pulmonary fibrosis.* PLoS One, 2014. **9**(2): p. e88362.

15. Lin, Q., et al., *RELMα Licenses Macrophages for Damage-Associated Molecular Pattern Activation to Instigate Pulmonary Vascular Remodeling.* J Immunol, 2019. **203**(11): p. 2862-2871.

16. Chen, G., et al., *Polarizing the T helper 17 response in Citrobacter rodentium infection via expression of resistin-like molecule α.* Gut Microbes, 2014. **5**(3): p. 363-8.

17. Munitz, A., et al., *Resistin-like molecule alpha enhances myeloid cell activation and promotes colitis.* J Allergy Clin Immunol, 2008. **122**(6): p. 1200-1207.e1.

18. Batugedara, H.M., et al., *Hematopoietic cell-derived RELMα regulates hookworm immunity through effects on macrophages.* J Leukoc Biol, 2018.

19. Krljanac, B., et al., *RELMα-expressing macrophages protect against fatal lung damage and reduce parasite burden during helminth infection.* Sci Immunol, 2019. **4**(35).

20. Sutherland, T.E., et al., *Ym1 induces RELMα and rescues IL-4Rα deficiency in lung repair during nematode infection.* PLoS Pathog, 2018. **14**(11): p. e1007423.

21. Chen, G., et al., *Comparison of RELMα and RELMβ Single- and Double-Gene-Deficient Mice Reveals that RELMα Expression Dictates Inflammation and Worm Expulsion in Hookworm Infection.* Infect Immun, 2016. **84**(4): p. 1100-1111.

22. Nair, M.G., et al., *Alternatively activated macrophage-derived RELM-{alpha} is a negative regulator of type 2 inflammation in the lung.* J Exp Med, 2009. **206**(4): p. 937-52.

23. Pesce, J.T., et al., *Retnla (relmalpha/fizz1) suppresses helminth-induced Th2-type immunity.* PLoS Pathog, 2009. **5**(4): p. e1000393.

24. Knipper, J.A., et al., *Interleukin-4 Receptor α Signaling in Myeloid Cells Controls Collagen Fibril Assembly in Skin Repair.* Immunity, 2015. **43**(4): p. 803-16.

25. Cook, P.C., et al., *Alternatively activated dendritic cells regulate CD4+ T-cell polarization in vitro and in vivo.* Proc Natl Acad Sci U S A, 2012. **109**(25): p. 9977-82.

26. Ferrer-Font, L., et al., *High-dimensional analysis of intestinal immune cells during helminth infection.* Elife, 2020. **9**.

27. Smith, K.A., et al., *Concerted IL-25R and IL-4Rα signaling drive innate type 2 effector immunity for optimal helminth expulsion.* Elife, 2018. **7**.

28. Tomfohr, J., J. Lu, and T.B. Kepler, *Pathway level analysis of gene expression using singular value decomposition.* BMC Bioinformatics, 2005. **6**: p. 225.

29. Frishberg, A., et al., *ImmQuant: a user-friendly tool for inferring immune cell-type composition from gene-expression data.* Bioinformatics, 2016. **32**(24): p. 3842-3843.

30. Behnke, J.M., et al., *Cellular and serological responses in resistant and susceptible mice exposed to repeated infection with Heligmosomoides polygyrus bakeri.* Parasite Immunol, 2003. **25**(6): p. 333-40.

31. Brailsford, T.J. and J.M. Behnke, *The dynamics of trickle infections with Heligmosomoides polygyrus in syngeneic strains of mice.* Int J Parasitol, 1992. **22**(3): p. 351-9.

32. Tuan, T.L., et al., *Increased plasminogen activator inhibitor-1 in keloid fibroblasts may account for their elevated collagen accumulation in fibrin gel cultures.* Am J Pathol, 2003. **162**(5): p. 1579-89.

33. Eitzman, D.T., et al., *Bleomycin-induced pulmonary fibrosis in transgenic mice that either lack or overexpress the murine plasminogen activator inhibitor-1 gene.* J Clin Invest, 1996. **97**(1): p. 232-7.

34. Rothlin, C.V., et al., *TAM receptor signaling in immune homeostasis.* Annu Rev Immunol, 2015. **33**: p. 355-91.

35. Sanin, D.E., et al., *A common framework of monocyte-derived macrophage activation.* Sci Immunol, 2022. **7**(70): p. eabl7482.

36. Su, Q., Y. Zhou, and R.A. Johns, *Bruton's tyrosine kinase (BTK) is a binding partner for hypoxia induced mitogenic factor (HIMF/FIZZ1) and mediates myeloid cell chemotaxis.* FASEB J, 2007. **21**(7): p. 1376-82.

37. Angelini, D.J., et al., *Hypoxia-induced mitogenic factor (HIMF/FIZZ1/RELM alpha) recruits bone marrow-derived cells to the murine pulmonary vasculature.* PLoS One, 2010. **5**(6): p. e11251.

38. Kolosova, I.A., et al., *Resistin-like molecule α stimulates proliferation of mesenchymal stem cells while maintaining their multipotency.* Stem Cells Dev, 2013. **22**(2): p. 239-47.

39. Chan, J.C., et al., *Accelerated skin wound healing in plasminogen activator inhibitor-1-deficient mice.* Am J Pathol, 2001. **159**(5): p. 1681-8.

CHAPTER Three – Choline Metabolism Promotes M2 Macrophage Polarization in Intestinal Infection With Helminth *Heligmosomoides polygyrus*

Sang Yong Kim[1], Peyman Ghorbani[2], Daniel Woo[3], Morgan D. Fullerton[2], Meera G. Nair[3]

[1]Department of Microbiology, University of California, Riverside, Riverside, CA, USA

[2]Department of Biochemistry, Microbiology, and Immunology, University of Ottawa, Ottawa, Canada

[3]Division of Biomedical Sciences, School of Medicine, University of California, Riverside, Riverside, CA, USA

Abstract

Choline is an essential nutrient, functioning as a precursor for membrane phospholipid. In previous studies, LPS-induced M1 polarization induced the expression of choline transporter CTL1 and choline uptake, which promoted proinflammatory cytokine production. However, whether choline metabolism regulates M2 macrophage polarization and Th2 cytokine production in vivo is unclear. In vitro, CTL1 protein expression was induced in M2 macrophages polarized by IL-4 as in M1 macrophages. To determine the function of choline metabolism in M2 polarization in vivo, mice were infected with *Heligmosomoides polygyrus* (*H. polygyrus*) or *Nippostrongylus brasiliensis* (*N. brasiliensis*), intraperitoneally injected with choline kinase α inhibitor, RSM932-A or vehicle, and sacrificed at day 17 and 6 post-infection, respectively. RSM-932A treatment impaired weight gain in *H. polygyrus*-infected mice. Within the peritoneal cavity of *H. polygyrus*-infected mice, macrophages, eosinophils and B-1 lymphocytes were depleted by RSM-932A treatment, while monocytes and neutrophils were increased. Flow cytometric and immunofluorescence characterization of macrophages implicated RSM-932A treatment in preventing transition from monocytes to macrophages and M2 macrophage polarization in *H. polygyrus*-infected mice. This involved a significant reduction in expression of RELMα and CD206 and conversely increased expression of CD86 and PD-L1. Also, RELMα level in the serum and peritoneal fluid was downregulated by RSM-932A treatment in *H. polygyrus*-infected mice. In *N. brasiliensis*-infected mice, RELMα expression was downregulated by RSM-932A without M2 macrophage polarization of alveolar macrophages. The impaired activation

of macrophages was associated with some loss in optimal immunity to *H. polygyurs* with increased parasite egg burden but no differences in intestinal worm count. This study suggests that choline metabolism is required for M2 macrophage polarization and an optimal immune response against intestinal helminth infection.

Introduction

Choline is an important biomolecule for the normal function of all cells [1] because it has many functions in cells. Choline acts as a source of methyl groups to make S-adenosylmethionine, a part of acetylcholine, and a component of phosphatidylcholine and sphingomyelin [2]. These molecules are required for epigenetic regulation, neuro signaling, and producing cell membrane, thus aberrant choline metabolism can cause improper cell functioning. Phosphatidylcholine is the most abundant phospholipid in eukaryotic cells, which is produced by the Kennedy pathway [3]. After choline is uptaken by choline transporters, choline is phosphorylated by choline kinases in an ATP-dependent manner to produce phosphatidylcholine and sphingomyelin. The choline kinases are found ubiquitously in eukaryotic cells [3, 4]. The rate of phosphatidylcholine synthesis can be affected by choline kinase activity [5-7]. Overexpression of choline kinase was involved in cell proliferation as DNA synthesis induced by growth factors requires phosphocholine as a secondary messenger [3]. However, the exact function of choline kinase alpha (ChoKα) in immune response has not been fully understood yet.

Depending on the type of immune response, metabolism in immune cells also changes, which greatly affects the efficiency of the immune response. The end products of the Kennedy pathway, phosphatidylcholine and sphingomyelin, are major components of the cell membrane, and aberrant regulation of this pathway will lead to abnormal immune responses. TRAF3 regulates B cell survival and expansion of the B cell compartment in secondary lymphoid organs [8]. In TRAF3-deficient mice, ChoKα expression was upregulated, increasing, phosphocholine and phosphatidylcholine

biosynthesis [9]. When ChoKα was pharmacologically inhibited, the prolonged survival of *Traf3*$^{-/-}$ B cells was decreased *in vitro* and *in vivo* [9]. Macrophages are also immune cells whose metabolism changes with activation, and vice versa. In M1 polarized bone marrow-derived macrophages (BMDMs) by LPS, choline transporter CTL1 expression was increased, inducing choline uptake and phosphatidylcholine [10, 11]. When CTL1 was inhibited by a pharmacological inhibitor or antibody, proinflammatory cytokines TNFα and IL-6 secretion was downregulated, but anti-inflammatory IL-10 secretion was increased in LPS-stimulated M1 BMDMs [10]. This altered cytokine secretion was involved in increased level of diacylglycerol and activation of protein kinase C. Choline uptake was also required for LPS-induced NLRP3 inflammasome activation and IL-1β production in BMDMs [11]. Inhibition of choline uptake and phosphorylation resulted in AMP-activated protein kinase (AMP), leading to mitophagy and termination of NLRP3 inflammasome activation [11].

Helminth infections polarize macrophages into M2 or alternatively activated macrophages (M2/AAMs), which express arginase-1, YM1, and RELMα [12-14]. M2 macrophages activated by Th2 cytokines such as IL-4 and IL-13 play a crucial role in protection against helminths [15]. M2 macrophages were accumulated around *H. polygyrus* larvae at 4 days post-infection and were required for a protective Th2 memory response [15]. Furthermore, proteins produced by M2 macrophage regulate immune response against helminth infection and tissue repair [16]. Arginase-1 catalyzes hydrolysis of arginine to urea and ornithine [17, 18]. Arginase-1 mediated parasite trapping and helminth killing both in *H. polygyrus* and *N. brasiliensis* infection [19-21].

Proteins derived from M2 macrophages are also functionally linked to each other. YM1 expressed during the innate phase of *N. brasiliensis* infection promoted Th2 cytokine production, but the one expressed during the adaptive phase inhibited the production of these cytokines [22]. YM1 in the adaptive phase induced lung repair following helminth infection by upregulating RELMα expression. RELMα was identified as a master regulator of Th2 immune response in *N. brasiliensis* infection [23-25]. Hematopoietic cell-derived RELMα and RELMα-expressing lung interstitial macrophages dampen Th2 immune response and protect the host from fatal lung damage. However, the mechanism by which M2 macrophage polarization and proteins are regulated has not been fully understood. In this study, mouse helminth infection models, *H. polygyrus* and *N. brasiliensis*, were employed to induce M2 polarization of macrophages in the peritoneal cavity and lung. When helminth-infected mice were injected with ChKα inhibitor, RSM-932A, M2 polarization was impaired and RELMα expression was decreased both in the peritoneal cavity and lung. This study demonstrates the importance of choline metabolism in the M2 polarization of macrophages and the requirement of proper metabolism for optimal immune response to mouse helminth infections.

Materials and Methods

Mice

6 to 7 weeks old female C57BL6/J mice were purchased from the Jackson Laboratory (Bar Harbor, ME) and housed five per cage under an ambient temperature with a 12-hour light/12 hours dark cycle. All animal procedures were approved by the UCR Institutional Animal Care and Use Committee (protocol A-20210017).

Heligomosomoides polygyrus and *Nippostrongylus brasiliensis*

Hp and Nb life cycle was maintained in mice as previously described.1,2 Mice were infected with 200 Hp L3 stage larvae or injected with PBS (naive group) through oral gavage. Mice were infected with 500 Nb L3 stage larvae or injected with PBS (naive group) through subcutaneous injection. Egg burden was measured at indicated day post-infection by counting eggs in feces with Mcmaster slide. To enumerate L5 stage Hp, the small intestines of infected mice were cut longitudinally, and larvae were isolated by fine forceps. Nb larvae were isolated after incubating the intestine in PBS for ≥ 2 hours at 37°C. Isolated larvae were counted on the petri dish with grids under the dissection microscope.

RSM-932A

RSM-932A (Cayman Chemical, Ann Arbor, MI) was reconstituted 30mg/ml in DMSO. For in vivo injection, RSM-932A was further diluted with DMSO and PBS to 1.5mg/ml. Mice were injected with 3mg/kg of RSM-932A or 40% DMSO in PBS (vehicle group) through intraperitoneal injection.

Flow Cytometry

Peritoneal exudate cells (PEC) were recovered in a total of 5 mL of ice-cold PBS. Cells were blocked with 0.6 µg Rat IgG and 0.6 µg anti-CD16/32 (93) for 5 min and stained for 30 min with antibodies to Ly6G (1A8), CD3e (145-2C11), PD-L1 (MIH6), CD86 (GL-1), CD4 (RM4-5), MERTK (2B10C42), CD301b (LOM-14), PD-L2 (TY25), CD5 (53-7.3), Ly6C (HK1.4), MHCII (M5/114.15.2) (BioLegend, San Diego, CA); CD8 (3B5), CD11b (M1/70) (Invitrogen, Waltham, MA); SiglecF (E50-2440) (BD Bioscience, San Jose, CA); CD206 (MR5D3) (BioRad, Hercules, CA). Cells were then washed and analyzed on a Novocyte (ACEA Biosciences, San Diego, CA) followed by data analysis using FlowJo v10.8.1 (Tree Star Inc.; Ashland, OR).

Immunofluorescence staining

Intestinal tissue was stored overnight in 4% PFA at 4°C. After 24 hours, tissue was removed from 4% PFA and incubated for 24 hours in 30% sucrose. Intestines were blocked in OCT and sectioned at 10µm. Tissue sections were incubated with polyclonal rabbit anti-CD86 (ThermoFisher, Waltham, MA), APC-conjugated anti-RELMα (DS8RELM) (Invitrogen, Waltham, MA), and biotinylated anti-CD206 (C068C2) (BioLegend, San Diego, CA) antibodies overnight at 4°C. Tissue sections were then incubated with Cy3-conjugated goat anti-rabbit antibodies (Abcam, Waltham, MA) and Cy2-conjugated streptavidin (Jackson ImmunoResearhch, West Grove, PA) for 2 hours at 4°C and mounted with VECTASHEILD HardSet Antifade Mounting Medium (Vector Laboratories,

Newark, CA) followed by imaging with BZ-X800 microscope (Keyence, Itasca, IL). Positive cells were counted by QuPath 0.3.2 software.

RELMα ELISA

Anti-RELMα capture and biotinylated detection antibodies were used according to previously described protocol.3

Statistical analysis

Data are presented as mean ± SEM and statistical analysis was performed by Graphpad Prism 9 software. Data was assessed by the unpaired student t-test, one-way ANOVA followed by post-hoc Tukey's test for multiple comparison. Data collected over several timepoints was analyzed by two-way ANOVA with post-Sidak multiple test was performed. (*, $P \leq 0.05$; **, $P \leq 0.01$; ***, $P \leq 0.001$; ****, $P \leq 0.0001$) Experiments with primary infection were repeated 3 times with n=3-5 per group for each experiment, and experiments with secondary and Nb infection were done one time.

Results

Choline phosphorylation is required for M2 macrophage polarization and B cell responses in intestinal helminth infection.

The importance of choline phosphorylation in in vivo M2 macrophage polarization was evaluated by infection with *Heligmosomoides polygyrus* (*H. polygyrus*), a parasitic nematode that colonizes the small intestine of mice and drives protective M2 macrophage responses.4 Mice were orally infected with *H. polygyrus* larvae and left for 8 days to allow parasite development to adults within the intestinal lumen, followed by treatment with RSM-932A or vehicle every two days. As control for infection, naïve mice were also treated with RSM-932A. RSM-932A treatment significantly decreased weight gain in *H. polygyrus*-infected mice, but this was not infection-specific since naïve mice also suffered from decreased weight gain in response to RSM-932A (Figure 7A and B). These findings are consistent with a previous study which reported that choline supply is required for weight gain.5 Intestinal *H. polygyrus* infection induces significant peritoneal cavity inflammation and M2 macrophage responses,6 therefore the effect of RSM-932A was examined by flow cytometric analysis of the peritoneal cavity cells at day 17 post-infection. *H. polygyrus* infection caused more than 10-fold increase in peritoneal cells compared to naïve mice, but there was no significant difference between vehicle and RSM-932A naïve nor injected groups (Fig 7C and D). Next, the effect of RSM-932A treatment on the immune cell population composition was examined by flow cytometry (Figure 3A). t-SNE plot analysis revealed striking effects of RSM-932A treatment on immune cell composition that were more pronounced in *H. polygyrus*

infection (Figure 7E). There was a significant drop in eosinophils and B-1 cells in RSM-932A-treated mice, while there was an induction in monocytes and neutrophils, both by frequency and total cell numbers (Figure 7E-G). Peritoneal macrophages were also decreased by RSM-932A in the peritoneal cavity of both naive and infected mice (Fig 8A and B). Macrophage polarization was examined by surface expression of M2 marker CD206 and M1 marker CD86 and PDL1 (Figure 8C and D). Compared to vehicle treated mice, M2 macrophage surface marker CD206 was significantly decreased with RSM-932A treatment, while M1 macrophage markers CD86 and PD-L1 were increased, supporting the suppressive effect of RSM-932A on M2 macrophage polarization in vitro. RELMα expression has been shown to be upregulated in M2 polarized macrophages in various type 2 immune response models.7-9 Moreover, RELMα gene was the most downregulated gene by choline kinase inhibition in vitro, thus RELMα expression level was quantified in the serum and peritoneal fluid by ELISA (Figure 8E and F). *H. polygyrus* infection increased RELMα levels in the serum and peritoneal fluid, but this was significantly decreased with RSM-932A treatment (Figure 8E and F). M2 macrophage responses was further examined at the infection site by immunofluorescent staining of intestinal tissue, which revealed decreased CD206+ and RELMα+ cells following RSM-932A treatment (Figure 8G and H). M2-polarized macrophages have been shown to play an important role in reducing helminth parasite burden,10,11 however, there were no significant differences in egg and worm burden (Figure 8I). The chronic effects of RSM-932A treatment were also examined in a vaccination model for Hp involving secondary infection with Hp, where M2 macrophages are critical for

protection12 In this chronic model, RSM-932A treatment induced significantly increased monocyte and neutrophil responses and decreased B1 cell responses (Figure 9B). Additionally, RSM-932A treatment led to a switch in macrophage polarization phenotype with increased CD86 surface expression and decreased expression of CD206 and RELMα, in both the peritoneum and intestine (Figure 9C-F). This deficiency in M2 macrophage polarization was associated with a significant but short-lived effect on parasite fecundity, with increased egg burdens at week 10 post-infection, but no significant differences in intestinal worm burdens (Figure 9G). To determine if choline kinase signaling had broader impacts in other helminth infections, the effect of RSM-932A treatment was examined in infection with *Nippostrongylus brasiliensis*, a natural rodent parasite the acutely infects the lung and small intestine, and drives M2 macrophage polarization and RELMα expression3,9 RSM-932A treatment inhibited weight gain but had no significant effects on bronchio-alveolar macrophage responses nor parasite burden (Figure 10E). However, immunofluorescent staining of the naïve and infected lungs revealed that *Nippostrongylus brasiliensis* induced RELMα expression in the lung airway epithelial cells and parenchyma, however, this was abrogated with RSM-932A treatment, while more CD86 expression was observed (Figure 10F). These data suggest that the effect of choline kinase signaling in promoting RELMα expression is applicable in many helminth infection settings. Overall, these data confirm a role for choline kinase signaling in shaping the immune cell response in intestinal helminth infection including promoting M2 macrophage polarization and RELMα expression without impacting parasite burden.

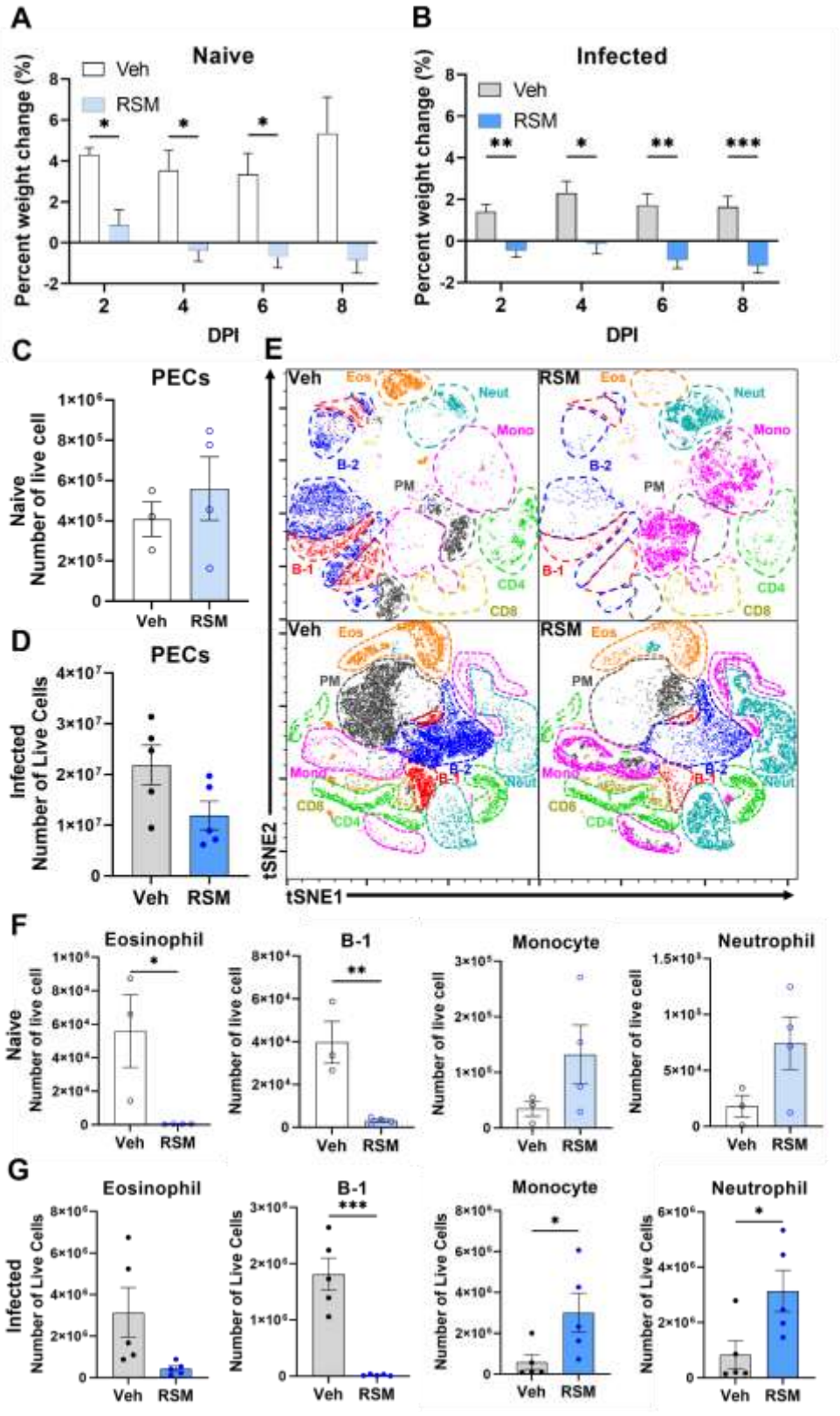
A
Naive
Veh
RSM
Percent weight change (%)
DPI
B
Infected
Veh
RSM
Percent weight change (%)
DPI
C
PECs
Naive
Number of live cell
Veh
RSM
D
PECs
Infected
Number of Live Cells
Veh
RSM
E
Veh
RSM
Eos
Neut
Mono
B-2
PM
B-1
CD4
CD8
tSNE2
tSNE1
F
Eosinophil
B-1
Monocyte
Neutrophil
Naive
Number of live cell
Veh
RSM
G
Eosinophil
B-1
Monocyte
Neutrophil
Infected
Number of Live Cells
Veh
RSM

Figure 7. RSM-932A treatment inhibits weight gain and changes overall immune cell populations in intestinal helminth infection. C57BL6/J mice were infected with 200 *H. polygyrus* L3 larvae through oral gavage and intraperitoneally injected with vehicle or RSM-932A every 2 days from day 8 followed by sacrifice at day 17 post-infection. (A-B) Weight change compared to weight before vehicle or RSM-932A injection was calculated at multiple time points after vehicle and RSM-932A injection. (C-D) Total cells in peritoneal exudate fluid were enumerated. (E) Immune cells in the peritoneal exudate fluid were plotted in the tSNE plots. (F-G) The number of eosinophils, B-1 cells, monocytes, and neutrophils was determined by flow cytometry. Values represent means ± SEM (n = 3 - 5 mice per group), and representative data from 3 independent experiments was presented. Two-way ANOVA with post-Sidak multiple comparison test and student t-test were performed, and P values less than 0.05 were considered statistically significant. (*, $P \leq 0.05$; **, $P \leq 0.01$; ***, $P \leq 0.001$; ****, $P \leq 0.0001$)

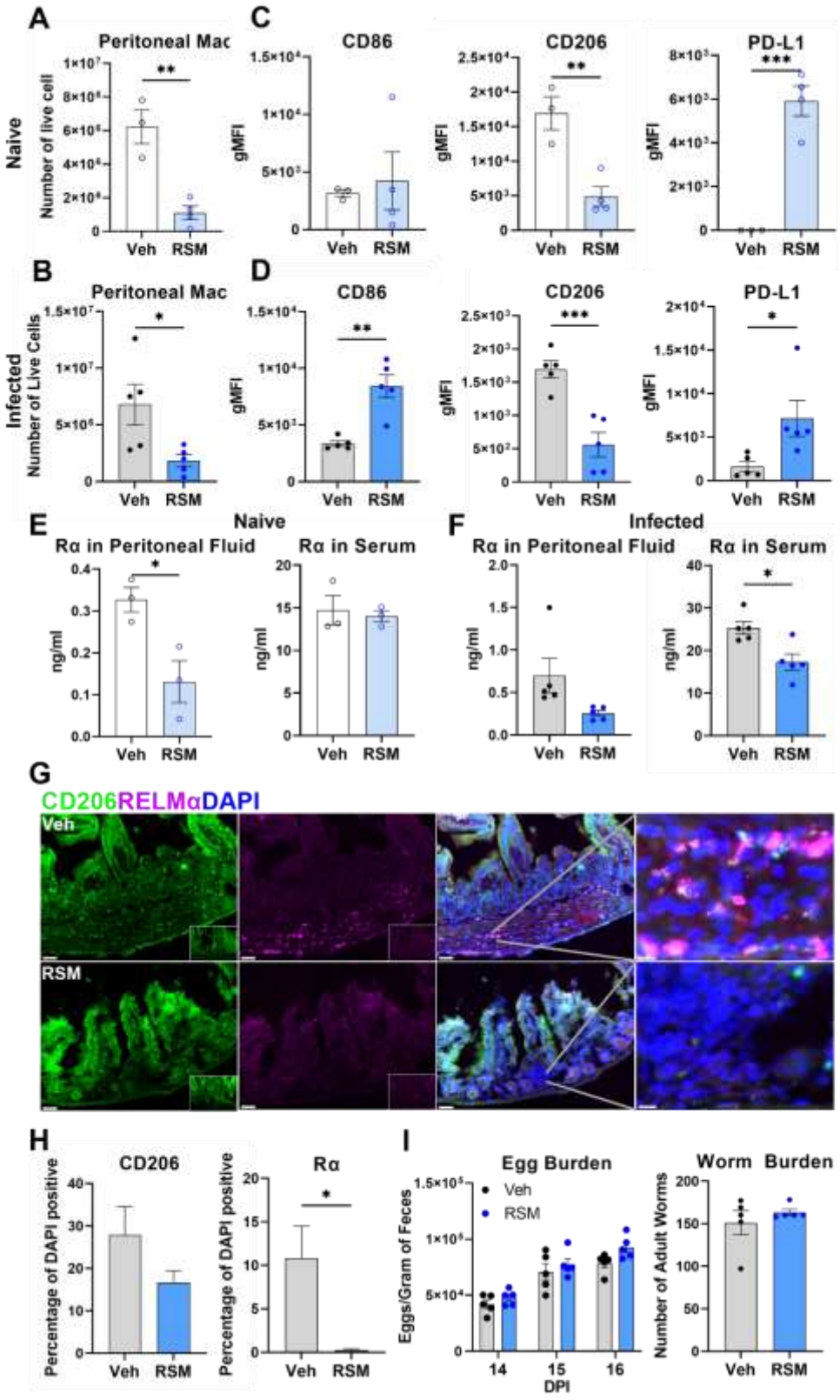
A
Peritoneal Mac
Naive
Number of live cell
Veh
RSM
C
CD86
CD206
PD-L1
gMFI
B
Peritoneal Mac
Infected
Number of Live Cells
D
CD86
CD206
PD-L1
E
Naive
Rα in Peritoneal Fluid
Rα in Serum
ng/ml
F
Infected
G
CD206RELMαDAPI
Veh
RSM
H
CD206
Rα
Percentage of DAPI positive
I
Egg Burden
Eggs/Gram of Feces
DPI
Worm Burden
Number of Adult Worms

Figure 8. RSM-932A inhibits M2 macrophage polarization in the peritoneal cavity and intestine in intestinal helminth infection. C57BL6/J mice were intraperitoneally injected with vehicle or RSM-932A every 2 days from day 0 to day 8 followed by sacrifice at day 9 post-injection. (A-B) Peritoneal macrophage number was determined by flow cytometry. (C-D) The geometric mean fluorescent intensity of CD86, CD206, and PD-L1 in peritoneal macrophages was evaluated by flow cytometry. (E and F) The concentration of RELMα in the serum and peritoneal fluid were measured by ELISA. (G and H) (G) CD206 and RELMα positive cells in the small intestine were imaged by a fluorescent microscope and (H) counted. (scale bar = 50um) Images of the small intestine from naive mice are presented in insets. (I) Eggs in feces were counted at multiple time points after infection, and adult worms were isolated from the small intestine and enumerated on the day of sacrifice. Values represent means ± SEM (n = 3 - 5 mice per group), and representative data from 3 independent experiments was presented. Two-way ANOVA with post-Sidak multiple comparison test and student t-test were performed, and P values less than 0.05 were considered statistically significant. (*, $P \leq 0.05$; **, $P \leq 0.01$; ***, $P \leq 0.001$; ****, $P \leq 0.0001$)

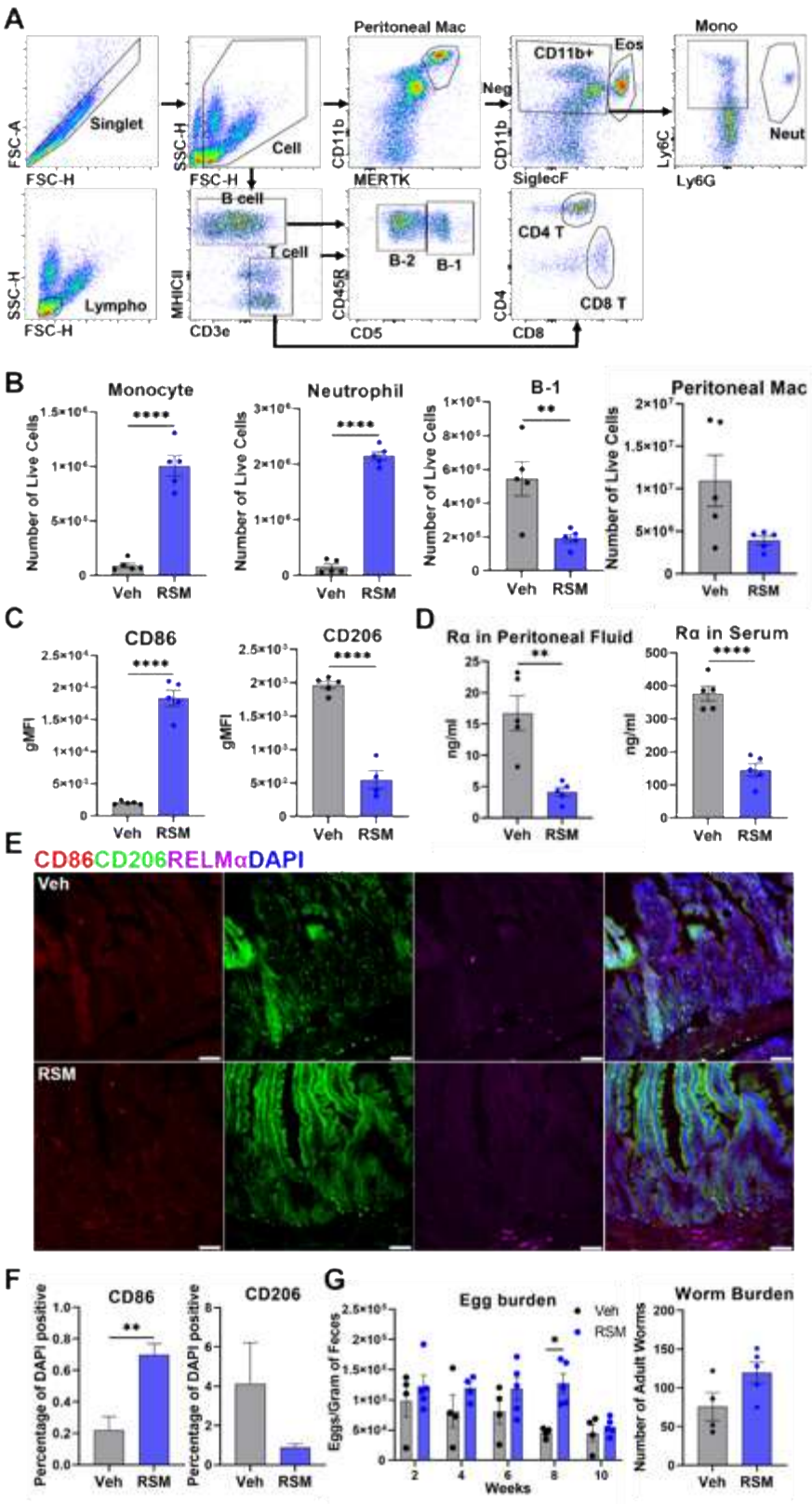
A
Singlet
FSC-A
FSC-H
Cell
SSC-H
FSC-H
Peritoneal Mac
CD11b
MERTK
Neg
CD11b+
Eos
CD11b
SiglecF
Mono
Ly6C
Neut
Ly6G
Lympho
SSC-H
FSC-H
B cell
T cell
MHCII
CD3e
B-2
B-1
CD45R
CD5
CD4 T
CD8 T
CD4
CD8
B
Monocyte
Neutrophil
B-1
Peritoneal Mac
Number of Live Cells
Veh
RSM
C
CD86
CD206
gMFI
D
Rα in Peritoneal Fluid
Rα in Serum
ng/ml
E
CD86CD206RELMαDAPI
Veh
RSM
F
CD86
CD206
Percentage of DAPI positive
G
Egg burden
Eggs/Gram of Feces
Weeks
Worm Burden
Number of Adult Worms

Figure 9. RSM-932A reduces M2 polarization of peritoneal macrophages and has a modest effect on parasite burden in secondary intestinal helminth infection.

C57BL6/J mice were infected with 200 *H.poly* L3 larvae through oral gavage and intraperitoneally injected with vehicle or RSM-932A every 2 days from day 2 post-infection during the entire experiment. Mice were treated with an anti-helminthic drug at day 25 post-infection and challenge infected at day 42 post-infection followed by sacrifice at day 52 post-infection. For a long-term challenge infection, mice were infected with 200 L3 larvae and injected with vehicle or RSM-932A two or three times per week during the entire experiment. Then, mice were treated with an anti-helminthic drug at day 93 post-infection and challenge infected at day 107 post-infection followed by sacrifice at day 117 post-infection. (A) Gating strategy of peritoneal exudate cells (B) The number of monocytes, neutrophils, B-1 cells, and peritoneal macrophages was determined by flow cytometry. (C) The geometric mean fluorescent intensity of CD86 and CD206 in peritoneal macrophages was evaluated by flow cytometry. (D) The concentration of RELMα in the serum and peritoneal fluid were measured by ELISA. (E-F) (E) CD86, CD206, and RELMα positive cells in the small intestine were imaged by a fluorescent microscope and (F) counted. (G) Eggs in feces were counted at multiple time points after infection, and adult worms were isolated from the small intestine and enumerated on the day of sacrifice. Values represent means ± SEM (n = 4 - 5 mice per group), and data from a single experiment was presented. Two-way ANOVA with post-Sidak multiple comparison test and student t-test were performed, and P values less than 0.05 were

considered statistically significant. (*, $P \leq 0.05$; **, $P \leq 0.01$; ***, $P \leq 0.001$; ****, $P \leq 0.0001$)

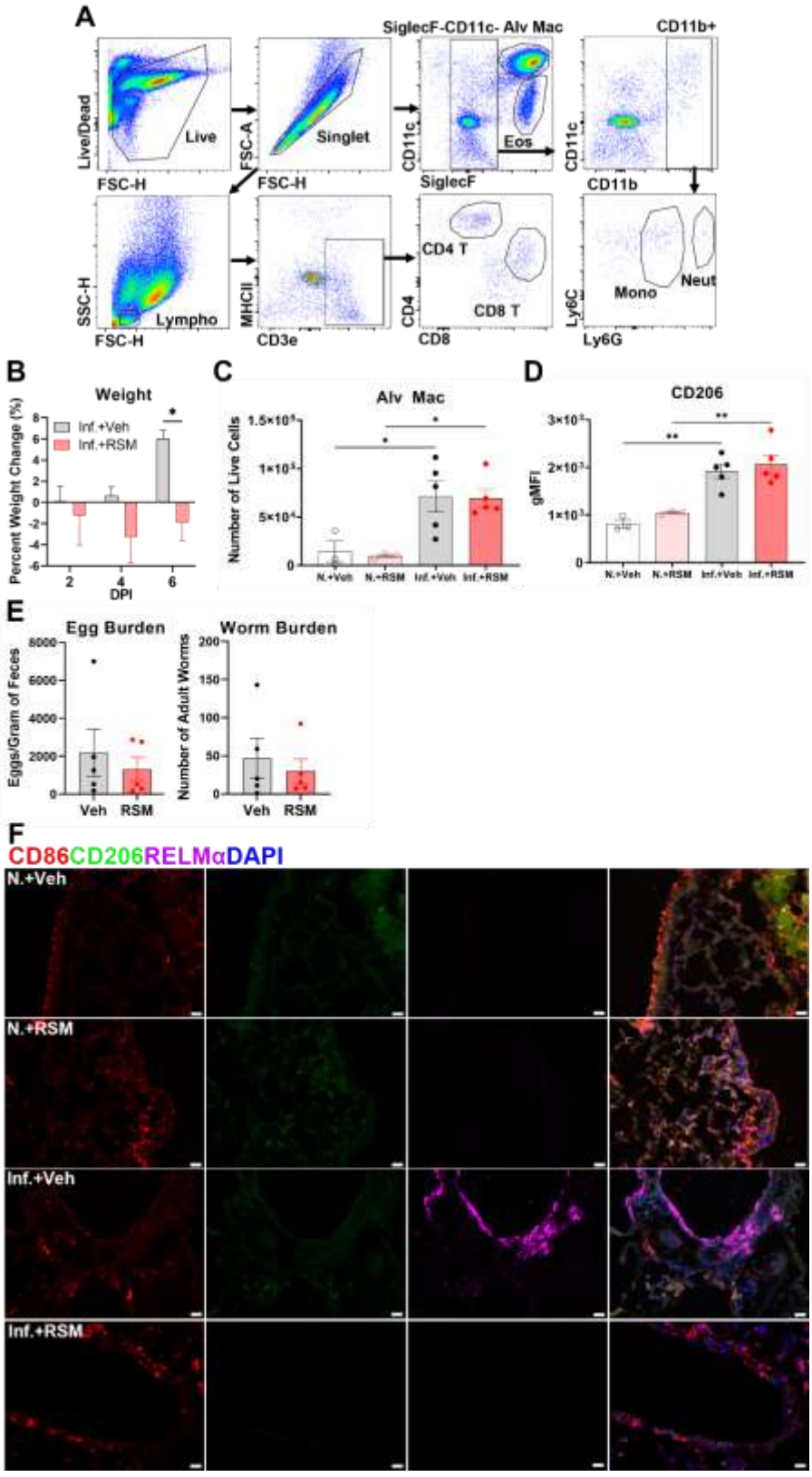
A
SiglecF-CD11c- Alv Mac
CD11b+
Live/Dead
Live
FSC-A
Singlet
CD11c
Eos
SiglecF
CD11c
CD11b
FSC-H
FSC-H
SSC-H
Lympho
FSC-H
MHCII
CD3e
CD4 T
CD8 T
CD4
CD8
Ly6C
Mono
Neut
Ly6G
B
Weight
Inf.+Veh
Inf.+RSM
Percent Weight Change (%)
DPI
C
Alv Mac
Number of Live Cells
N.+Veh
N.+RSM
Inf.+Veh
Inf.+RSM
D
CD206
gMFI
E
Egg Burden
Eggs/Gram of Feces
Veh
RSM
Worm Burden
Number of Adult Worms
F
CD86CD206RELMαDAPI
N.+Veh
N.+RSM
Inf.+Veh
Inf.+RSM

Figure 10. Intraperitoneal injection of RSM-932A has no effect on lung M2 macrophage polarization or parasite burden in infection with rodent hookworm *Nippostrongylus brasiliensis*. C57BL6/J mice were infected with 500 *N.brasiliensis* L3 larvae subcutaneously and intraperitoneally injected with vehicle or RSM-932A every 2 days from day 0 followed by sacrifice at day 6 post-infection. (A) Gating strategy of bronchio-alveolar lavage fluid cells (B) Weight change compared to weight before vehicle or RSM-932A injection was calculated at multiple time points after injection. (C) The number of alveolar macrophages was determined by flow cytometry. (D) The geometric mean fluorescent intensity of CD206 in alveolar macrophages was measured by flow cytometry. (E) Eggs in feces and adult worms in the small intestine were enumerated at 6 days post-infection. (F) CD86, CD206, and RELMα positive cells were imaged by a fluorescent microscope. Values represent means ± SEM (n = 3-5 mice per group), and data from a single experiment was presented. Two-way ANOVA with post-Sidak multiple comparison test, one-way ANOVA post-Tukey test, and student t-test were performed, and P values less than 0.05 were considered statistically significant. (*, $P \leq 0.05$; **, $P \leq 0.01$; ***, $P \leq 0.001$; ****, $P \leq 0.0001$)

Discussion

In this study, the function of choline metabolism in M2 macrophage polarization in helminth infection was investigated. Many people in underdeveloped countries are afflicted with helminth infections due to poor sanitation and hygiene. Even if anti-helminthic drugs are available, this is still insufficient to eradicate helminth infections in this area because of the development of anti-helminthic drug resistance and evasion of host immune response by worms. Moreover, many people have poor nutritional status in these countries, which results in a metabolic change. Thus, how changes in metabolism affect the immune response against helminths must be studied to develop an appropriate treatment for people living in the endemic area. Choline is a precursor of the substances that make up the cell membrane and is produced in small amounts in the body, so the rest of the essential intake should be supplemented by food. In the previous study, Choline deficiency inhibited weight gain and improved glucose tolerance in genetically-induced obese mice [26]. In Figure 7, weight gain was significantly decreased when ChKα was inhibited by RSM-932A in both naive and *H. polygyrus*-infected mice, indicating that an intact Kennedy pathway is required for weight gain.

Type 2 immune activation by helminth infections induces alternative activation and a metabolic change of macrophages that are required for parasite trapping or tissue repair [27]. Whereas choline uptake and metabolism were shown to be required for proinflammatory response in LPS-induced M1 macrophages [10, 11], the function of choline metabolism has not been well characterized in M2 macrophages. *H. polygyrus* infection induces proliferation and M2 polarization of macrophages, and eosinophilia in

the peritoneal cavity [28, 29]. Repeated peritoneal injection of RSM-932A decreased macrophages, eosinophils, and B-1 cells but increased monocytes and neutrophils in *H. polygyrus*-infected mice. RSM-932A had a direct effect on BMDMs [10, 11], but it should be determined if these changes originated from the effect of RSM-932A on T cell activation despite no significant differences in CD8 and CD4-positive T cell numbers. Since M2 polarization induces the proliferation of macrophages, there must be more cell membrane synthesis. The inhibition of phosphatidylcholine and sphingomyelin production by RSM-932A probably contributed to less peritoneal macrophage proliferation in mice. RELMα expression is a trademark of M2 macrophages and was recently identified as a marker for monocyte-derived tissue-resident macrophages [14, 30]. These studies support a lower level of RELMα in RSM-932A-injected mice, reflecting lower M2 macrophage numbers but higher monocyte numbers in the peritoneal cavity. It is possible that choline metabolism mediates macrophage derivation from monocytes before peritoneal macrophages undergo M2 polarization. RSM-932A downregulated M2 polarization of macrophage also in the small intestine of *H. polygyrus*-infected mice, but interestingly, there was no significant difference in parasite burden between vehicle and RSM-932A-injected mice. *H. polygyrus* larvae reside in the small intestine, and the immune response is robustly activated in the submucosal layer. However, it is difficult to deliver the drug directly and efficiently into the small intestine, so RSM-932A was delivered through intraperitoneal injection. Inhibition of M2 macrophage polarization by peritoneal RSM-932A was probably not enough to completely limit the Th2 immune response against *H. polygyrus*. Therefore, it should be

determined how much RSM-932A is translocated into the small intestine and affects the immune response against *H. polygyrus* in the small intestine after peritoneal injection. Another function of M2 macrophages is arising memory Th2 immune response against secondary *H. polygyrus* infection [15]. Long-term RSM-932A injection made the changes in peritoneal immune cell populations and downregulation of M2 macrophage polarization more pronounced and increased the parasite burden after secondary infection. This indicates that RSM-932A has a greater effect on the function of M2 macrophage in the adaptive immune response than in the innate immune response against *H. polygyrus*.

Lastly, mice were infected with *N. brasiliensis*, which has the lung phase, to demonstrate the importance of choline metabolism in the M2 polarization of lung macrophages. Intraperitoneal injection of RSM-932A had no effect on immune cell populations, M2 macrophage polarization, and parasite burden in the lung, which was also caused by inefficient delivery. Thus, intratracheal or intranasal injection of RSM-932A probably will have more drastic effects on the immune response against *N. brasiliensis*. However, RELMα expression was suppressed by RSM-932A in the lung of *N. brasiliensis*-infected mice despite of low efficiency of delivery, indicating that RSM-932A regulates more specifically RELMα expression rather than M2 macrophage polarization in the lung.

Collectively, this chapter demonstrates that ChKα activity is required for M2 polarization of macrophages and appropriate immune response against intestinal helminth. Signaling pathways and mechanisms through which choline metabolism

regulates M2 macrophage polarization and RELMα expression should be investigated in future studies.

References

1. Zeisel, S.H. and K.A. da Costa, *Choline: an essential nutrient for public health.* Nutr Rev, 2009. **67**(11): p. 615-23.

2. Zeisel, S.H., *Choline: critical role during fetal development and dietary requirements in adults.* Annu Rev Nutr, 2006. **26**: p. 229-50.

3. Gibellini, F. and T.K. Smith, *The Kennedy pathway--De novo synthesis of phosphatidylethanolamine and phosphatidylcholine.* IUBMB Life, 2010. **62**(6): p. 414-28.

4. Rontein, D., et al., *Plants synthesize ethanolamine by direct decarboxylation of serine using a pyridoxal phosphate enzyme.* J Biol Chem, 2001. **276**(38): p. 35523-9.

5. Carman, G.M. and S.A. Henry, *Phospholipid biosynthesis in the yeast Saccharomyces cerevisiae and interrelationship with other metabolic processes.* Prog Lipid Res, 1999. **38**(5-6): p. 361-99.

6. Aoyama, C., H. Liao, and K. Ishidate, *Structure and function of choline kinase isoforms in mammalian cells.* Prog Lipid Res, 2004. **43**(3): p. 266-81.

7. Ramírez de Molina, A., et al., *Choline kinase as a link connecting phospholipid metabolism and cell cycle regulation: implications in cancer therapy.* Int J Biochem Cell Biol, 2008. **40**(9): p. 1753-63.

8. Moore, C.R., et al., *Specific deletion of TRAF3 in B lymphocytes leads to B-lymphoma development in mice.* Leukemia, 2012. **26**(5): p. 1122-7.

9. Gokhale, S., et al., *Elevated Choline Kinase α-Mediated Choline Metabolism Supports the Prolonged Survival of TRAF3-Deficient B Lymphocytes.* J Immunol, 2020. **204**(2): p. 459-471.

10. Snider, S.A., et al., *Choline transport links macrophage phospholipid metabolism and inflammation.* J Biol Chem, 2018. **293**(29): p. 11600-11611.

11. Sanchez-Lopez, E., et al., *Choline Uptake and Metabolism Modulate Macrophage IL-1β and IL-18 Production.* Cell Metab, 2019. **29**(6): p. 1350-1362.e7.

12. Maizels, R.M., et al., *Helminth parasites--masters of regulation.* Immunol Rev, 2004. **201**: p. 89-116.

13. Reece, J.J., M.C. Siracusa, and A.L. Scott, *Innate immune responses to lung-stage helminth infection induce alternatively activated alveolar macrophages.* Infect Immun, 2006. **74**(9): p. 4970-81.

14. Nair, M.G., et al., *Chitinase and Fizz family members are a generalized feature of nematode infection with selective upregulation of Ym1 and Fizz1 by antigen-presenting cells.* Infect Immun, 2005. **73**(1): p. 385-94.

15. Anthony, R.M., et al., *Memory T(H)2 cells induce alternatively activated macrophages to mediate protection against nematode parasites.* Nat Med, 2006. **12**(8): p. 955-60.

16. Kim, S.Y. and M.G. Nair, *Macrophages in wound healing: activation and plasticity.* Immunol Cell Biol, 2019. **97**(3): p. 258-267.

17. Gordon, S., *Alternative activation of macrophages.* Nat Rev Immunol, 2003. **3**(1): p. 23-35.

18. Wynn, T.A., *Fibrotic disease and the T(H)1/T(H)2 paradigm.* Nat Rev Immunol, 2004. **4**(8): p. 583-94.

19. Esser-von Bieren, J., et al., *Antibodies trap tissue migrating helminth larvae and prevent tissue damage by driving IL-4Rα-independent alternative differentiation of macrophages.* PLoS Pathog, 2013. **9**(11): p. e1003771.

20. Esser-von Bieren, J., et al., *Antibody-mediated trapping of helminth larvae requires CD11b and Fcγ receptor I.* J Immunol, 2015. **194**(3): p. 1154-63.

21. Chen, F., et al., *Helminth resistance is mediated by differential activation of recruited monocyte-derived alveolar macrophages and arginine depletion.* Cell Rep, 2022. **38**(2): p. 110215.

22. Sutherland, T.E., et al., *Ym1 induces RELMα and rescues IL-4Rα deficiency in lung repair during nematode infection.* PLoS Pathog, 2018. **14**(11): p. e1007423.

23. Chen, G., et al., *Comparison of RELMα and RELMβ Single- and Double-Gene-Deficient Mice Reveals that RELMα Expression Dictates Inflammation and Worm Expulsion in Hookworm Infection.* Infect Immun, 2016. **84**(4): p. 1100-1111.

24. Batugedara, H.M., et al., *Hematopoietic cell-derived RELMα regulates hookworm immunity through effects on macrophages.* J Leukoc Biol, 2018.

25. Krljanac, B., et al., *RELMα-expressing macrophages protect against fatal lung damage and reduce parasite burden during helminth infection.* Sci Immunol, 2019. **4**(35).

26. Wu, G., et al., *Choline Deficiency Attenuates Body Weight Gain and Improves Glucose Tolerance in ob/ob Mice.* J Obes, 2012. **2012**: p. 319172.

27. Lechner, A., S. Bohnacker, and J. Esser-von Bieren, *Macrophage regulation & function in helminth infection.* Semin Immunol, 2021. **53**: p. 101526.

28. Huang, S.C., et al., *Metabolic Reprogramming Mediated by the mTORC2-IRF4 Signaling Axis Is Essential for Macrophage Alternative Activation.* Immunity, 2016. **45**(4): p. 817-830.

29. Rzepecka, J., K. Donskow-Schmelter, and M. Doligalska, *Heligmosomoides polygyrus infection down-regulates eotaxin concentration and CCR3 expression on lung eosinophils in murine allergic pulmonary inflammation.* Parasite Immunol, 2007. **29**(8): p. 405-13.

30. Sanin, D.E., et al., *A common framework of monocyte-derived macrophage activation.* Sci Immunol, 2022. **7**(70): p. eabl7482.

CHAPTER FOUR – Epithelial Cell-Derived RELMα Facilitates Influenza A Virus Infection of Epithelial cells in The Lung

Sang Yong Kim[1], James Stumpff[2], Roksana Shirazi[1], Daniel Diaz[3], Juliet Morrison[1], Meera G. Nair[3]

[1]Department of Microbiology, University of California, Riverside, Riverside, CA, USA

[2]Department of Cell, Molecular, and Developmental Biology, University of California, Riverside, Riverside, CA, USA

[3]Division of Biomedical Sciences, School of Medicine, University of California, Riverside, Riverside, CA, USA

Abstract

RELMα is a small secreted protein originally identified in T helper type 2 cytokine inflammatory settings such as allergy and helminth infection. However, RELMα is also produced in the acute settings of lung injury and hypoxia, suggesting potential relevance for RELMα in non-Th2 cytokine-biased inflammatory responses. Influenza A virus (IAV) infection causes damage to the lung, triggering acute respiratory distress syndrome (ARDS). We characterized RELMα expression and investigated its function in murine influenza infection with the A/California/04/2009 (H1N1) strain. Influenza infection of wild type mice led to significantly increased airway epithelial cell production of RELMα while circulating serum RELMα levels were unchanged in naïve and infected mice. Using RELMα-deficient mice, where the RELMα gene was deleted and replaced with the reporter tdTomato gene ($Retnla^{tdT/tdT}$), we found that RELMα-deficient mice had a lower viral burden in the lung compared to wild type mice. There was a positive correlation between RELMα concentration in the bronchio-alveolar lavage fluid (BALF) and IAV burden in the lung, and RELMα directly enhanced IAV infection of lung epithelial cells *in vitro* and *in vivo* independently of immune cells. Together, these data demonstrate that RELMα is expressed by IAV-infected epithelial cells, where it has a non-protective role in enhancing viral burden.

Introduction

Influenza infection is a global health concern causing an estimated 290,00-650,000 deaths every year globally due to respiratory diseases. IAV has a broad spectrum of hosts including humans, swine, horses, marine mammals, and birds [1]. IAV infection results in a wide range of symptoms from mild respiratory disease to severe pneumonia, ARDS, and even death [2-4]. IAV genome consists of 8 RNA segments, which encode RNA polymerase subunits, viral structural and non-structural proteins. Influenza A virus changes its antigens by accumulating point mutations and reassorting genes between different subtypes, which are called antigenic drift and shift, respectively [5, 6]. Influenza surface glycoproteins hemagglutinin (HA) and neuraminidase (NA) undergo antigenic drift and shift frequently [7, 8], and there are 18 HA subtypes and 11 NA subtypes. Various combinations of HA and NA decide IAV subtypes. IAV enters host cells by binding to sialic acid linked to cell surface galactose on glycoproteins or glycolipids through HA [9, 10]. HA is the primary target of current influenza virus vaccines [11], and NA is also a target of vaccine development [12]. This mandates the development of the new vaccine every year the new variant emerges, which is costly and resource-demanding. Therefore, the identification of host factors that are effective in regulating immune response and decreasing tissue damage following IAV infection may provide a new strategy to decrease loss and waste cause by IAV infection.

Differentiated epithelial cells in the upper and lower respiratory tract such as ciliated cells, club cells, and type 1 and 2 alveolar epithelial cells are primary targets of IAV infection, and viruses actively replicate in epithelial cells in the respiratory system

[13, 14]. Therefore, lung epithelial cells serve as the primary defense against influenza infection through various mechanisms. Influenza infection induces apoptosis of epithelial cells, which limits the further propagation of viruses and production of proinflammatory cytokines [15]. Epithelial cells also produce the type 1 and type 3 interferons after viral infection to activate antiviral responses in neighboring cells [14]. Moreover, epithelial cells express a variety of cytokines and chemokines that cause an inflammatory response in the lung. There is a cascade of cytokine production in epithelial cells starting with IFNα, TNFα, IL-1α, and IL-β followed by IL-6, followed by IL-6, CXCL1, monocyte chemoattractant proteins (MCPs), and macrophage inflammatory proteins (MIPs) after influenza infection [16]. The function of these antiviral and proinflammatory cytokines is well studied in IAV infection, but anti-inflammatory cytokines or other Th2-related proteins are not well characterized.

RELMα was first discovered in mouse bronchio-alveolar lavage fluid (BALF) with an experimentally induced asthma model [17]. In a mouse chronic hypoxia model of pulmonary hypertension, RELMα was expressed in the pulmonary vasculature, bronchial epithelial cells, and type 2 pneumocytes with vasoconstrictive and angiogenic functions [18]. RELMα was also upregulated by gp130 cytokine, Oncostatin M (OSM), and required for the expression of matrix remodeling genes, including *Col1a1*, *Col3a1*, *Mmp13*, *Timp1* [19]. Infection with the rat hookworm *Nippostrongylus brasiliensis* strongly upregulates RELMα in the lung, and its function is well characterized in this model [20-22]. While RELMα expressed by immune cells dampens the Th2 immune response to protect the host from fatal lung damage caused by *N. brasiliensis* infection,

the function of epithelial cell-derived RELMα was skewed toward damaged lung repair [20-22]. Unlike helminth infections, RELMα has a pathogenic function in *Citrobacter* infection by activating IL-23/Th17 axis [23]. However, the pathogenic function of RELMα has not been still studied well and the role of RELMα in viral infection has never been explored. This study identified that RELMα is upregulated by IAV infection in lung epithelial cells, and it induces infection of neighboring epithelial cells.

Materials and Methods

Mice

Retnla^{tDT} transgenic mice were generated by genOway (Lyon, France) by targeting *Retnla* Exon 2-4 using cre recombinase and Flp-mediated excision and replacement with the tDT reporter gene. Briefly, mice were bred with a genOway proprietary Cre deleter C57BL/6 mouse line to generate constitutive *Retnla*$^{tDT/+}$ mice. *Retnla*$^{tDT/+}$ heterozygote mice were crossed with C57BL/6J mice to generate littermate homozygote (tdT/tdT) and WT (+/+) mice after two generations, then bred in-house. Mice were genotyped by PCR and RELMα serum ELISA. Mice were age matched (6 to 14 weeks old), sex-matched for experiments, and housed five per cage under an ambient temperature with a 12 hours light/12 hours dark cycle. Mice were intranasally challenged with PBS or 10^2 or 10^3 PFU of pH1N1 A/California/04/2009 viruses and sacrificed at day 7 or 9 post-infection.

Viruses

pH1N1 A/California/04/2009 and Venus reporter expressing A/California/04/2009 viruses were a kind gift from Dr. Morrison (Department of Microbiology, University of California, Riverside). Virus stocks were propagated in specific-pathogen-free eggs (Charles River Laboratories) and titrated by plaque assays on MDCK cells.

Cytokine quantification

For sandwich ELISA, capture and biotinylated detection antibodies were used according to previously described protocols: RELMα (eBioscience, San Diego, CA) [24].

Immunofluorescence staining

The right lobe of mouse lung was inflated with 400µl of 2 parts of OCT and 1 part of 4% PFA and 30% sucrose PBS solution and stored overnight in 4% PFA and 30% sucrose in PBS solution at 4°C. After 24 hours, tissue was removed from the solution and incubated for 24 hours in 30% sucrose. Lungs were blocked in OCT, sectioned at 10µm, and stained by H&E. For immunofluorescent staining, sections were incubated with rabbit anti-RELMα (Peprotech, Rock Hill, NJ), APC-conjugated Rat anti-RELMα (eBioscience), rabbit anti-NS1 (Invitrogen, Waltham, MA), and Griffonia Simplicifolia Lectin I (GSL I) (Vector Laboratories, Newark, CA) overnight at 4°C. Sections were incubated with anti-Rabbit fluorochrome-conjugated antibody for 2 hours at RT then counterstained with DAPI. NS1 distribution was scored based on expression and location of NS1 in the lung (0: Nothing, 1: a few NS1 in airway epithelium, 2: several in airway epithelium, 3: a lot in airway epithelium, 4: several in airway epithelium and parenchyma, 5: a lot in airway epithelium and parenchyma).

Plaque assay

The left lobe of the mouse lung was homogenized in 3% FBS, and 1mM EDTA in 1ml PBS. MDCK cells were seeded in 6-well culture plates and incubated at 37°C in 5% CO2 for 24 hours. 10-fold serial dilutions of lung homogenates were prepared in a solution containing 1x PBS, 0.21% BSA, 1% Pen/Strep, and 1% Ca/Mg. Cells were washed once with PBS before adding 200 ml of the serial dilutions. Plates were incubated at 37°C and were rocked side-to-side and forward-to-back every 15 minutes to distribute virus

inoculum over the monolayer of cells for 1 hour. TPCK-treated (1 mg/ml) was added at a 1:1000 ratio to a supplemented 2X DMEM (2X DMEM, 2% Pen/Strep, 0.42% BSA, 20 mM HEPES, 0.24% NaHCO3, 0.02% DEAE-Dextran) before mixing with 1.5% Oxoid Agar at a 1:1 ratio. 2 ml of the agar overlay was added to each well and allowed to cool for 15 min at room temperature before transferring to the 37°C incubator. Plates were incubated for 96 hours. After incubation, plates were fixed with 1 ml of a 3.7% formaldehyde solution and incubated for 10 minutes to neutralize infectious virus. Overlay was flicked out with a spatula and stained for 20 min with crystal violet (0.095% crystal violet, 2.8% ethanol, 19% methanol). Plates were rinsed in tap water and plaques were counted to determine viral titers.

MLE-12

MLE-12 cells were cultured in HITES Media (DMEM/F-12 with HEPES, 1X Insulin-Transferrin-Selenium, 2% FBS, 100U/ml Penicillin-Streptomycin, 2mM L-glutamine (Gibco, Waltham, MA), 10 nM Hydrocortisone, 10nM β-estradiol (Sigma-Aldrich, St. Louis, MO) at 37°C in 5% CO2. MLE-12 cells were infected with 0.01 MOI of Venus reporter expressing pH1N1 A/California/04/2009 viruses. At indicated time points, the supernatant was removed, and cells were stained with Hoechst 33342 (ThermoFisher, Waltham, MA), followed by imaging with BZ-X00 (Keyence, Osaka, Japan). Venus-positive cells were counted by QuPath 0.2.3 [25]. After imaging, cells were harvested with supernatant and used for plaque assay.

Pleural macrophage and lung epithelial cell isolation

Pleural cells were collected by washing the pleural cavity with 500µl of ice-cold PBS two times. Half of the mouse lung was perfused with 10ml of ice-cold PBS and instilled with 800µl of 1U/ml Dispase (STEMCELL, Vancouver, Canada) and 100µl of 1% low melting point agarose (ThermoFisher). Lungs were incubated on ice for 2 minutes and incubated in 5ml of HBSS solution (Lonza, Bend, OR) at room temperature for 45 minutes. Lungs were minced with a scalpel in 5ml of DMEM containing 25mM HEPES (Corning, Tewksbury, MA), 1X Penicillin-Streptomycin (Gibco), and antimycotic solution (ThermoFisher) and passed through 70µm and 40µm nylon filters. Filtered cells were spun down at 340g for 7 minutes and incubated with 3ml of ACK lysis buffer (Gibco) to get lung single cell suspension. Pleural cells were incubated with biotinylated anti-MERTK antibody (BAF591, R&D system, Minneapolis, MN) and lung single cell suspension was CD325 microbeads (Miltenyi Biotec, Gaithersburg, MD). Cells were sorted with MS or LS columns (Miltenyi Biotec) with the manufacturer's instructions.

RNA isolation and qRT-PCR

RNA was isolated with RNeasy mini kit (Qiagen, Germantown, MD) and qRT-PCR was run with GoTaq® qPCR and RT-qPCR Systems (Promega, Madison, WI) with the manufacturer's instructions. *Epcam* Forward: CGT GAG GAC CTA CTG GAT CAT, *Epcam* Reverse: GTC CAC GTC GTC TTG TGT TTT, *Retnla* Forward: CAA GGA ACT TCT TGC CAA TCC AG, *Retnla* Reverse: CCA AGA TCC ACA GGC AAA GCC

A, HA Forward: GGA CAT GCT GCC GTT ACA C, HA Reverse: AGC TCA GTG TCA TCA TTT GAA AGG T

Statistical analysis

Data are presented as mean ± SEM and statistical analysis was performed by GraphPad Prism 9 software. Data was assessed by one-way ANOVA followed by post-hoc Tukey's test for multiple comparison, or the unpaired t-test for 2-group comparisons. For data collected over several timepoints, two-way ANOVA with post-Sidak multiple test was performed. *, $p \leq 0.05$; **, $p \leq 0.01$; ***, $p \leq 0.001$, ****, $p \leq 0.001$. Pearson coefficients between two variables were computed by GraphPad Prism 9 software. Experiments were repeated 2-3 times with n=3-5 per group for each experiment.

ETHICS STATEMENT

All protocols for animal use and euthanasia were approved by the University of California Riverside Institutional Animal Care and Use Committee (https://or.ucr.edu/ori/committees/iacuc.aspx; protocol A-20180023 and 20210017) and were in accordance with National Institutes of Health guidelines. Animal studies are in accordance with the provisions established by the Animal Welfare Act and the Public Health Services (PHS) Policy on the Humane Care and Use of Laboratory Animals.

Results

IAV infection upregulates RELMα expression in the bronchial epithelium and epithelial cells.

RELMα induction and its function have been demonstrated in both bacteria and helminth infections [20, 21, 23, 26], but they have not been studied in viral infections. RELMα was first discovered in the pulmonary vasculature, bronchial epithelial cells, and type 2 pneumocytes under hypoxic conditions [18], but the following study also showed that RELMα is strongly expressed by alternatively activated macrophages [27]. *Retnla*$^{+/+}$ (WT) and *Retnla*$^{tdT/tdT}$ (KO) mice were intranasally infected with A/California/04/2009 (H1N1) strain and sacrificed at day 7 or 9 post-infection. Mice begin to recover lung inflammation and damage at day 7, and RELMα induced these processes in helminth infections [20, 21]. Thus, we hypothesized that RELMα affects immune response and tissue repair in the lung after IAV infection. Serum and bronchoalveolar lavage fluid (BALF) were collected from naive and infected mice at day 7 and 9 post-infection to check the systemic and site-specific RELMα upregulation by IAV infection. RELMα was not systemically induced by IAV infection showing a slight difference in the RELMα level between WT naive and infected mice (Figure 11A). However, IAV infection increased RELMα expression in the BALF both at day 7 and 9 post-infection, indicating that RELMα is mainly expressed in the bronchial epithelium (Figure 11B). To confirm if RELMα upregulation by IAV infection is specific for the bronchial epithelium, RELMα and macrophage maker, Griffonia Simplicifolia Lectin (GSL), were imaged in the lung of WT infected mice by immunofluorescence staining (Figure 11C). RELMα expression was

concentrated and lined with airway epithelium, but GSL was spotted in the parenchyma of the lung, indicating that IAV infection induces bronchial epithelium-specific RELMα expression rather than immune cells.

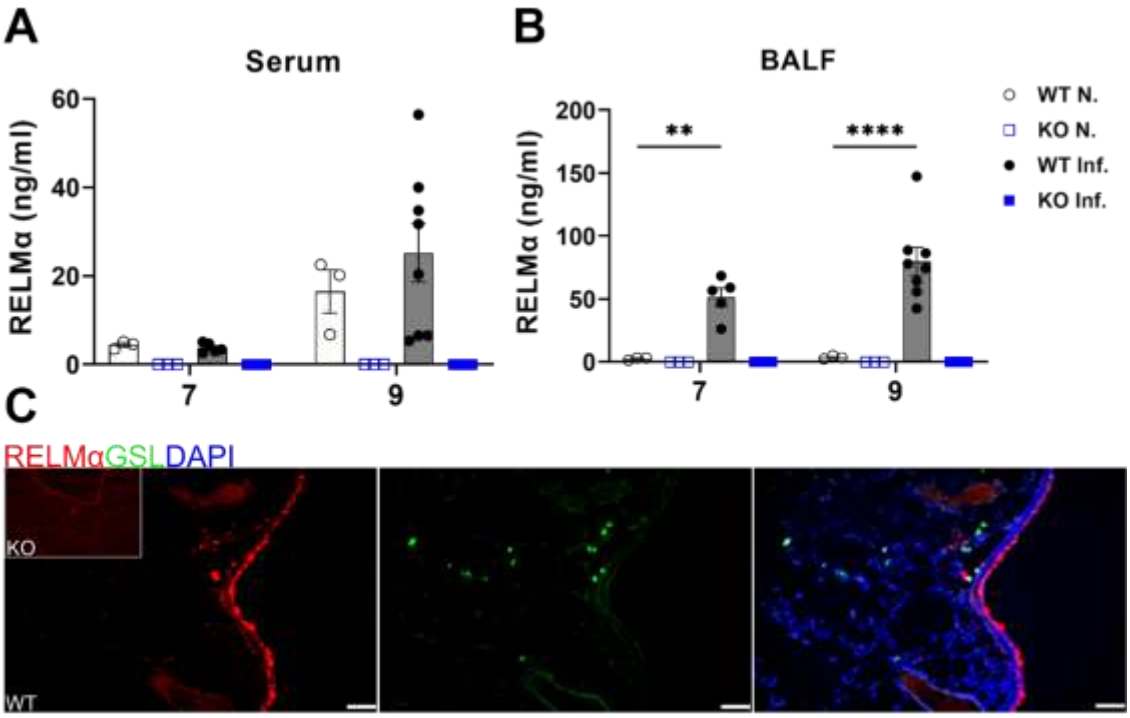

Fiugre 11. IAV infection upregulates RELMα expression in the bronchial epithelium and epithelial cells. *Retnla*$^{+/+}$ (WT) and *Retnla*$^{tdT/tdT}$ (KO) mice were intranasally injected with PBS (Naive) 10^2 PFU of IAV (Infected), followed by sacrifice at day 7 and 9. (A and B) RELMα in the serum and BALF at 7 and 9 days post-infection was quantified by ELISA. (C) Lung sections of WT-infected mice at day 9 post-infection was stained with anti-RELMα antibody, GSL, and counterstained with DAPI. The image was obtained by the immunofluorescent microscope. (Scale bar=50μm) Data from 2 independent experiments (day 9) and 1 experiment (day 7) were presented as mean ± SEM (n = 3-5 per group).

RELMα is colocalized with viral protein NS1 and positively correlated with IVA burden in the lung.

Airway and alveolar epithelial cells produce sialic acid glycan as receptors, which are the primary target of infection [2, 28, 29]. Since RELMα was upregulated by IAV infection in the bronchial epithelium, RELMα may affect lung epithelial cells and the IAV infections of these cells. NS1 is a viral non-structural protein that has an important immunomodulatory function such as inhibiting interferon production by host cells [30]. RELMα and NS1 were stained in the lungs of WT and KO infected mice to validate if RELMα changes IAV infections and distributions. NS1 was mainly detected and colocalized with RELMα in the bronchial epithelium (Figure 12A), suggesting that IAV infection induces RELMα expression in the bronchial epithelium or RELMα expressing cells are more susceptible to IAV infection. Interestingly, while NS1 was highly expressed in the airway epithelium and even parenchyma of WT infected lungs, there were less NS1 expression and distribution in KO infected lungs (Figure 12B). Distribution of NS1 in WT and KO infected lungs was scored, and WT infected mice had significantly higher NS1 distribution score compared to KO infected mice, indicating that RELMα accelerated IAV propagation and spreading in the lung (Figure 12C). This data led us to quantify actual IAV burden in WT and KO infected lungs, and plaque assay can measure live viruses in the lung. Plaque assays were done with WT and KO infected lung homogenates at day 7 and 9, and the viral burden was significantly lower in KO lungs than in WT lungs at day 7 post-infection (Figure 12D). More strikingly, live viruses were not detectable in KO lungs at day 9 whereas there was still live virus in WT-infected

lungs (Figure 12E). To determine if viral burden is statistically correlated with RELMα level in the bronchial epithelium at day 7 and 9 post-infection, Pearson coefficients were calculated between two variables (Figure 12F). R-value was 0.47, and p-value was 0.03, indicating that the RELMα level in the BALF is positively correlated with the IAV burden in the lung.

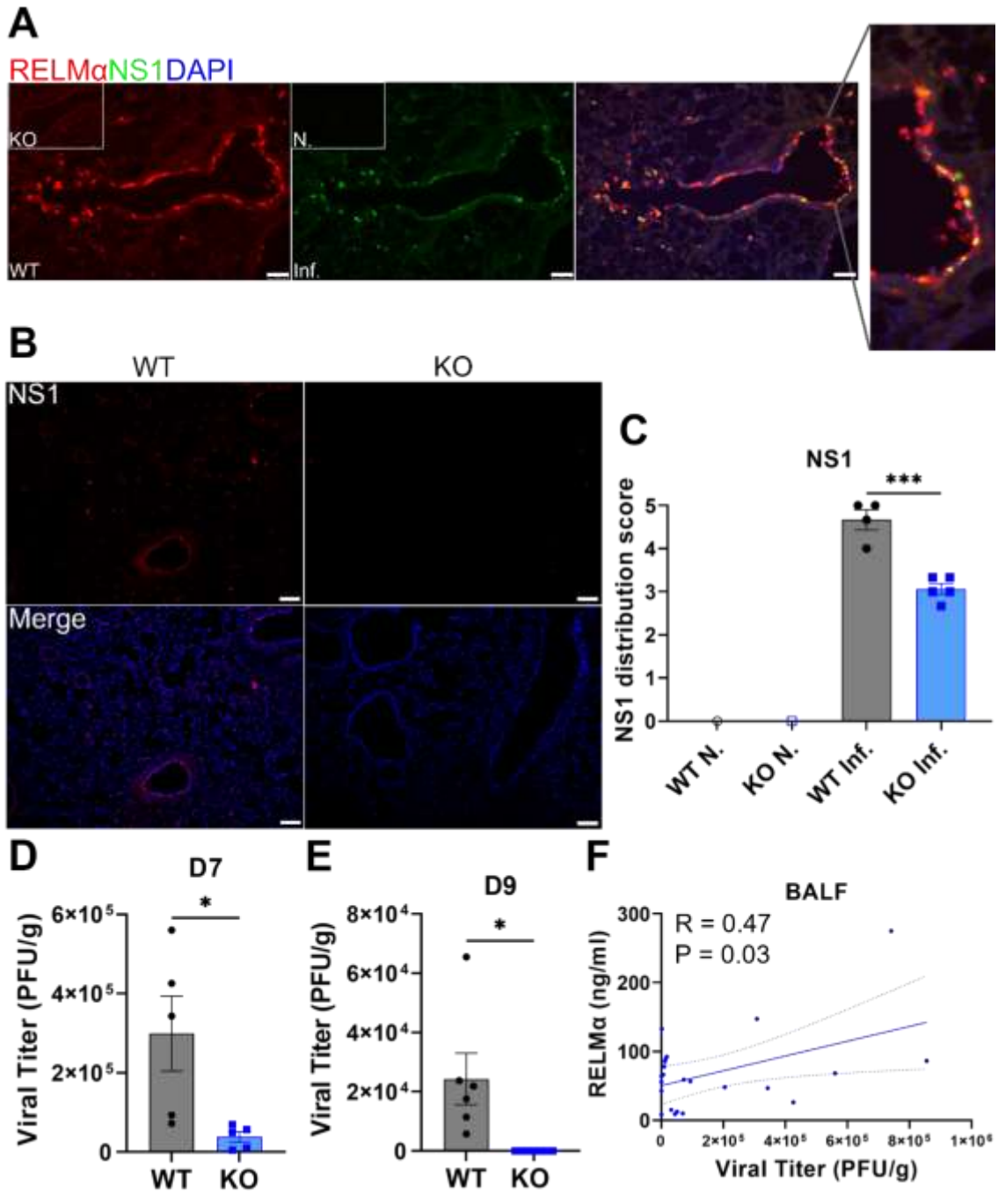
A
RELMαNS1DAPI
KO
WT
N.
Inf.
B
WT
KO
NS1
Merge
C
NS1
***
NS1 distribution score
WT N.
KO N.
WT Inf.
KO Inf.
D
D7
*
Viral Titer (PFU/g)
WT
KO
E
D9
*
Viral Titer (PFU/g)
WT
KO
F
BALF
R = 0.47
P = 0.03
RELMα (ng/ml)
Viral Titer (PFU/g)

Figure 12. RELMα is colocalized with viral protein NS1 and positively correlated with IAV burden in the lung. *Retnla*$^{+/+}$ (WT) and *Retnla*$^{tdT/tdT}$ (KO) mice were intranasally injected with PBS (naïve) 10^2 PFU of IAV (Infected), followed by sacrifice at day 7 and 9. (A) The lung section of WT-infected mice at day 7 post-infection was stained with anti-RELMα and NS1 antibody, and counterstained with DAPI. The image was obtained by the immunofluorescent microscope. (Scale bar=50μm) (B and C) Lung sections from WT and KO infected mice at day 7 post-infection were stained with anti-NS1 antibody, and NS1 distribution was scored. (Scale bar=50μm) (D and E) Viral burden in the lung was measured by plaque assay. (F) The correlation between RELMα in the BALF and lung viral burden at day 7 and 9 post-infection was calculated by Pearson correlation coefficients. Data from 2 independent experiments (day 9) and 1 experiment (day 7) were presented as mean ± SEM (n = 3-5 per group).

RELMα induces IAV infection of mouse lung epithelial cells in vitro and *in vivo.*

The lung is made up of very complex structures with various structural and resident immune cells. Influenza infection will recruit countless immune cells into the lungs, which can also be affected by RELMα. To see if RELMα affects the immune response to IAV, immune cell composition and cytokine level in the BALF was analyzed by flow cytometry and cytometric bead array. However, there was no significant difference in immune cell populations and cytokine levels between WT and KO (data are not shown). Therefore, we hypothesized that RELMα directly affects lung epithelial cells and induces infection with IAV. MLE-12 cell is a mouse type 2 alveolar epithelial cell line, which is one of the primary targets of IAV infection. MLE-12 cells were pretreated with a low and high concentration of RELMα followed by infection with Venus expressing IAV at 0.01 MOI to visualize infected cells. After infection, RELMα was added back to cells, and cells were visualized and collected at 48 and 72 hours post-infection. When MLE-12 cells were treated with a low concentration of RELMα (100ng/ml), there was no induction of infection of cells with IAV, but high concentrations of RELMα (1000ng/ml) induced IAV infection in MLE-12 cells (Figure 13A and B). In addition, live virus burden in a mixture of supernatant and cell lysate was measured by plaque assay. In contrast to Venus-positive cell images and counting, a low concentration of RELMα also increased IAV in the supernatant and cell lysate mixture both at 48 and 72 hours post-infection, and a high concentration of RELMα still increased IAV in the mixture at 72 hours post-infection, suggesting that RELMα increase infection and release of IAV in epithelial cells *in vitro* (Figure 13C).

Next, lung epithelial cells were isolated with magnetic activated cell sorting (MACS) to determine whether the higher level of IAV in the lungs was attributed to lung epithelial cells and whether the effect on promoting IAV infection in lung epithelial cells is the same even in actual inflammatory environments. The purity of isolated lung epithelial cells was confirmed by cytospin followed by staining surface markers of lung epithelial cells and macrophages, and the expression of markers was compared with pleural macrophages. In lung epithelial cells, MERTK, a macrophage marker, expression was lower compared to macrophages, but there was higher expression of cytoskeletal protein β-Actin and epithelial cell marker EPCAM, (Figure 13D). Quantitative real-time PCR result (qRT-PCR) of *Epcam* showed that *Epcam* expression was significantly higher in sorted lung epithelial cells than in pleural macrophages, indicating high purity of lung epithelial cells (Figure 13E). RELMα gene expression was robustly induced in WT infected mice compared to naive mice, validating dominant RELMα protein expression in the bronchial epithelium (Figure 13F). Lastly, viral HA gene expression was significantly higher in WT infected mice, demonstrating that RELMα facilitates infection of lung epithelial cells with IAV *in vivo* (Figure 13G).

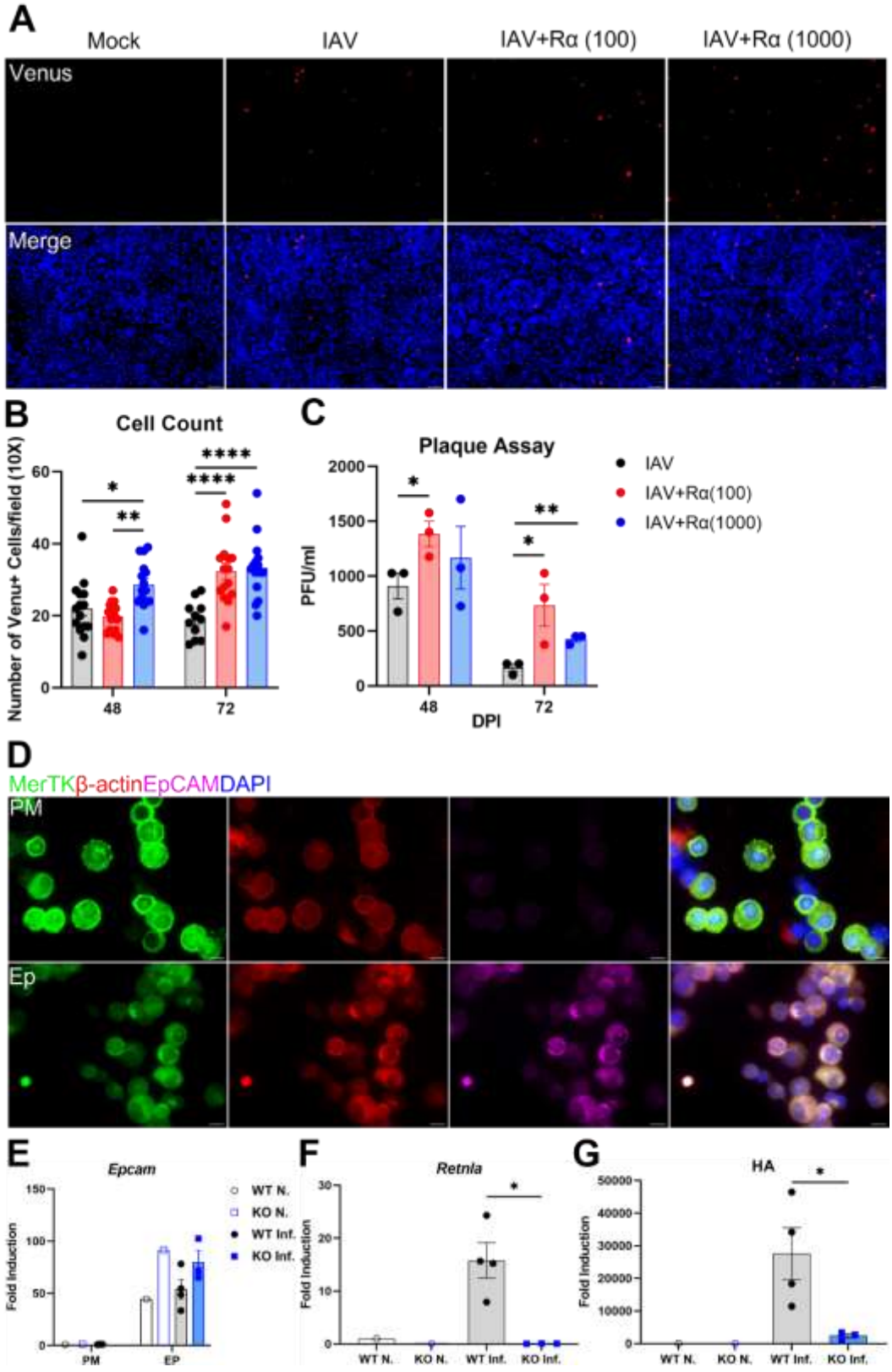
A
Mock
IAV
IAV+Rα (100)
IAV+Rα (1000)
Venus
Merge
B
Cell Count
Number of Venu+ Cells/field (10X)
48
72
C
Plaque Assay
PFU/ml
DPI
IAV
IAV+Rα(100)
IAV+Rα(1000)
D
MerTKβ-actinEpCAMDAPI
PM
Ep
E
Epcam
Fold Induction
WT N.
KO N.
WT Inf.
KO Inf.
F
Retnla
G
HA

Figure 13. RELMα induces IAV infection of mouse lung epithelial cells *in vitro* and *in vivo*. MLE-12 cells were pre-treated with PBS or RELMα, followed by infection with reporter IAV expressing Venus fluorescent protein at 0.01 MOI. *Retnla*$^{+/+}$ (WT) and *Retnla*$^{tdT/tdT}$ (KO) mice were intranasally injected with PBS (Naive) 10^3PFU of IAV (Infected), followed by sacrifice at day 7. Pleural macrophages and lung epithelial cells were isolated by magnetic-activated cell sorting. (A) MLE-12 cells were counterstained with Hoechst 33342 and Venus-expressing cells were imaged at 48 hours post-infection by the fluorescent microscope. (B) Venus-positive cells were counted more than 10 fields of 10X images. (C) Cell lysates were collected at 48 and 72 hours post-infection, and viral burden in the lysates were quantified by plaque assay. (D) Pleural macrophages and lung epithelial cells were spun down with the cytospin centrifuge and stained with anti-MERTK, RELMα, and EPCAM antibodies, followed by counterstaining with DAPI. Then, cells were imaged by the fluorescent microscope (Scale bar=10μm) (E-G) RNA was extracted from sorted pleural macrophages and lung epithelial cells, and *Epcam* expression in both cell types*, Retnla,* and HA expression in epithelial cell were quantified by qRT-PCR. Representative data from 3 independent experiments was presented as in Fig A-C mean ± SEM (n = 3 per group). Data from 1 experiment was presented in Fig D-G as mean ± SEM (n = 3-4 per group).

DISCUSSION

RELMα is a pleiotropic protein, which is expressed by diverse cell types such as epithelial cells and immune cells and upregulated by different stimulus [31]. RELMα induced by various cells and stimulation has different functions in a context-dependent manner. In this study, we showed for the first time that RELMα was induced by IAV infection and the novel pathogenic function of RELMα in viral infections. RELMα expression in epithelial cells is mostly IL-4rα-dependent, but it was also shown in the absence of type 2 inflammation [23, 32]. In the latter case, the mechanism by which RELMα is upregulated has not been fully understood yet. A previous study showed that Oncostatin M, one of the gp130 cytokines, elevated the expression of RELMα in airway epithelial cells. Interestingly, OSM was upregulated by H3N2 IAV infection in human the nasal epithelium, suggesting that RELMα upregulation by IAV infection in lung epithelial cells may be mediated by OSM through the gp130 receptor pathway. Gp130 cytokines are also referred to the IL-6 family of cytokines, which include Interleukin-6 (IL-6), Interleukin-11 (IL-11), Interleukin-27 (IL-27), leukemia inhibitory factor (LIF), oncostatin M (OSM), ciliary neurotrophic factor (CNTF), cardiotrophin-1 (CT-1), novel neurotrophin-1/B cell stimulating factor-3 or cardiotrophin-like cytokine (CLC), and neuropoietin (NP) [33, 34]. Although it was not as much as OSM, IL-6 also increased the expression of RELMα in airway epithelial cells [19]. IL-6 expression was promoted with suppressor of cytokine signaling-3 (SOCS3) by IAV infection, which inhibits IL-6-associated signal transducer and activator of transcription 3 (STAT3) [35]. In SOCS3-deficient mice, acute lung damage, mortality, and viral load were decreased after IAV

infection, indicating that IAV simultaneously induces SOCS3 with IL-6 to downregulate IL-6/STAT3-mediated immune responses. In another study, IL-6 was shown to downregulates acute lung injury following IAV infection by inhibiting proliferation, migration, and survival of lung fibroblasts as well as decreasing apoptosis of lung epithelial cells [36]. Thus, regulation of RELMα and IAV infection by gp130 cytokines through its receptor should be further studied in the future.

When RELMα is expressed in the Th2 immune environment in the lung, it downregulates inflammation and accelerates the repair of damaged tissue [20-22]. However, RELMα-derived from lung epithelial cells expedited infection of adjacent epithelial cells with IAV without the intervention of other cells. RELMα not only induces IAV infection but also delayed clearance of viruses directly in lung epithelial cells *in vitro* and *in vivo*. Since IAV enters host cells through interaction with sialic acid through HA, it will be worthwhile to investigate if RELMα regulates sialic acid level on the cell surface. Many studies showed that RELMα activates phosphatidylinositol 3-kinase (PI3K)/AKT and ERK pathway [18, 37]. Hypoxia-induced RELMα expression, which increased the number of $Sca1^{+}/CD45^{-}$ progenitor cells in the lung [37]. RELM activated proliferation of mesenchymal stem cells through PI3K/Akt and Erk pathway. In addition, RELMα inhibited apoptosis of mouse lung fibroblast induced by TNFα and cycloheximide (CHX) [38]. RELMα treated with TNFα/CHX elevated phosphorylation of AKT in mouse lune fibroblast, which is required for inhibition of apoptosis. Thus, RELMα is probably upregulated by IAV infection to limit host tissue damage and facilitate tissue repair caused by inflammation through PI3K/Akt pathway. However, the

bivalent role of PI3K in influenza virus infection and host cell defense was identified in another study [39]. IAV infection also induces the PI3K-Akt signaling pathway and it was required for activation of the anti-viral genes by IRF3 [39]. Interestingly, IAV titers were significantly reduced when PI3K was inhibited by wortmannin, increasing the accumulation of viruses on the surface of cells not in the endosome, indicating that PI3K activation induces virus uptake. This proves that viruses exploit host anti-viral components to facilitate their survival. Therefore, the effect of synergistic PI3K/Akt pathway activation by RELMα and IAV infection on IAV host cell entry should be further investigated.

References

1. Webster, R.G., et al., *Evolution and ecology of influenza A viruses.* Microbiol Rev, 1992. **56**(1): p. 152-79.

2. Chen, X., et al., *Host Immune Response to Influenza A Virus Infection.* Front Immunol, 2018. **9**: p. 320.

3. Herold, S., et al., *Influenza virus-induced lung injury: pathogenesis and implications for treatment.* Eur Respir J, 2015. **45**(5): p. 1463-78.

4. Hogan, B.L., et al., *Repair and regeneration of the respiratory system: complexity, plasticity, and mechanisms of lung stem cell function.* Cell Stem Cell, 2014. **15**(2): p. 123-38.

5. Both, G.W., et al., *Antigenic drift in influenza virus H3 hemagglutinin from 1968 to 1980: multiple evolutionary pathways and sequential amino acid changes at key antigenic sites.* J Virol, 1983. **48**(1): p. 52-60.

6. Webster, R.G., et al., *Molecular mechanisms of variation in influenza viruses.* Nature, 1982. **296**(5853): p. 115-21.

7. Das, S.R., et al., *Defining influenza A virus hemagglutinin antigenic drift by sequential monoclonal antibody selection.* Cell Host Microbe, 2013. **13**(3): p. 314-23.

8. Bhatt, S., E.C. Holmes, and O.G. Pybus, *The genomic rate of molecular adaptation of the human influenza A virus.* Mol Biol Evol, 2011. **28**(9): p. 2443-51.

9. Gottschalk, A., *Chemistry of virus receptors*, in *The viruses: biochemical, biological and biophysical properties* F. Burnet and W. Stanley, Editors. 1959, Academic Press: New York, NY.

10. Palese, P. and M.L. SHAW, *Orthomyxoviridae: the viruses and their replication*, in *Fields virology*, D.M. Knipe and P.M. Howley, Editors. 2007, Lippincott Williams and Wilkins: Philadelphia, PA.

11. Krammer, F., *The human antibody response to influenza A virus infection and vaccination.* Nat Rev Immunol, 2019. **19**(6): p. 383-397.

12. Sylte, M.J. and D.L. Suarez, *Influenza neuraminidase as a vaccine antigen.* Curr Top Microbiol Immunol, 2009. **333**: p. 227-41.

13. Krammer, F., et al., *Influenza.* Nat Rev Dis Primers, 2018. **4**(1): p. 3.

14. Sanders, C.J., P.C. Doherty, and P.G. Thomas, *Respiratory epithelial cells in innate immunity to influenza virus infection.* Cell Tissue Res, 2011. **343**(1): p. 13-21.

15. Cheung, C.Y., et al., *Induction of proinflammatory cytokines in human macrophages by influenza A (H5N1) viruses: a mechanism for the unusual severity of human disease?* Lancet, 2002. **360**(9348): p. 1831-7.

16. Bielefeldt-Ohmann, H., *Cytokines in animal health and disease / [edited by Michael J. Myers, Michael P. Murtaugh]*. 1995: Marcel Dekker.

17. Holcomb, I.N., et al., *FIZZ1, a novel cysteine-rich secreted protein associated with pulmonary inflammation, defines a new gene family.* EMBO J, 2000. **19**(15): p. 4046-55.

18. Teng, X., et al., *FIZZ1/RELMalpha, a novel hypoxia-induced mitogenic factor in lung with vasoconstrictive and angiogenic properties.* Circ Res, 2003. **92**(10): p. 1065-7.

19. Ho, L., et al., *RELMα is Induced in Airway Epithelial Cells by Oncostatin M Without Requirement of STAT6 or IL-6 in Mouse Lungs In Vivo.* Cells, 2020. **9**(6).

20. Batugedara, H.M., et al., *Hematopoietic cell-derived RELMα regulates hookworm immunity through effects on macrophages.* J Leukoc Biol, 2018.

21. Krljanac, B., et al., *RELMα-expressing macrophages protect against fatal lung damage and reduce parasite burden during helminth infection.* Sci Immunol, 2019. **4**(35).

22. Sutherland, T.E., et al., *Ym1 induces RELMα and rescues IL-4Rα deficiency in lung repair during nematode infection.* PLoS Pathog, 2018. **14**(11): p. e1007423.

23. Osborne, L.C., et al., *Resistin-like molecule α promotes pathogenic Th17 cell responses and bacterial-induced intestinal inflammation.* J Immunol, 2013. **190**(5): p. 2292-300.

24. Chen, G., et al., *Comparison of RELMα and RELMβ Single- and Double-Gene-Deficient Mice Reveals that RELMα Expression Dictates Inflammation and Worm Expulsion in Hookworm Infection.* Infect Immun, 2016. **84**(4): p. 1100-1111.

25. Bankhead, P., et al., *QuPath: Open source software for digital pathology image analysis.* Sci Rep, 2017. **7**(1): p. 16878.

26. Gundra, U.M., et al., *Vitamin A mediates conversion of monocyte-derived macrophages into tissue-resident macrophages during alternative activation.* Nat Immunol, 2017. **18**(6): p. 642-653.

27. Nair, M.G., et al., *Chitinase and Fizz family members are a generalized feature of nematode infection with selective upregulation of Ym1 and Fizz1 by antigen-presenting cells.* Infect Immun, 2005. **73**(1): p. 385-94.

28. van Riel, D., et al., *Seasonal and pandemic human influenza viruses attach better to human upper respiratory tract epithelium than avian influenza viruses.* Am J Pathol, 2010. **176**(4): p. 1614-8.

29. Shinya, K., et al., *Avian flu: influenza virus receptors in the human airway.* Nature, 2006. **440**(7083): p. 435-6.

30. Qian, W., et al., *The C-Terminal Effector Domain of Non-Structural Protein 1 of Influenza A Virus Blocks IFN-β Production by Targeting TNF Receptor-Associated Factor 3.* Front Immunol, 2017. **8**: p. 779.

31. Pine, G.M., H.M. Batugedara, and M.G. Nair, *Here, there and everywhere: Resistin-like molecules in infection, inflammation, and metabolic disorders.* Cytokine, 2018. **110**: p. 442-451.

32. Dasgupta, P., et al., *Transfer of in vivo primed transgenic T cells supports allergic lung inflammation and FIZZ1 and Ym1 production in an IL-4Rα and STAT6 dependent manner.* BMC Immunol, 2011. **12**: p. 60.

33. White, U.A. and J.M. Stephens, *The gp130 receptor cytokine family: regulators of adipocyte development and function.* Curr Pharm Des, 2011. **17**(4): p. 340-6.

34. Fasnacht, N. and W. Müller, *Conditional gp130 deficient mouse mutants.* Semin Cell Dev Biol, 2008. **19**(4): p. 379-84.

35. Liu, S., et al., *Influenza Virus-Induced Robust Expression of SOCS3 Contributes to Excessive Production of IL-6.* Front Immunol, 2019. **10**: p. 1843.

36. Yang, M.L., et al., *IL-6 ameliorates acute lung injury in influenza virus infection.* Sci Rep, 2017. **7**: p. 43829.

37. Kolosova, I.A., et al., *Resistin-like molecule α stimulates proliferation of mesenchymal stem cells while maintaining their multipotency.* Stem Cells Dev, 2013. **22**(2): p. 239-47.

38. Chung, M.J., et al., *Antiapoptotic effect of found in inflammatory zone (FIZZ)1 on mouse lung fibroblasts.* J Pathol, 2007. **212**(2): p. 180-7.

39. Ehrhardt, C., et al., *Bivalent role of the phosphatidylinositol-3-kinase (PI3K) during influenza virus infection and host cell defence.* Cell Microbiol, 2006. **8**(8): p. 1336-48.

CHAPTER FIVE – CX3CR1-Expressing Myeloid Cells Regulate Host–Helminth Interaction and Lung Inflammation

Sang Yong Kim[1], Mark A. Barnes[2], Suhas Sureshchandra[3], Andrea R. Menicucci[3], Jay J. Patel[2], Ilhem Messaoudi[3], and Meera G. Nair[2]

[1]Department of Microbiology, University of California, Riverside, CA, USA

[2]Division of Biomedical Sciences, School of Medicine, University of California, Riverside, CA, USA

[3]Department of Molecular Biology and Biochemistry, School of Biological Sciences University of California, Irvine, CA, USA

A version of this chapter was published in Advanced Biology, 2022.

Abstract

Many helminth life cycles, including hookworm, involve a mandatory lung phase, where myeloid and granulocyte subsets interact with the helminth and respond to infection-induced lung injury. To evaluate these innate subsets in *Nippostrongylus brasiliensis* infection, reporter mice for myeloid cells ($CX3CR1^{GFP}$) and granulocytes ($PGRP^{dsRED}$) are employed. *Nippostrongylus* infection induces lung infiltration of reporter cells, including $CX3CR1^{+}$ myeloid cells and $PGRP^{+}$ eosinophils. Strikingly, $CX3CR1^{GFP/GFP}$ mice, which are deficient in CX3CR1, are protected from *Nippostrongylus* infection with reduced weight loss, lung leukocyte infiltration, and worm burden compared to $CX3CR1^{+/+}$ mice. This protective effect is specific for CX3CR1 as CCR2-deficient mice do not exhibit reduced worm burdens. *Nippostrongylus* co-culture with lung $Ly6C^{+}$ monocytes or $CD11c^{+}$ cells demonstrates that $CX3CR1^{GFP/GFP}$ monocytes secrete more pro-inflammatory cytokines and actively bind the parasites causing reduced motility. RNA sequencing of $Ly6C^{+}$ or $CD11c^{+}$ cells shows *Nippostrongylus*-induced gene expression changes, particularly in monocytes, associated with inflammation, chemotaxis, and extracellular matrix remodeling pathways. Analysis reveals cytotoxic and adhesion molecules as potential effectors against the parasite, such as *Gzma* and *Gzmb*, which are elevated in $CX3CR1^{GFP/GFP}$ monocytes. These studies validate a dual innate cell reporter for lung helminth infection and demonstrate that CX3CR1 impairs monocyte–helminth interaction.

Introduction

Soil-transmitted helminths afflict over one billion individuals worldwide, where they can cause debilitating symptoms, including growth retardation, organ pathology and failure [1]. Given the development of anthelminthic drug resistance [2, 3], and the occurrence of re-infection after drug treatment [4, 5], understanding how to trigger protective immune effector responses offers valuable therapeutic insight to promote helminth elimination by the host. Helminths are macroparasites with complex life cycles that frequently involve tissue migration through many organs, leading to tissue pathology and inflammation [6]. Immune effector responses at these sites of incoming larval parasites are especially critical in preventing long-term infections. In particular, the lung is a main infection site for many helminths, including hookworms *Necator americanus* and *Ancylostoma duodenale*, where the infectious larvae migrate through the lung as an essential developmental step before reaching the small intestine [7].

While clinical symptoms of pulmonary helminth infection in humans have been reported, including coughing, wheezing, and potentially respiratory failure, investigation of the immune-mediated mechanisms within the lung against the helminth are less well understood, and rely on *in vivo* models such as murine helminth infection. One such murine model is infection with *Nippostrongylus brasiliensis*, a natural helminth parasite of rodents, which has a transient migratory phase through the lung prior to reaching the small intestine, mimicking pulmonary hookworm infection [8]. Previous studies have shown that pulmonary immune responses, including neutrophils and macrophages, are critical against *Nippostrongylus* [9, 10]. These studies utilized secondary challenge with

Nippostrongylus to show that $CD4^+$ derived T helper type 2 cytokines and neutrophils promoted lung macrophage interaction and killing of *Nippostrongylus* larval parasites. The importance of other innate cells such as eosinophils have also been investigated, showing modest effects of eosinophils in promoting secondary effector responses to *Nippostrongylus* [11-13]. Eosinophil-dependent resistance was not required for resistance to the primary infection but was necessary for resistance to the secondary infection, which involves immobilizing worms and inhibiting their progression to the gut. These studies highlight the importance of innate effector cells in the lung, and prompted our study to investigate innate cells in *Nippostrongylus* infection. We focused on lung monocytes, which have been less well studied in lung helminth infection, although they are recruited and have important antimicrobial functions to a variety of other lung pathogens, and also can differentiate into dendritic cells and macrophages [14-16]. To this end, we investigated the CX3CR1 signaling pathway in influencing lung cell infiltration and activation in response to *Nippostronglyus* infection.

CX3CR1 is a G-protein coupled receptor that binds the chemokine CX3CL1/fractalkine. CX3CR1 is expressed on monocytes, where it is critical for effective monocyte adhesion and transmigration through the endothelium into the tissues. Within the tissue, and dependent on the inflammatory environment, CX3CR1-expressing monocytes differentiate into dendritic cells and macrophages, with essential protective functions against many pathogens, including bacteria and viruses [17, 18]. CX3CR1 signaling also occurs in response to injury and fibrosis. In murine models of spinal cord injury and stroke, CX3CR1-deficient mice have ameliorated neural outcomes associated

with a reparative phenotype in CX3CR1-expressing microglia and macrophages [19, 20]. In pulmonary and peritoneal fibrosis models, CX3CR1 signaling is also detrimental, exacerbating fibrosis. Further, in infection with *Schistosoma japonicum*, acute hepatic granuloma formation and liver pathology is increased by CX3CR1 signaling, with little effect on parasite burdens.[21] Together, these studies suggest that CX3CR1 signaling is important for optimal effector responses to multiple pathogens, but needs to be tightly regulated to reduce inflammatory outcomes and tissue pathology. However, CX3CR1 signaling in pulmonary helminth infection has not previously been examined. We utilized CX3CR1-GFP knockout/knock-in transgenic mice to determine the kinetics of CX3CR1-expressing cells in the lung and investigate their role in infection with *Nippostrongylus brasiliensis*. To evaluate granulocyte lung subsets at the same time, we generated dual reporters by crossing $CX3CR1^{GFP}$ mice to reporter mice for PGRP-S, a peptidoglycan recognition protein identified in neutrophil granules.[22] Following *Nippostrongylus* infection, we observed $CX3CR1^{GFP}$ and $PGRP^{dsRed}$ cells in the lung and small intestine of infected mice. Flow cytometric characterization showed that these subsets were significantly increased at day 7 post-infection in the lung but not peripherally in the blood. The $CX3CR1^{GFP}$ subsets were composed mainly of $Ly6C^{+}$ monocytes and $CD11c^{+}$ DCs, while the main $PGRP^{dsRed}$ cells in the lung were eosinophils, identifying $PGRP^{dsRed}$ mice as useful reporters to visualize and track eosinophils. Comparison of $CX3CR1^{+/+}$ and $CX3CR1^{GFP/GFP}$ mice revealed that CX3CR1-deficient mice were more protected against *Nippostrongylus* infection, associated with reduced infection-induced weight loss, lung leukocyte infiltration, and intestinal parasite burdens. In contrast, CCR2 deficiency

did not show striking effects in *Nippostrongylus* infection. *Nippostrongylus* larval parasite co-culture with $CD11c^+$ or $Ly6C^+$ sorted from the infected lungs identified $Ly6C^+$ monocytes as the functional downstream effectors in CXCR1-deficient mice, with increased expression of proinflammatory cytokines, and enhanced binding to the parasite, leading to reduced worm motility. RNA-seq analysis was performed on $Ly6C^+$ monocytes and $CD11c^+$ cells sorted from the infected lungs of $CX3CR1^{GFP/+}$ and $CX3CR1^{GFP/GFP}$ mice. The most differentially expressed genes was observed in $Ly6C^+$ monocytes in response to infection, and the CX3CR1-deficient $Ly6C^+$ monocytes demonstrated increased cytotoxic molecules and enhanced chemokines compared to $CX3CR1^{GFP/+}$ monocytes. In contrast, $CD11c^+$ CX3CR1-expressing cells represented a heterogeneous macrophage/dendritic population with some infection-induced changes in gene expression but no significant gene expression changes between $CX3CR1^{GFP/+}$ and $CX3CR1^{GFP/GFP}$ $CD11c^+$ cells. Together, these studies validate a dual reporter for myeloid and granulocyte subsets in *Nippostrongylus* infection, and identify a previously unrecognized role for CX3CR1 signaling in promoting infection-induced weight loss and leukocyte infiltration and impairing optimal effector responses to *Nippostrongylus*, in part through effects on monocytes.

Materials and Methods

Animals

The following studies were performed using eight to ten weeks old mice. CX3CR1^{GFP}/PGRP-S^{dsRed} double transgenic mice were generated as previously described [23], and maintained in vivaria at the University of California Riverside (UCR). Briefly, GFP-expressing Cx3cr1^{tm1Litt} mice from Jackson Laboratory (Bar Harbor, ME) were crossed with PGRP-S dsRed transgenic mice. Colonies of wild-type C57BL/6 and RFP-expressing transgenic Ccr2$^{tm2.1Ifc}$ mice were obtained from Jackson Laboratory and maintained in UCR vivaria. CX3CR1^{GFP}/CCR2^{RFP} mice were generated by crossing Cx3cr1^{tm1Litt} mice and Ccr2$^{tm2.1Ifc}$ mice, originally obtained from Jackson Laboratory. All animal procedures were approved by the UCR Institutional Animal Care and Use Committee https://or.ucr.edu/ori/committees/iacuc.aspx; protocol A-20180023.

Nippostrongylus brasiliensis (Nb) culture, infection, and ATP assay

Nb life cycle was maintained in Sprague-Dawley rats obtained from Harlan Laboratories (Indianapolis, IN). L3 stage infective Nb larvae were extracted from feces of previously infected rats. Mice were subject to subcutaneous injection of 500 L3 Nb or PBS for naïve groups. Mice were euthanized and tissue was harvested at days 3, 4, 7, 10, and 29 post-infection. Nb eggs in feces of infected mice were quantified using a McMaster chamber between days 6-10 after infection. To enumerate and extract L5 stage Nb, small intestines of infected mice were cut longitudinally and incubated in PBS for ≥ 2 hours at 37°C. Following extraction from the small intestine Nb were washed 3 times, then homogenized

in PBS. ATP levels were quantified in Nb homogenates using CellTiter-Glo Luminescent Cell Viability Assay (Promega; Madison, WI), according to the manufacturer's instructions.

Immunofluorescence

Lungs were inflated through the trachea with a solution containing ⅓ 1% PFA/30% sucrose and ⅔ optimal cutting temperature (OCT) compound (Sakura Finetek USA; Torrance, CA), then placed in 4% PFA/30% sucrose for 2 hours at room temperature. Following fixation, lung tissue was embedded into OCT and sectioned at 10µm. Lung sections were treated overnight with StartingBlock Blocking Buffer (ThermoFisher Scientific; Waltham, MA). Endogenous GFP and DsRed were visualized in mounting medium with DAPI (VECTASHIELD; Burlingame, CA) using a 20x objective on an epifluorescent microscope.

Flow cytometry analysis and cell sorting

Lung tissue was minced, then incubated with 30µg/mL DNAse I (Sigma-Aldrich; St Louis, MO) and 1mg/mL Collagenase/Dispase (Roche Diagnostics; Indianapolis, IN) for 30 minutes in a 37°C shaking incubator. Single-cell suspensions were obtained by passing digested tissue over a 70µm cell strainer. Whole blood was collected from the mesenteric vein and mixed with 4% Sodium citrate. Leukocytes were separated from whole blood using Histopaque 1077 (Sigma-Aldrich). Cells were blocked with 25µg/mL of Rat IgG and anti-CD16/32 (clone 2.4G2; BD Biosciences; San Jose, CA), then stained for flow

cytometry analysis with CD11b (M1/70), CD11c (N418), F4/80 (BM8), Ly6C (HK1.4), MHC II (AF6-120.1), NK1.1 (PK136) from eBioscience (San Diego, CA); CD206 (MR5D3) from Bio-Rad (Hercules, CA); biotinylated Siglec F from R&D Systems (Minneapolis, MN); and CD3 (145-2C11), CD4 (RM4-5), Ly6G (IA8) from BD Biosciences (San Jose, CA). For flow cytometry cell sorting, cells were blocked as above and stained with CD11c and Ly6C. Data for analysis were collected using an LSRII (Becton Dickinson; Franklin Lakes, New Jersey); sorted cells were collected using FACSAria (Becton Dickinson), with over 90% purity of the post-sorted cells. Data were analyzed using FlowJo v10.7.1 (Tree Star, Ashland, OR).

RNA Sequencing Bioinformatics Analysis

Flow cytometry-sorted cells were collected in RLT buffer (Qiagen; Hilden, Germany), and RNA was extracted and DNAse-treated using RNeasy Mini Kit (Qiagen) according to the manufacturer's protocol. cDNA libraries were synthesized using Clontech SMARTer Stranded RNA-Seq kit (Mountain View, CA) with multiplexing primers. Quality of RNA and cDNA libraries were analyzed using 2100 BioAnalyzer (Agilent Technologies; Santa Clara, CA), then samples were sequenced with Illumina HiSeq2500 (San Diego, CA). Quality reports of RNA-Seq reads were generated using FASTQC (version 0.11.5), and reads were trimmed using TrimGalore (version 0.4.1) (http://www.bioinformatics.babraham.ac.uk/projects/trim_galore/) ensuring a minimum Phred Quality Score of at least 20, read lengths of at least 50 base pairs and removing any remaining adapters. The trimmed reads were then aligned to Mus musculus genome

(GRCm38) from Ensembl using splice aware short read aligner Bowtie2/TopHat in a strand-specific manner [24, 25]. Gene level counts were summarized based on Ensembl gene annotations (GRCm38.84) using GenomicRanges package in R [26], counting reads that align to exonic regions only. Raw gene expression data have been submitted to NCBI GEO (SRA Project PRJNA744529). Differential gene expression (DEG) analysis was performed using edgeR package in R [27]. Briefly, genes with 0 counts in more than 50% of samples analyzed (lowly expressed genes) were excluded from differential testing. Data were normalized using TMM (Trimmed Mean of Means) normalization to account for compositional differences in libraries. Overall dispersion and differential metrics were computed using negative binomial GLM (Generalized Linear Models) functions in edgeR. DEGs were defined as those with fold change ≥ 1 and a false discovery rate (FDR) of ≤ 5%. Heatmaps were generated after normalizing raw counts using the RPKM (Reads Per Kilobase per Million Mapped Reads) method [28]. Functional enrichment of these DEGs was completed using DAVID Functional Annotation Tools to identify over-representative gene ontologies (GO) and KEGG pathways of interest (FDR ≤ 5%) [29].

In vitro Nb motility and cellular adherence, and cytokine quantification

$Ly6C^+$ and $CD11c^+$ cells from Nb-infected lungs of $CX3CR1^{+/+}$ and $CX3CR1^{GFP/GFP}$ were enriched with magnetic assisted cell sorting (MACs) using biotinylated Ly6C (HK1.4; Abcam) and Streptavidin microbeads, or CD11c microbeads (Miltenyi Biotech; San Diego, CA), which resulted in ~70% purity. $0.25x10^6$ cells were plated in 48 well plates with 25 L3 stage Nb in the presence of 1:50 serum from the day 7 infected corresponding mouse

group (WT serum for WT cells and KO serum for KO cells) according to previously reported methodologies [30]. Cells and Nb larvae were co-cultured for 4 days at 37°C. Nb motility was assessed as previously described,[31] and cellular adherence was quantified by counting numbers of cells attached to each worm (n=6 per group, 3 replicate wells). Culture supernatants were collected for cytokine quantification by cytokine bead array, inflammation panel (Thermoscientific).

Statistical Analysis

Values are reported as means ± standard error of the mean (SEM). Multiple experiments were performed and combined for final data analysis, and data were analyzed by the unpaired t-test for 2-group comparison or one-way ANOVA for multiple groups comparison followed by post-Tukey or Dunnett's multiple comparison test where appropriate using Graphpad Prism 9 (Graphpad Software, La Jolla, CA). For data collected over several time points, two-way ANOVA with post-Tukey or Sidak's multiple comparison test was performed. Comparisons with P values less than 0.05 were considered statistically significant.

Acknowledgments

These studies were supported by the National Institutes of Health/NIAID (R01AI153195 to MGN; R01AI091759 to MGN and MB). The authors would like to thank David D. Lo for provision of the PGRPredCx3CR1GFP transgenic mice; Spencer H. Wang, Jessica C. Jang, and Hashini M. Batugedara for assistance with experiments; Holly Eckelhoefer and

John Weger of the UC Riverside Genomics core (Riverside, CA) for assistance with cell sorting and RNA sequencing.

Results

Dynamic changes in CX3CR1-expressing myeloid cells and PGRP-expressing eosinophils in the helminth-infected lung.

The transgenic reporter GFP knock-in/knock out CX3CR1 (Cx3cr1) mouse offers the opportunity to track myeloid cells and investigate the function of CX3CR1 signaling,[32] while the dsRedPGRP-S (Pglyrp1) mice, in which the dsRed transgene, under the control of the Pglyrp1 promoter, is integrated into the genome, are reporters for a peptidoglycan recognition protein present in neutrophil granules [22, 23]. We generated dual reporter transgenic mice, $CX3CR1^{GFP/+}PGRP^{dsRed}$ to determine their utility in tracking innate cells in helminth infection. Immunofluorescent imaging of lung and small intestine cryosections demonstrated strong GFP and dsRed signal in cells within the lung parenchyma and lamina propria of the small intestine (Figure 14A). Comparison of cryosections from naive or day 7 post-*Nippostrongylus* infection, when the adult parasites are present in the small intestine [33], revealed infection-induced infiltration of reporter cells. This was particularly evident in the lung, reflecting the inflammatory response to the transient migration (day 2-3 post-infection) of the helminth parasites, which is evident even after the parasite has left the lung (day 3-4 post-infection). CX3CR1-positive cells were increased in the infected lungs but not the intestine, while PGRP-positive cells were increased in the lung and to a lesser extent in the small intestine. Given that these innate reporter cell subsets had not previously been investigated in pulmonary helminth infection, we utilized flow cytometry to characterize these subsets in the lung and determine their kinetics over the course of helminth infection. Flow cytometric analysis

of single-cell suspensions from naive or infected CX3CR1$^{GFP/+}$PGRP^{dsRed} mice showed distinct single and double GFP/dsRed positive cells following infection (Figure 14B). Further gating and overlay with reporter negative wild-type (WT) mice revealed that the double-positive cells were in fact artifacts consisting of autofluorescent alveolar macrophages (Figure 14B and Figure 16A-C). This is consistent with prior studies showing that alveolar macrophages do not express CX3CR1 [32], therefore we gated out these cells in subsequent analysis. The CX3CR1^{+} cells from the infected lungs were composed of three main subsets: CD11c^{+} dendritic cells (DC), interstitial macrophages (IM), and Ly6C^{+} monocytes with minimal contributions from CD3^{+} T cells and NK1.1^{+} Natural Killer (NK) cells (Figure 16D).

PGRP is reported to be a granule protein found in neutrophils and M cells [22, 23]. Unexpectedly, we observed that most of the PGRP^{+} cells in the infected lung, especially at day 7 post-infection were in fact eosinophils, followed by neutrophils (Figure 14B and Figure 16C). To evaluate if the reporter protein was effective for live cell imaging, lung cells were isolated from Nb-infected CX3CR1$^{+/+}$PGRP^{Neg}, CX3CR1$^{+/+}$PGRP^{DsRed}, and CX3CR1$^{+/GFP}$PGRP^{DsRed} mice and co-cultured with Nb L3 larvae. CX3CR1 and PGRP single-positive cells exhibited strong signal and bound to the larvae suggesting that these reporter mice are also a valuable tool to image myeloid and granulocyte subsets (Fig 14C).

Flow cytometry analysis at various timepoints post-infection showed that both CX3CR1^{+} cells and PGRP^{+} cells peaked at day 7 post-infection in the lung (Figure 15A). The frequency of CX3CR1^{+}CD11c^{+} cells in the lung increased 11 times (1% to 11%), and

CX3CR1^{+} monocytes increased 2.5 times (2% to 5%) at day 7 post-infection compared to naive mice. Lung eosinophils in the PGRP^{+} cell subset were also significantly increased (5-fold) at day 7 post-infection, but there were no significant differences in the frequency of these cells in the blood (Figure 15B), indicating that infection-induced changes in these subsets occurred mostly at the infection site. These significant changes in eosinophils and CX3CR1^{+} myeloid cells were transient, with recovery to naive frequencies at day 10 post-infection. Together, this data shows dynamic changes in lung innate effector cells in response to helminth infection. These included significant but transient increases in myeloid cells and eosinophils, which can be efficiently tracked by transgenic mouse reporters for CX3CR1 and PGRP respectively.

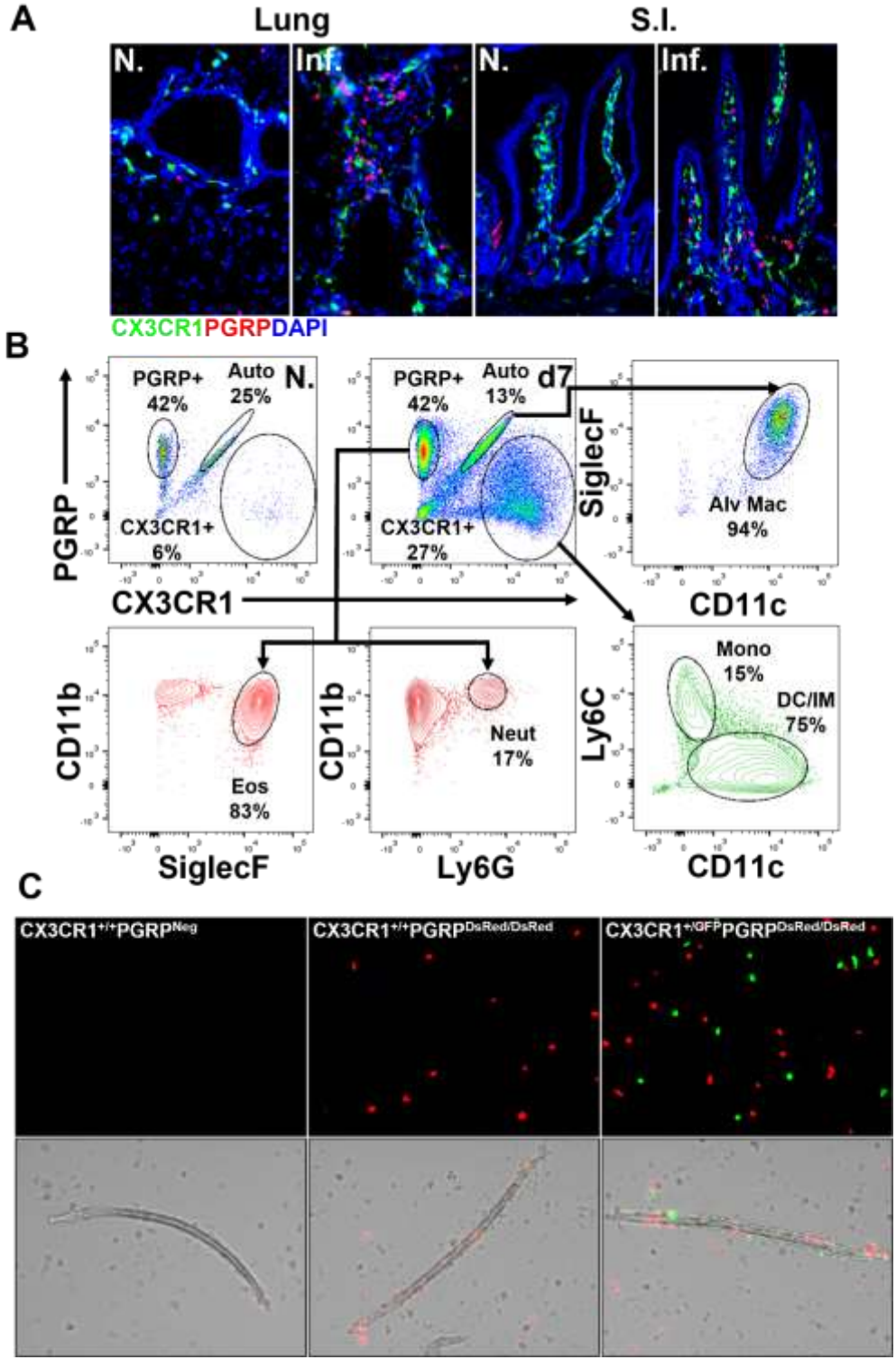
A
Lung
S.I.
N.
Inf.
N.
Inf.
CX3CR1PGRPDAPI
B
PGRP+
42%
Auto
25%
N.
CX3CR1+
6%
PGRP
CX3CR1
PGRP+
42%
Auto
13%
d7
CX3CR1+
27%
SiglecF
Alv Mac
94%
CD11c
CD11b
Eos
83%
SiglecF
CD11b
Neut
17%
Ly6G
Ly6C
Mono
15%
DC/IM
75%
CD11c
C
CX3CR1+/+PGRPNeg
CX3CR1+/+PGRPDsRed/DsRed
CX3CR1+/GFPPGRPDsRed/DsRed

Figure 14. *Nippostrongylus* infection induces lung infiltration of CX3CR1^{+} myeloid cells and PGRP^{+} eosinophils. CX3CR1$^{+/GFP}$/PGRP^{dsRED} transgenic mice were infected with 500 L3 *Nippostrongylus*, followed by analysis of lung and blood at day 7 post-infection. **(A)** CX3CR1-GFP and PGRP-DsRed signal in frozen lung and small intestine (S.I.) sections. **(B)** Temporal changes in CX3CR1 and PGRP cell populations were assessed by flow cytometry. **(C)** Lung cells were isolated from CX3CR1$^{+/+}$PGRP^{Neg}, CX3CR1$^{+/+}$PGRP^{DsRed}, and CX3CR1$^{+/GFP}$PGRP^{DsRed} mice at 7 days post-infection, and co-cultured with *Nb* L3 larvae. Data are representative of 2 experiments in (A and B) and of 1 experiment in (C).

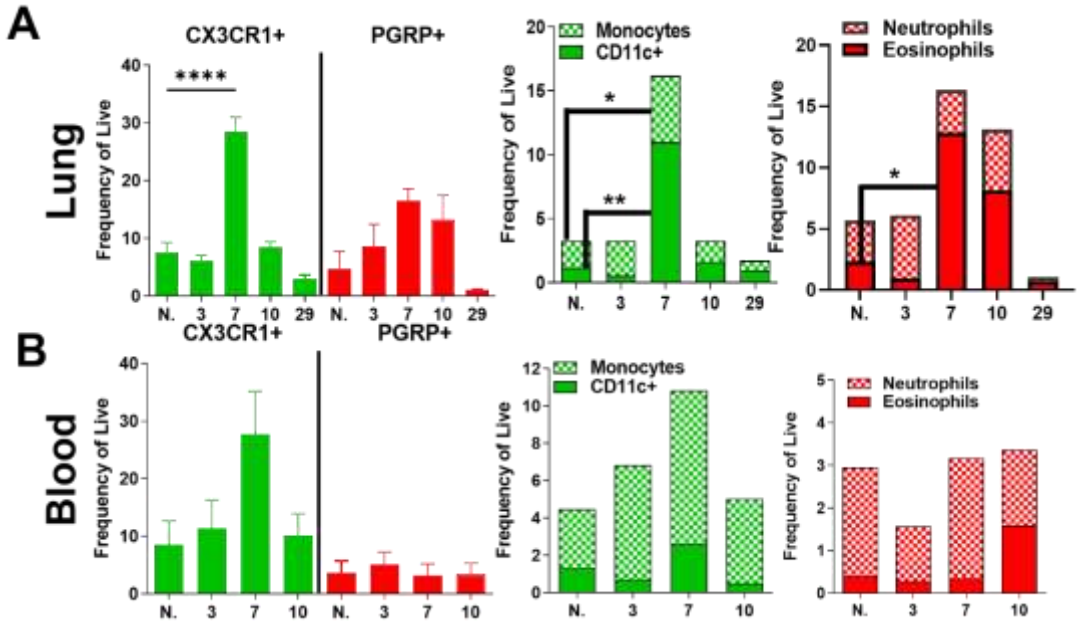

Figure 15. The recruitment of CX3CR1+ monocytes and CD11c+ cells peaked at day 7 post-infection. CX3CR1$^{+/GFP}$/PGRP^{DsRed} transgenic mice were infected with 500 *Nippostrongylus* L3, followed by analysis of lung and blood at various time points post-infection. (A-B) CX3CR1 and PGRP populations and subpopulations were quantified in (A) the lung and (B) blood. Values represent means ± SEM (n = 3-6 animals per time point), and data are representative of 2 experiments. One-way ANOVA with Dunnett's multiple comparison test and two-way ANOVA with post-Tukey multiple comparison test were performed, and P values less than 0.05 were considered statistically significant. (*, P≤ 0.05; **, P≤ 0.01; ***, P≤ 0.001; ****, P≤ 0.0001)

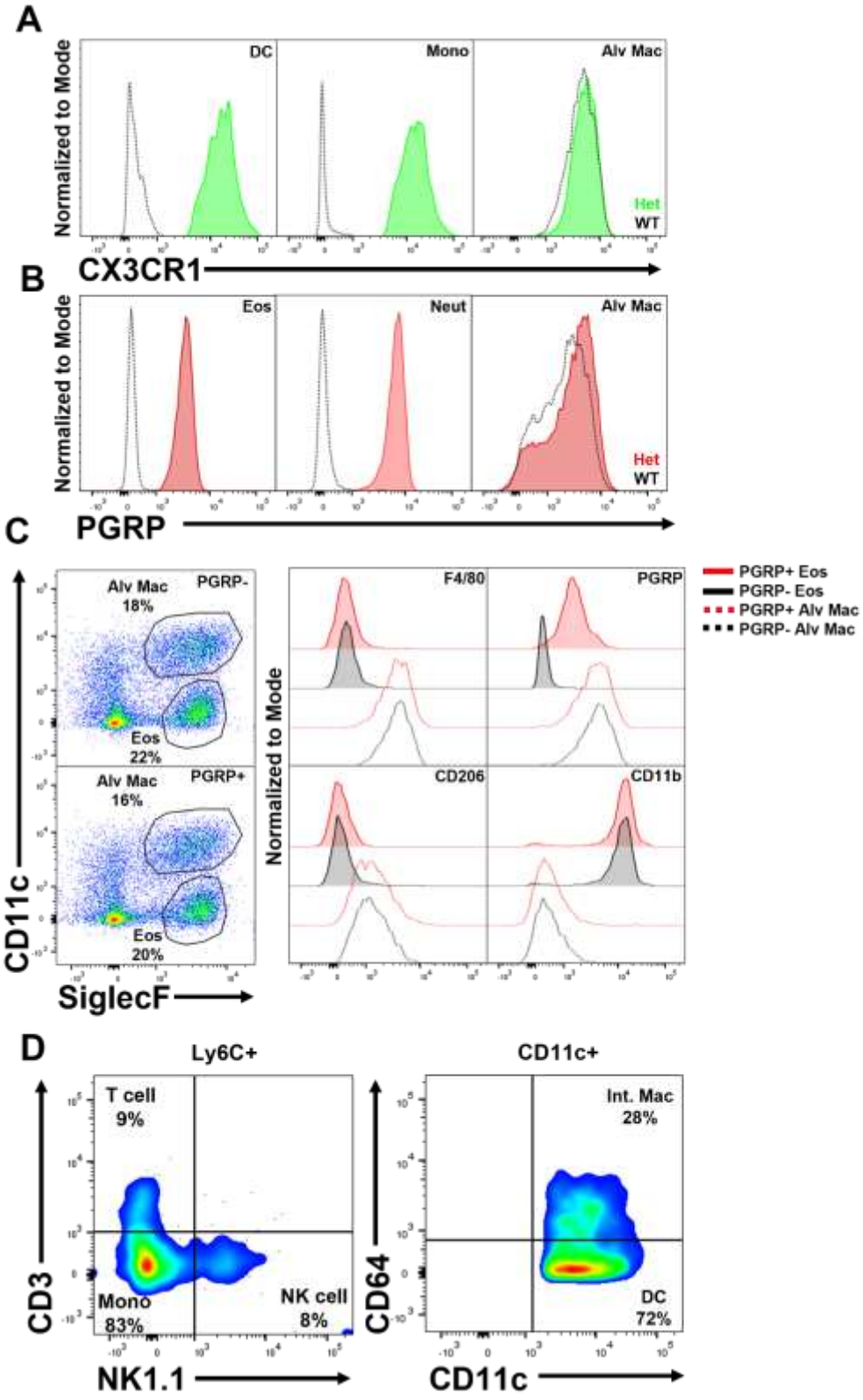
A
DC
Mono
Alv Mac
Normalized to Mode
Het
WT
CX3CR1
B
Eos
Neut
Alv Mac
Normalized to Mode
Het
WT
PGRP
C
Alv Mac
18%
PGRP-
Eos
22%
Alv Mac
16%
PGRP+
Eos
20%
CD11c
SiglecF
F4/80
PGRP
CD206
CD11b
Normalized to Mode
PGRP+ Eos
PGRP- Eos
PGRP+ Alv Mac
PGRP- Alv Mac
D
Ly6C+
T cell
9%
Mono
83%
NK cell
8%
CD3
NK1.1
CD11c+
Int. Mac
28%
DC
72%
CD64
CD11c

Figure 16. Characterization of CX3CR1^{+} cells and PGRP^{+} cells in the lung.

CX3CR1$^{+/GFP}$/PGRP^{dsRED} (Het) transgenic mice and control wild-type (WT) mice were infected with 500 L3 *Nippostrongylus*, followed by analysis of lung at day 7 post-infection. **(A)** CX3CR1 expression, represented as median fluorescence intensity (MFI), was compared in dendritic cells, monocytes, and alveolar macrophages. **(B-C)** MFI of PGRP was compared in eosinophils, neutrophils, and alveolar macrophages. **(D)** Cell types in CX3CR1^{+}Ly6C^{+} and CX3CR1^{+}CD11c^{+} cells were analyzed at day 7 after infection by flow cytometry. Data are representative of 2 experiments.

CX3CR1-deficient mice show improved outcomes to Nippostrongylus infection.

To determine the role of CX3CR1 signaling in helminth infection, wild-type (WT) and CX3CR1$^{GFP/GFP}$ (KO) mice were infected with *Nippostrongylus*. Both WT and KO mice exhibited infection-induced weight loss at days 2 and 3 post-infection (Figure 17A), consistent with the pathologic consequence of parasite migration through the lung. However, KO mice had ameliorated outcomes with significantly reduced infection-induced weight loss compared to WT mice. Since a higher weight loss is typically associated with stronger inflammatory responses, the number of immune cells in the lung was enumerated (Figure 17B). Consistent with the reduced weight loss, lung leukocyte counts were significantly lower in KO mice. Different immune cell populations in the lung were analyzed by flowcytometry, and monocytes, alveolar macrophages, and CD11c^{+} cells were significantly decreased in infected KO mice, which is consistent with the importance of CX3CR1 signaling for myeloid subset recruitment (Fig 17C). Although there was a significant increase in eosinophil frequency in KO mice, there were no differences in lung eosinophil or neutrophil numbers between WT and KO mice. The expression of CD206 (mannose receptor), a surrogate for M2 macrophage activation [34], was significantly increased in alveolar macrophages and in CD11c^{+} cells from KO mice compared to WT mice, suggesting increased M2 polarization in the absence of CX3CR1 signaling. M2 polarized macrophages are important effector cells against lung migrating larvae such as *Nippostrongylus* [6, 9], therefore we tested the hypothesis that KO mice may have improved innate responses to *Nippostrongylus* leading to reduced parasite burdens. Intestinal worm counts at day 7 post-infection confirmed an almost 3-fold

decrease in worm burdens and an 8-fold decrease in fecal egg counts (Figure 17D). This was associated with decreased parasite viability, measured by ATP quantification of adult worms recovered from the intestine.

We tested whether this protective effect was specific for CX3CR1 deficiency, or if deficiency in myeloid cell recruitment through another chemokine receptor such as CCR2, also resulted in lower lung leukocyte infiltration and parasite burdens. CCR2 deficiency ($CCR2^{RFP/RFP}$) did not have any significant effect on infection-induced weight loss or worm burden (Figure 18A and B). This was despite significantly reduced lung leukocyte numbers and strikingly decreased infiltration of monocytes (33-fold) (Figure 18C), which validated the mice and confirmed that monocyte responses were CCR2-dependent. Additionally, CCR2 deficiency resulted in reduced frequency and numbers of alveolar macrophages, which may reflect deficiencies in monocyte-derived alveolar macrophages which have been identified in response to lung infection [35, 36]. Nonetheless, we observed significantly increased surface expression of CD206 in CCR2-deficient alveolar macrophages suggesting that CCR2 deficiency, similar to CX3CR1 deficiency, may also cause M2 macrophage activation. We validated the CCR2 reporter, showing that $Ly6C^{+}$ monocytes were RFP-positive (Figure 18D). Thus, deficiency in CCR2 signaling did not significantly affect worm clearance although this receptor was important for recruiting monocytes and influenced macrophage M2 polarization. In contrast, CX3CR1 signaling had an unexpected and detrimental role in helminth infection, where it promoted lung myeloid cell responses and infection-induced pathology, but impaired M2 macrophage activation and optimal worm clearance.

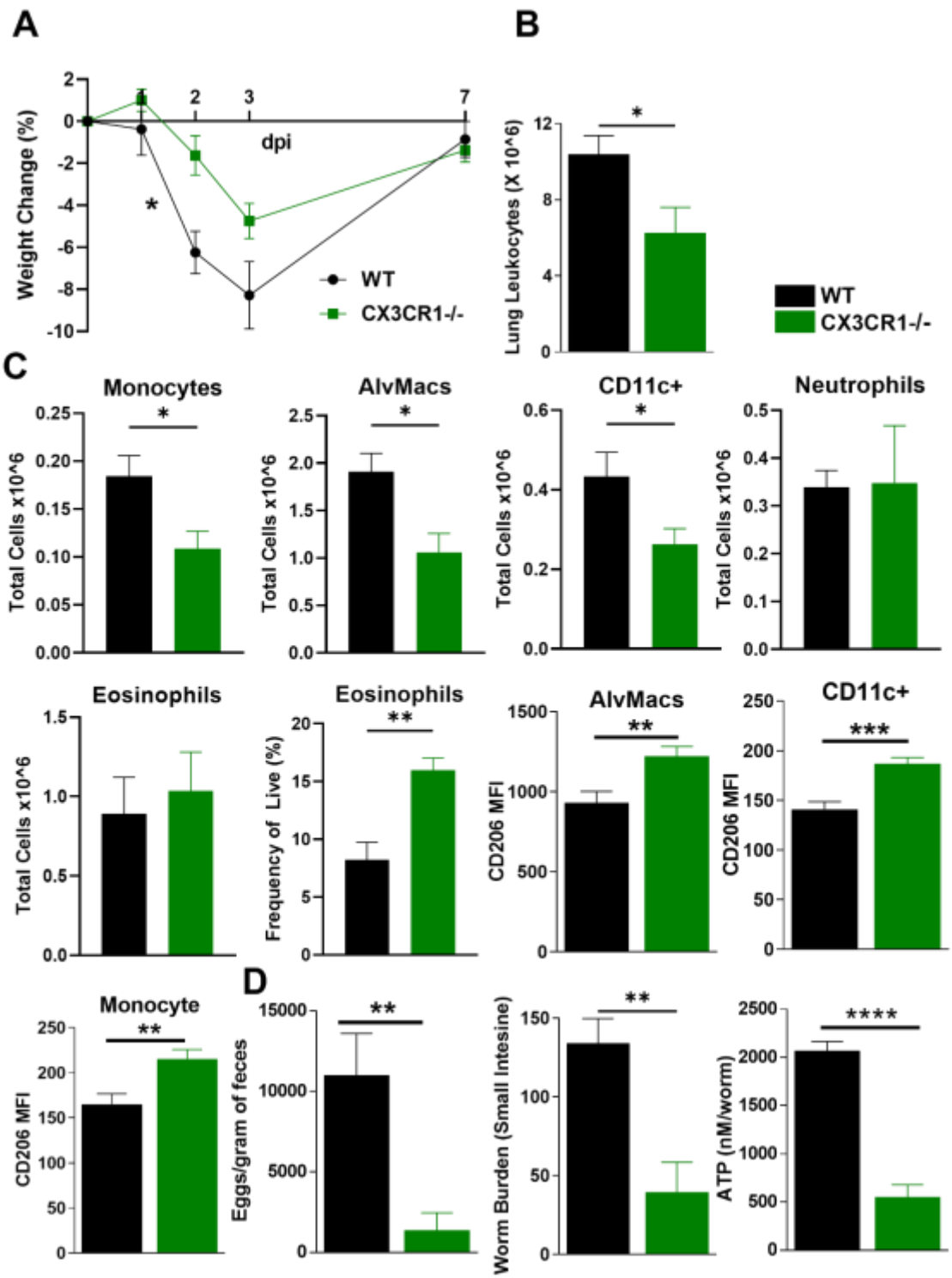
A
Weight Change (%)
dpi
WT
CX3CR1-/-
B
Lung Leukocytes (X 10^6)
WT
CX3CR1-/-
C
Monocytes
AlvMacs
CD11c+
Neutrophils
Eosinophils
Eosinophils
AlvMacs
CD11c+
Total Cells x10^6
Frequency of Live (%)
CD206 MFI
D
Monocyte
Eggs/gram of feces
Worm Burden (Small Intesine)
ATP (nM/worm)

Figure 17. CX3CR1 deficiency reduces *Nippostrongylus* parasite burden and decreases infection-induced weight loss and lung leukocyte infiltration. CX3CR1 wild-type (WT) or CX3CR1$^{GFP/GFP}$ (-/-) mice were infected subcutaneously with 500 *Nippostrongylus* L3. (A) Infection-induced weight loss compared to pre-infection weight was calculated at multiple time points. (B) Total lung leukocytes were enumerated. (C) Myeloid and granulocyte subsets were determined and CD206 median fluorescence intensity (MFI) in alveolar macrophages, monocytes and CD11c^{+} lung cells were evaluated by flow cytometry. (D) Parasite burden was evaluated at day 7 post-infection by fecal egg count, intestinal worm count and measurement of worm viability by ATP quantification of adult worms dissected from the small intestine. Values represent means ± SEM (n = 6-7 per group), and data is representative of 3 experiments. Two-way ANOVA with post-Sidak multiple comparison test and the unpaired t-test were performed, and P values less than 0.05 were considered statistically significant. (*, P≤ 0.05; **, P≤ 0.01; ***, P≤ 0.001; ****, P≤ 0.0001)

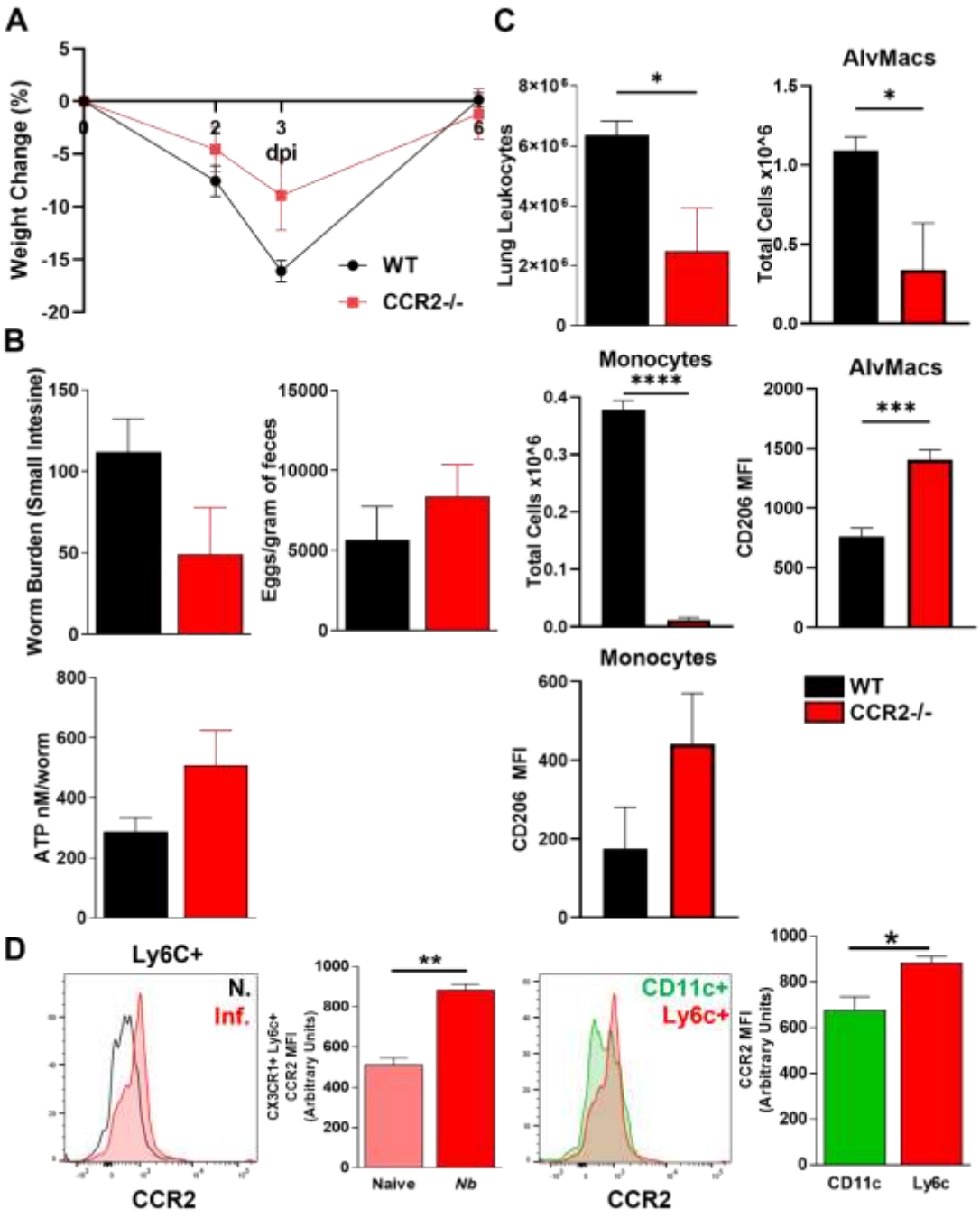
A
Weight Change (%)
dpi
WT
CCR2-/-
B
Worm Burden (Small Intesine)
Eggs/gram of feces
ATP nM/worm
C
Lung Leukocytes
AlvMacs
Total Cells x10^6
Monocytes
CD206 MFI
WT
CCR2-/-
D
Ly6C+
N.
Inf.
CCR2
CX3CR1+ Ly6c+ CCR2 MFI (Arbitrary Units)
Naive
Nb
CD11c+
Ly6c+
CD11c
Ly6c

Figure 18. Lack of CCR2 does not protect against Nb-induced pathology. CCR2 wild-type (WT) or $CCR2^{RFP/RFP}$ (-/-) mice were infected subcutaneously with 500 *Nippostrongylus* L3. **(A)** Infection-induced weight loss compared to pre-infection weight was calculated at multiple time points. **(B)** Parasite burden was evaluated at day 7 post-infection by fecal egg count, intestinal worm count and measurement of worm viability by ATP quantification of adult worms dissected from the small intestine. **(C)** Total lung counts for total leukocytes, and myeloid subsets were determined and CD206 median fluorescence intensity (MFI) in alveolar macrophages and $CD11c^+$ monocytes were evaluated by flow cytometry. **(D)** CCR2-RFP expression, represented as median fluorescence intensity (MFI), was compared in naïve and infected $CX3CR1^+$ $Ly6C^+$ cells, as well as infected $CX3CR1^+$ CD11c and $CX3CR1^+$ $Ly6C^+$ cells. Values represent means ± SEM (n = 4 per group) and data are representative of one experiment. Two-way ANOVA with post-Sidak multiple comparison test and the unpaired t-test were performed, and P values less than 0.05 were considered statistically significant. (*, $P \leq 0.05$; **, $P \leq 0.01$; ***, $P \leq 0.001$; ****, $P \leq 0.0001$)

CX3CR1-deficient Ly6C$^+$ monocytes are more active against the Nippostrongylus parasites and secrete more proinflammatory cytokines.

Both CCR2 and CX3CR1 deficiency led to decreased myeloid cell recruitment in the lung, however, the reduced parasite burden in CX3CR1 KO mice suggests that CX3CR1 signaling may have functional effects beyond its chemotactic function that impairs the innate immune response to parasitic worms. Given that Ly6C$^+$ monocytes and CD11c$^+$ myeloid cells were the main CX3CR1$^+$ cells in the lung at day 7 post-infection (see Figure 14), we investigated if CX3CR1 deficiency in these subsets affected their effector function against *Nippostrongylus* parasites. In in vivo infection, *Nippostrongylus* infectious L3 larvae migrate to the lung triggering innate effector cells, therefore we investigated this lung cell interaction in vitro by co-culture of lung cells with *Nippostrongylus* L3 parasites based on previously established methodologies [30]. CD11c$^+$ and Ly6C$^+$ cells were enriched by magnetic bead purification of dissociated lung cells from day 7-infected CX3CR1 WT and KO mice followed by co-culture with L3 *Nippostrongylus* larvae (Figure 19A). Microscopic visualization of co-cultures at day 3 revealed that both WT and KO CD11c$^+$ cells were effective at binding the larval parasite. In comparison, WT Ly6C$^+$ monocytes showed minimal larval binding, while KO Ly6C$^+$ monocytes exhibited strikingly increased adherence to the worm (Figure 19B). Quantification of cell numbers per worm confirmed a more than 4-fold increase in binding of KO Ly6C$^+$ compared to WT Ly6C$^+$ monocytes, with no significant difference between WT and KO CD11c$^+$ cells (Figure 19C). We evaluated the outcome of enhanced cell binding by quantifying larval motility, and confirmed that co-culture with cells from

all four groups led to reduced larval motility compared to larvae cultured alone. Co-culture with Ly6C^{+} KO monocytes resulted in significantly reduced larval motility compared to WT monocytes, consistent with more efficient binding to the worm. Measurement of proinflammatory cytokines in the co-culture supernatants revealed that KO monocytes secreted 10-fold more TNFα and IL-6, and 20-fold more MCP-1 than WT monocytes (Figure 19D). In contrast, there was no difference between WT and KO CD11c^{+} cells, nor differences in secretion of IFNγ, IL-10 or IL-12 in any of the groups (data not shown). We investigated if addition of live *Nippostrongylus* larvae was necessary for this cytokine production by lung cells in the co-culture, but observed that there were no significant differences in cytokine production between lung cells alone, or cells incubated with *Nippostrongylus* larvae (Figure 19E and data not shown). Together, our data indicate that CX3CR1 deficiency has targeted effects on monocytes infiltrating the helminth-infected lung, including increased proinflammatory cytokines and adherence to the parasite, which leads to improved effector responses against the parasite.

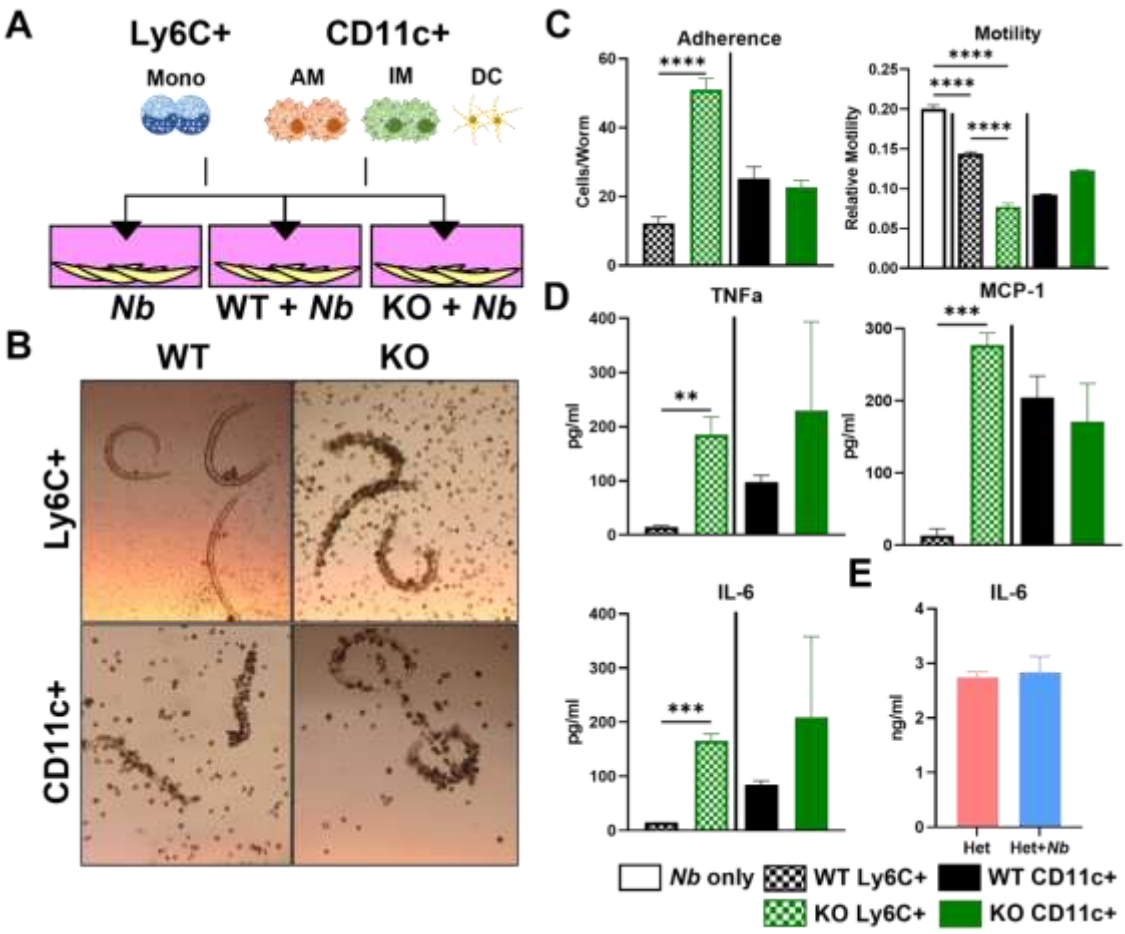
A
Ly6C+
CD11c+
Mono
AM
IM
DC
Nb
WT + Nb
KO + Nb
B
WT
KO
Ly6C+
CD11c+
C
Adherence
Cells/Worm
Motility
Relative Motility
D
TNFa
pg/ml
MCP-1
pg/ml
IL-6
pg/ml
E
IL-6
ng/ml
Het
Het+Nb
Nb only
WT Ly6C+
WT CD11c+
KO Ly6C+
KO CD11c+

Figure 19. CX3CR1-deficient Ly6c+ monocytes secrete more proinflammatory cytokines and actively bind *Nippostrongylus* L3 parasites. (A) Schematic representation of magnetic assisted cell sorting (MACs) of cells from CX3CR1 wild-type (WT) and CX3CR1$^{GFP/GFP}$ (KO) *Nippostrongylus*-infected lungs, and co-culture with L3 *Nippostrongylus* parasites. (B) Representative micrographs of Ly6c+ and CD11c+ cells from WT or KO mice adhered to L3 Nb. (C) Cellular adherence and relative *Nippostrongylus* motility were assessed at day 3 co-culture. (D) Cytokines and chemokines in WT and KO cell co-culture medium were measured. (E) IL-6 secretion by lung cells isolated from *Nippostrongylus*-infected CX3CR1$^{+/GFP}$PGRP^{DsRed} (Het) mice cultured with or without *Nippostrongylus* larvae. Values represent means ± SEM (n = 5 animals, n = 3-4 for cell culture replicates) and are representative of 3 experiments in (C and D) and 1 experiment in (E). The unpaired t-test was performed, and P values less than 0.05 were considered statistically significant. (*, P≤ 0.05; **, P≤ 0.01; ***, P≤ 0.001; ****, P≤ 0.0001)

RNA expression profiling of Ly6C$^+$ and CD11c$^+$ subsets reveals Nippostrongylus-induced and CX3CR1-dependent changes particularly in lung Ly6C$^+$ monocytes

Our previous data identified an unexpected role for CX3CR1 signaling in the lung in impairing effector responses to helminth parasites, therefore we investigated potential differences between CX3CR1$^{+/GFP}$ (Het) and CX3CR1$^{GFP/GFP}$ (KO) lung by RNA-sequencing analysis, focusing on Ly6C$^+$ and CD11c$^+$ cells as the main CX3CR1-expressing subsets in the lung. PGRP$^+$CX3CR1 Het and KO mice were infected with *Nippostrongylus* L3, and we validated, as before, reduced parasite burden and lung leukocyte counts in the KO mice (Figure 21A). To determine infection-induced changes in the CX3CR1-expressing subsets, we also examined PBS-treated Het mice. At day 7 post *Nippostrongylus* infection, CX3CR1$^+$GFP$^+$ subsets were sorted based on Figure 20A, where the gating strategy included removing PGRP$^+$ cells to minimize contamination from granulocytes and alveolar macrophages. We evaluated gene expression changes between naïve and infected groups, CD11c$^+$ and Ly6C$^+$ cells, and CX3CR1-Het and KO genotype. Ly6C$^+$ cells exhibited the most differential gene expression according to infection status (naïve vs infected, n=180) and according to genotype (CX3CR1 Het vs KO, n=20) (Figure 20B). Functional enrichment of differentially expressed genes in CX3CR1-expressing Ly6C$^+$ monocytes from naïve or infected lungs revealed that *Nippostrongylus* infection was associated with changes in genes involved with migration (e.g. regulation of cell migration, monocyte chemotaxis), inflammation (e.g. inflammatory response, cellular response to TNF), and tissue remodeling (e.g. collagen fibril organization, angiogenesis, ECM receptor interaction)

(Figure 20C and D). Heatmap of the most differentially expressed genes in monocytes following infection suggests infection-induced increases in chemokines (*Ccl12, Ccl24, Ccl7, Cxcl16*) and matrix metalloproteinases (*Mmp14, Mmp19, Timp1*), indicating that monocytes were involved in promoting leukocyte recruitment to the infected tissue and in tissue remodeling (Fig 20E). In contrast, several collagen-encoding genes were downregulated upon infection (*Col1a1, Col1a2, Col14a1*), suggesting decreased function in collagen matrix deposition.

When comparing Cx3CR1 Het and KO Ly6C+ monocytes sorted from infected lungs, most DEG were upregulated in Ly6C$^+$ KO cells, and indicated enhanced chemotactic and cytotoxic responses. These included *Ugcg*, *Sh2d2a, Eomes*, *Gzma* and *Gzmb*, which are associated with innate and adaptive effector cell responses, especially cytotoxic NK and CD8 T cell function [37-39]. y6C$^+$ KO cells expressed significantly decreased *Maged1,* a gene identified in NK cells which triggers cell death. Downregulation of this gene may suggest the increased longevity of the CX3CR1-deficient monocytes [40, 41]. *Ets1*, which mediates vascular inflammation and remodeling, was upregulated in KO Ly6C$^+$ cells. Ets-1 is a known activator of CCL2, which supports the increased monocyte activity in the co-culture data [42, 43]. Unexpectedly, *Ccl3* was also significantly reduced in KO Ly6C$^+$ cells, which is in contrast to the significantly upregulated secretion of another chemokine, MCP-1/CCL2, in the co-cultures. This result may reflect differences between RNA and protein levels, the different chemokines, or differences between the *in vivo* versus *in vitro* environment. Cytotoxic genes are usually expressed in CD8 and NK cells and not typically in

monocytes, however, the flow cytometry characterization suggested that Ly6C^{+}CX3CR1^{-} expressing subset had minimal contamination from these cytotoxic effector subsets (see Figure 16D). To investigate this further, we utilized ImmQuant for digital cell quantification of the RNA-seq datasets based on the immunological genome (Figure 22) [44]. Overall, the top cell hits for the sorted Ly6C^{+} subsets were monocytes from various lymphoid tissues. Although most of the datasets used for ImmQuant reflect naive conditions and lymphoid organs, these findings support our sorting strategy for monocytes. While Ly6C^{+} cells from infected Het mice did not show similarities to NK nor CD8 T cells, KO Ly6C^{+} cells matched NK and CD8 T cell subsets, albeit at a lower score than that for monocytes. It is possible that the Ly6C^{+} KO cells may be monocytes that acquire NK and CD8 T cell cytotoxic characteristics in the absence of CX3CR1 signaling. Alternatively, there may be more contamination of CD8 and NK cells in the KO subset. Despite these caveats, our data indicate that CX3CR1 deficiency promotes cytotoxic functions, which may be linked to the improved immunity and damage to the *Nippostrongylus* parasites.

Compared to monocytes, there were minimal gene expression changes in CD11c^{+} cells, with only 65 DEG between naïve and infected groups, and no significant DEG were found between CX3CR1 Het and KO cells (Figure 21B). These findings may reflect the greater heterogeneity in the CD11c^{+} lung subsets, which would mask any significant gene expression changes. Additionally, there was no functional difference between Het and KO CD11c+ cell when co-cultured with *Nb* larvae (see Figure 22). ImmQuant analysis of the CD11c^{+} subsets supported a heterogeneous subset with gene expression profiles that

matched both DCs and macrophages from a variety of tissues including the lung (Figure 22). Comparison of DEG between Het CD11c+ cells sorted from naïve and infected lungs indicated most DEG were downregulated genes in infection (52 downregulated vs 13 upregulated). Downregulated genes were associated with proliferation (*Pou2f2*) [45], anti-inflammatory function (*CD300e*) [46], and cell adhesion (*Itga1*, *Itgb7*), suggesting that the $CD11c^+$ subset was more quiescent in the infected lungs. Interestingly, $CD11c^+$ cells from infected lungs also had reduced expression of the angiotensin-converting enzyme *Ace*, which has been reported to in pulmonary granuloma formation [47]. Overall, these results demonstrate that *Nippostrongylus* infection induces gene expression changes, especially in CX3CR1-expressing lung monocytes, associated with chemokines, inflammation, and matrix remodeling pathways. These data also identify candidate cytotoxic and adhesion molecules as effectors against the parasite.

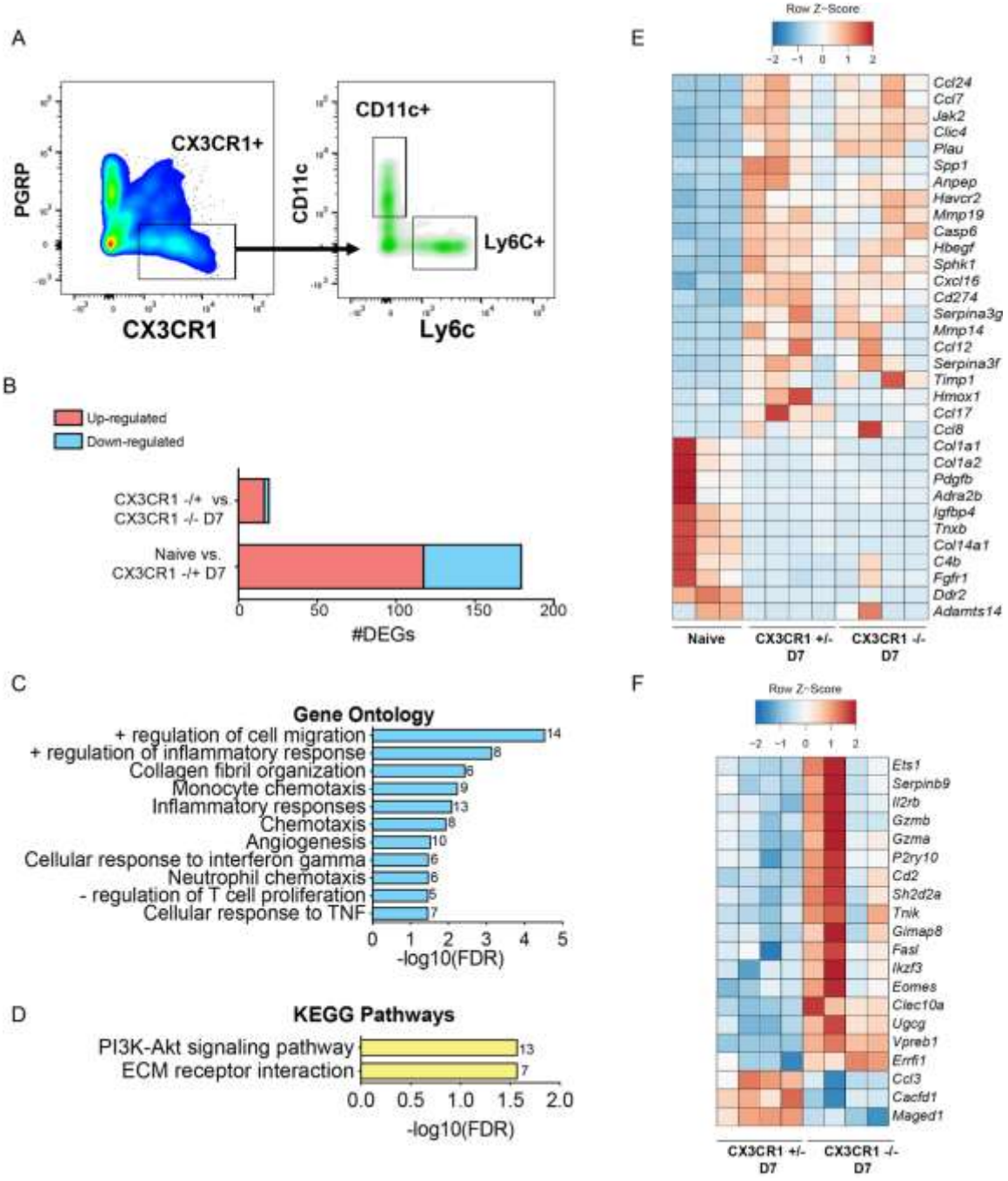
A
PGRP
CX3CR1+
CX3CR1
CD11c
CD11c+
Ly6C+
Ly6c
B
Up-regulated
Down-regulated
CX3CR1 -/+ vs.
CX3CR1 -/- D7
Naive vs.
CX3CR1 -/+ D7
0
50
100
150
200
#DEGs
C
Gene Ontology
+ regulation of cell migration
+ regulation of inflammatory response
Collagen fibril organization
Monocyte chemotaxis
Inflammatory responses
Chemotaxis
Angiogenesis
Cellular response to interferon gamma
Neutrophil chemotaxis
- regulation of T cell proliferation
Cellular response to TNF
14
8
6
9
13
8
10
6
6
5
7
0 1 2 3 4 5
-log10(FDR)
D
KEGG Pathways
PI3K-Akt signaling pathway
ECM receptor interaction
13
7
0.0 0.5 1.0 1.5 2.0
-log10(FDR)
E
Row Z-Score
-2 -1 0 1 2
Ccl24
Ccl7
Jak2
Clic4
Plau
Spp1
Anpep
Havcr2
Mmp19
Casp6
Hbegf
Sphk1
Cxcl16
Cd274
Serpina3g
Mmp14
Ccl12
Serpina3f
Timp1
Hmox1
Ccl17
Ccl8
Col1a1
Col1a2
Pdgfb
Adra2b
Igfbp4
Tnxb
Col14a1
C4b
Fgfr1
Ddr2
Adamts14
Naive
CX3CR1 +/- D7
CX3CR1 -/- D7
F
Row Z-Score
-2 -1 0 1 2
Ets1
Serpinb9
Il2rb
Gzmb
Gzma
P2ry10
Cd2
Sh2d2a
Tnik
Gimap8
Fasl
Ikzf3
Eomes
Clec10a
Ugcg
Vpreb1
Errfi1
Ccl3
Cacfd1
Maged1
CX3CR1 +/- D7
CX3CR1 -/- D7

Figure 20. RNA-sequencing analysis of lung Ly6C+ monocytes sorted from naive and infected CX3CR1$^{+/GFP}$ (Het) and Cx3CR1$^{GFP/GFP}$ (KO) mice.

CX3CR1$^{+/GFP}$PGRP^{DsRed} (Het) were injected with PBS control (naive) or infected with *Nippostrongylus* for 7 days, and compared to day 7-infected Cx3CR1$^{GFP/GFP}$ PGRP^{DsRed} (KO) mice. **(A)** Ly6c+ and CD11c+ cells within the live, single cell-gated CX3CR1 GFP+ cell populations were recovered via flow cytometry-assisted cell sorting from lung leukocytes of naïve CX3CR1$^{+/GFP}$ or infected CX3CR1$^{+/GFP}$ and CX3CR1$^{GFP/GFP}$ mice. **(B)** Bar graph summarizing transcriptional changes in monocytes - naïve CX3CR1$^{+/GFP}$ vs. infected CX3CR1$^{+/GFP}$ and infected CX3CR1$^{+/GFP}$ vs. CX3CR1$^{GFP/GFP}$ mice. X axis represents number of significantly different genes (log2 FC $\geq$ 1 and FDR $\leq$ 5%) up-regulated (red) or down-regulated (blue) under each comparison **(C-D)** Bar graphs representing functional enrichment – **(C)** Gene Ontologies (GO) and **(D)** KEGG pathways of differentially expressed genes within the naïve CX3CR1$^{+/GFP}$ group. Ontologies were predicted using DAVID (FDR $\leq$ 5%). Number of genes mapping to each term is annotated. **(E)** Clustered heatmap of DEGs discovered in naïve vs. infected CX3CR1$^{+/GFP}$ mapping to GO terms "inflammatory response", "regulation of cell migration", and "collagen fibril organization". **(F)** Clustered heatmap of DEGs discovered when comparing CX3CR1$^{GFP/GFP}$ to CX3CR1$^{+/GFP}$ Ly6c+ (F). n = 3-4 per group from one experiment.

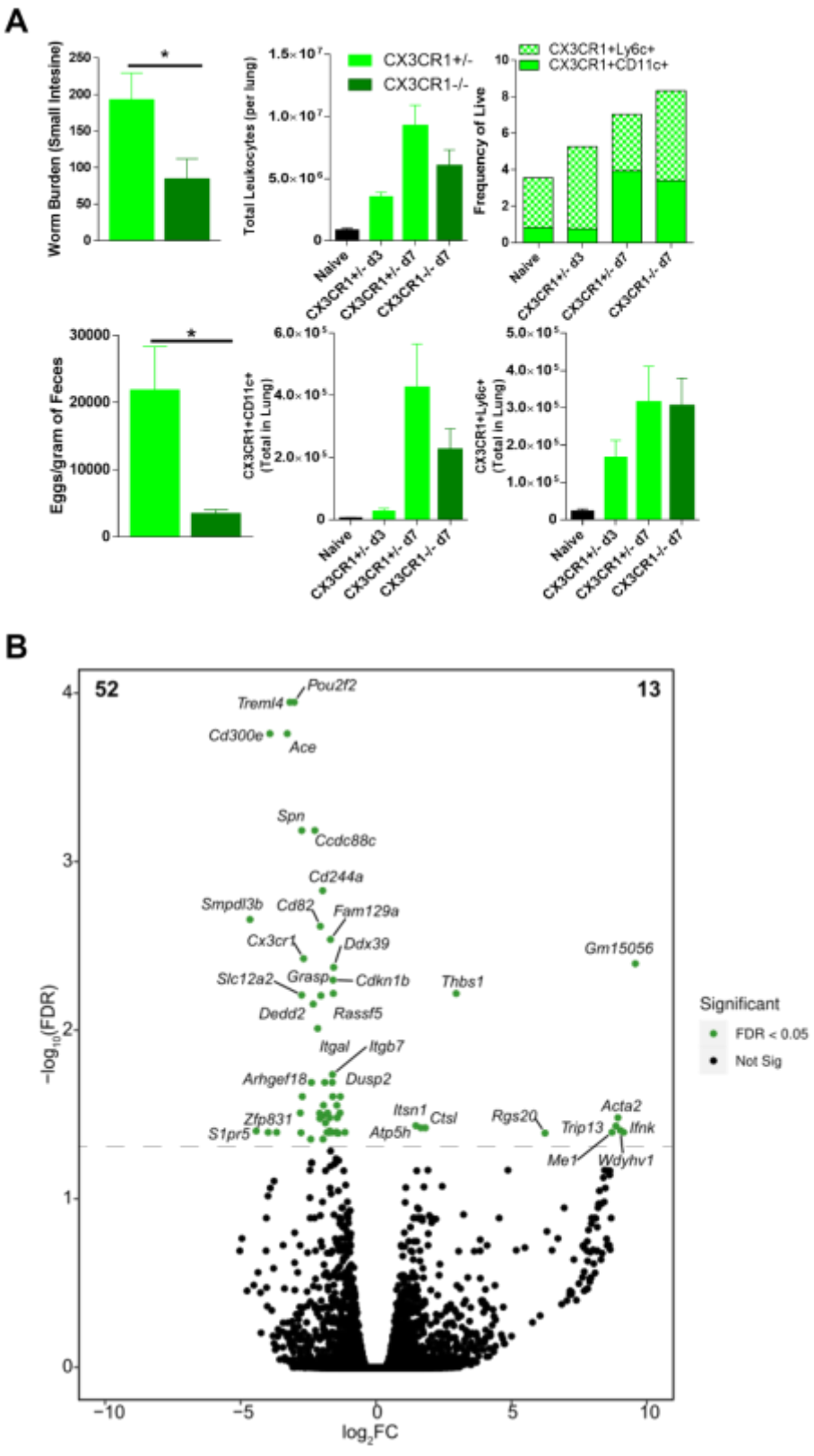
A
Worm Burden (Small Intesine)
Total Leukocytes (per lung)
CX3CR1+/-
CX3CR1-/-
Frequency of Live
CX3CR1+Ly6c+
CX3CR1+CD11c+
Eggs/gram of Feces
CX3CR1+CD11c+ (Total in Lung)
CX3CR1+Ly6c+ (Total in Lung)
Naive
CX3CR1+/- d3
CX3CR1+/- d7
CX3CR1-/- d7
B
52
13
Pou2f2
Treml4
Cd300e
Ace
Spn
Ccdc88c
Cd244a
Smpdl3b
Cd82
Fam129a
Cx3cr1
Ddx39
Gm15056
Slc12a2
Grasp
Cdkn1b
Thbs1
Dedd2
Rassf5
Itgal
Itgb7
Arhgef18
Dusp2
Itsn1
Ctsl
Rgs20
Acta2
Zfp831
S1pr5
Atp5h
Trip13
Ifnk
Me1
Wdyhv1
−log10(FDR)
log2FC
Significant
FDR < 0.05
Not Sig

Figure 21. Comparison of immune response and differentially expressed genes (DEGs) in CX3CR1$^{+/GFP}$ and CX3CR1$^{GFP/GFP}$ mice following *Nb* infection.

PGRP^{+}CX3CR1$^{GFP/+}$ (Het) and PGRP^{+}Cx3CR1$^{GFP/GFP}$ (KO) mice were injected with PBS (naive) or infected with *Nippostrongylus* for 7 days. **(A)** *Nb* and *Nb* eggs were quantified in the small intestine and fecal pellets of infected mice, respectively. Total leukocytes were isolated from lung tissue of naïve, day 3 and day 7 *Nb*-infected CX3CR1$^{+/GFP}$ mice, and day 7 *Nb*-infected CX3CR1$^{GFP/GFP}$ mice. Isolated leukocytes were evaluated by flow cytometry. **(B)** Volcano plot of differentially expressed genes within DCs from CX3CR1$^{GFP/+}$ (Het) Infected relative to naïve animals. X-axis represents fold change (log2 scale) and Y-axis represents statistical significance (-log10 scale). Genes statistically different between two conditions are colored green. Black dots represent genes that did not satisfy the statistical threshold (Fold change ≥ 1 and FDR ≤ 5%). Values represent means ± SEM (n = 3-5 per group). The unpaired t-test were performed, and P values less than 0.05 were considered statistically significant. (*, P≤ 0.05; **, P≤ 0.01; ***, P≤ 0.001; ****, P≤ 0.0001)

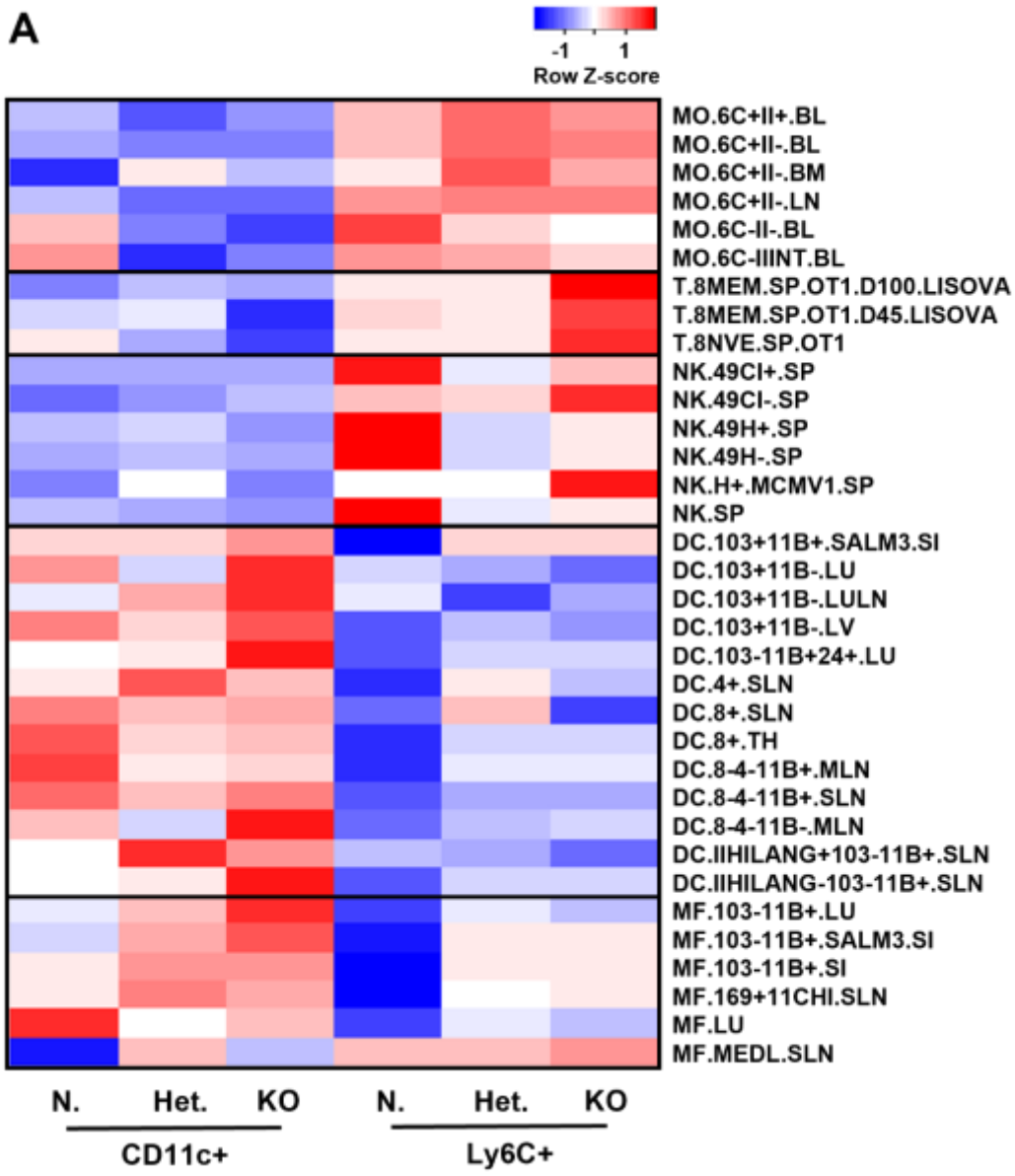
A
-1
1
Row Z-score
MO.6C+II+.BL
MO.6C+II-.BL
MO.6C+II-.BM
MO.6C+II-.LN
MO.6C-II-.BL
MO.6C-IIINT.BL
T.8MEM.SP.OT1.D100.LISOVA
T.8MEM.SP.OT1.D45.LISOVA
T.8NVE.SP.OT1
NK.49CI+.SP
NK.49CI-.SP
NK.49H+.SP
NK.49H-.SP
NK.H+.MCMV1.SP
NK.SP
DC.103+11B+.SALM3.SI
DC.103+11B-.LU
DC.103+11B-.LULN
DC.103+11B-.LV
DC.103-11B+24+.LU
DC.4+.SLN
DC.8+.SLN
DC.8+.TH
DC.8-4-11B+.MLN
DC.8-4-11B+.SLN
DC.8-4-11B-.MLN
DC.IIHILANG+103-11B+.SLN
DC.IIHILANG-103-11B+.SLN
MF.103-11B+.LU
MF.103-11B+.SALM3.SI
MF.103-11B+.SI
MF.169+11CHI.SLN
MF.LU
MF.MEDL.SLN
N.
Het.
KO
N.
Het.
KO
CD11c+
Ly6C+

Figure 22. Digital cell quantification with sorted cell RNA-seq. (A) Cell types in CX3CR1+Ly6C+ and CX3CR1+ CD11c+ cells were quantified by a digital cell quantification software Immquant, and significantly different cell types (t-test, $p<0.05$) were presented as a heatmap. N.: *CX3CR1*$^{+/-}$ naive, Het.: *CX3CR1*$^{+/-}$ infected, KO: *CX3CR1*$^{-/-}$ infected, Cell abbreviation (Mo: monocytes, MF: macrophages, DC: dendritic cells, T: t cells, NK: NK cells), Tissue abbreviation (BL: blood, BM: bone marrow, LN: lymph node, LU: lung, SLN: skin draining lymph node, SI: small intestine, LULN: mediastinal lymph node, LV: liver, TH: thymus, MLN: mesenteric lymph node, SP: spleen, Marker abbreviation (6C: Ly6C, II: MHCII, 103: CD103, 11B: CD11b, 169: CD169, 11C: CD11c, LANG: langerin, 8: CD8, 4: CD4, 49H: Ly49H, CI: Ly49C/I), etc. (MEDL: medullary, SALM3: day 3 post-infection with oral Salmonella Typhimurium, NVE: naïve, OT1: OT-1 mouse, MEM: memory, LISOVA: Listeria monocytogenes ovalbumin, MCMV: Murine Cytomegalovirus

DISCUSSION

The overall goals of this study were to characterize innate effector lung cells in response to *Nippostrongylus* infection, and to determine the function of chemokine receptor signaling through CX3CR1 and CCR2 in infection-induced inflammation and parasite clearance. Using dual reporters for CX3CR1 and PGRP, we show that CX3CR1-expressing monocytes and dendritic cells are induced in the *Nippostrongylus*-infected lungs, and identify the significant infection-induced infiltration of $PGRP^{dsRed}$ eosinophils. We found that eosinophils have strong $PGRP^{dsRed}$ signal that can be detected by fluorescence microscopy and flow cytometry, suggesting that this transgenic model may be useful to visualize eosinophils. PGRP proteins are critical innate sensors of bacterial peptidoglycan, triggering innate signaling to promote microbicidal responses.[48] Prior to these studies, PGRP expression in mice had been reported in the granules of neutrophils and M cells [22, 23]. However, a bovine study reported expression in eosinophils [49], which is in line with our findings. In that study, PGRP was microbicidal against the fungal pathogen *Cryptococcus* and gram-negative bacteria in which peptidoglycan was buried (*Salmonella*), suggesting a potential function for these proteins that may not be mediated by peptidoglycan recognition. Beyond its utility as a reporter for eosinophils and neutrophils, investigation of PGRP effector responses against helminth parasites may be warranted.

We investigated chemokine receptor signaling through CX3CR1 and CCR2, which are expressed in monocytes [32, 50, 51]. Monocytes infiltrate tissues in response to infection and injury, and have critical roles in various microbial infections, including

viral, bacterial, and protozoan [14-16, 52, 53]. However, few studies have investigated monocyte responses in helminth infection, or monocyte-helminth interaction. Here we identify both chemotactic and non-chemotactic functions for CX3CR1-expressing monocytes in *Nippostrongylu*s infection. Deficiency in CX3CR1 signaling led to reduced lung leukocyte infiltration, with reductions in monocyte and DC subsets, consistent with these cells requiring CX3CR1 for recruitment to inflamed tissues [32, 54]. Although lung alveolar macrophages do not express CX3CR1, they were also reduced in CX3CR1-deficient mice. In influenza infection studies, infiltrating monocytes differentiate into alveolar macrophages, referred to as monocyte-derived alveolar macrophages, which then downregulate CX3CR1 expression [55]. It is possible that the reduction in alveolar macrophages in *Nippostrongylus*-infected CX3CR1-deficient mice may reflect reduction in these monocyte-derived subsets.

Functionally, CX3CR1-deficient mice exhibited ameliorated outcomes to *Nippostrongylus* infection, including reduced infection-induced weight loss, and significantly reduced parasite burdens. This protective effect was not observed in CCR2-deficient mice, although these mice also had reduced monocyte and alveolar macrophage frequencies in the lung, consistent with the CCR2-mediated chemotaxis. These data therefore suggest a non-chemotactic function for CX3CR1 that is distinct from CCR2. Functional differences between CCR2 and CX3CR1 are supported by prior studies showing that inflammatory monocytes have high CCR2, while resident monocytes, as well as macrophages and DC in specific tissues, express CX3CR1 [56]. Overall, there is general consensus that CCR2 is specific for inflammatory monocytes, while CX3CR1 is

expressed on anti-inflammatory macrophages [57, 58]. Related to our findings, a study investigating pulmonary hypoxia reported that CX3CR1 deficiency was protective against hypoxia while CCL2 deficiency had no effect [59]. In our study with lung helminth infection, we observed that CX3CR1-deficient Ly6C^{+} monocytes were more effective at migrating and binding to the *Nippostrongylus* larvae, and also secreted higher levels of proinflammatory cytokines. These findings indicate an inhibitory function for CX3CR1 in suppressing effector responses in monocytes, and suggest that therapeutically targeting CX3CR1 signaling may enhance immunity to helminths through promoting tissue monocyte responses. In viral and fungal parasite infection, CX3CR1 signaling is protective for pathogen killing [54, 60], yet in our studies with helminth infection, CX3CR1 signaling impaired parasite clearance and was associated with reduced M2 macrophage activation. It is possible that CX3CR1 signaling influences the balance between M1/M2, favoring M1 macrophage activation instead of anti-helminthic M2 macrophage responses. Studies in neural tissue injury showed that CX3CR1 signaling exacerbates inflammation and CX3CR1 KO macrophages show a reparative phenotype [19, 20]. This is consistent with our findings, where we show that CX3CR1-deficient cells have higher expression of M2 marker CD206. Other studies in the lung investigated the function of CX3CR1 signaling in response to hypoxic pulmonary tension or bleomycin-induced fibrosis [59, 61], which trigger similar pathways and share disease etiologies with *Nippostrongylus* infection of the lungs [8]. Consistent with our findings, those studies showed that CX3CR1 deficiency led to increased inflammatory cytokines (CCL2, TNFα), however they noted a shift from M2 to M1 macrophage polarization in

CX3CR1-deficient mice. This highlights the complex role of CX3CR1 signaling in the lung, which may depend on the inflammatory context and stressor (e.g., hypoxia, chemical, infection).

To identify candidate downstream effectors of CX3CR1 signaling that regulate host-helminth interaction, we conducted RNA-seq on $CX3CR1^{GFP}$ positive $Ly6C^{+}$ and $CD11c^{+}$ cells sorted from the lungs of CX3CR1 Het or deficient mice. We found that the greatest changes in gene expression occurred in $Ly6C^{+}$ monocytes in response to *Nippostrongylus* infection, which were associated with pathways involved in chemotaxis, inflammation and extracellular matrix receptor interaction. These data indicate dynamic changes in monocytes recruited to the lung in response to helminth infection, where they secrete chemokines and cytokines as a positive feedback loop to enhance tissue inflammation. These monocytes are also likely involved in interaction with other immune cells as well as the matrix, as a response to injury. Based on studies in other infection models [52, 53], these monocytes may also differentiate into macrophages and dendritic cells with functions that are distinct from the tissue-resident subsets. We evaluated CX3CR1-dependent gene expression in $Ly6C^{+}$ monocytes, and found that CX3CR1 deficiency led to expression of genes associated with NK and CD8 T cells. We cannot exclude the possibility of contamination from these cell-types, however, this data indicates CX3CR1 deficiency leads to an exacerbated cytotoxic effector function, such as the increased expression of granzymes (*Gzma* and *Gzmb*) and *Serpinb9*. Granzyme A caused membrane damage-mediated cell death, cleavage of many intracellular substrates [62-66], and promotes proinflammatory cytokine expression, making it a candidate

effector molecule for the enhanced effector response to *Nippostrongylus* observed in the CX3CR1-deficient mice. Granzyme B was shown to be upregulated in human monocytes by activation of TLR8 signaling and induced antibody-dependent cellular cytotoxicity [67]. *Serpinb9*, an endogenous natural antagonist regulating excessive granzyme B activity was also upregulated in KO monocytes, indicating potential regulation of this pathway.[68] Granzyme expression has been reported in both human and rodent helminth infections [69], with divergent roles in the inflammatory response and anti-helminthic immunity. In infection with filarial nematode *Litomosomoides sigmodontis*, granzyme A deficiency increased susceptibility while deficiency in granzyme B promoted early inflammation and improved resistance [70]. Future experiments investigating the interplay between these effectors and regulators of the granzyme pathway, and how they might contribute to the enhanced cell binding to the larval parasite, may uncover new pathways that can be targeted to promote helminth killing. In conclusion, our study characterizes a dual reporter for innate myeloid and granulocyte subsets in pulmonary helminth infection, and identify a previously unrecognized role for CX3CR1 signaling in promoting infection-induced pathology and impairing optimal anti-helminth effector responses.

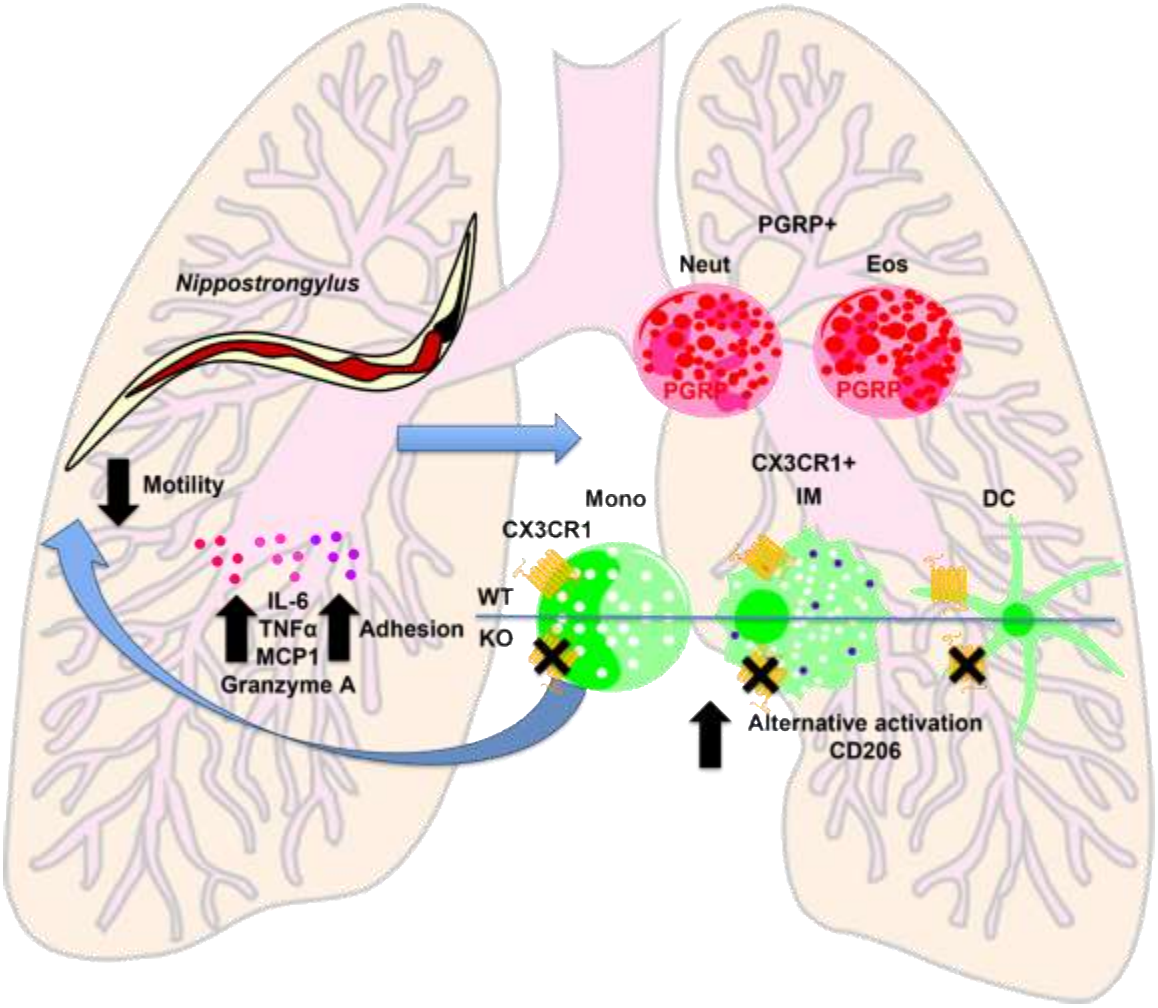

Figure 23. Immunomodulatory function of CX3CR1 in myeloid cells during helminth infection

References

1. Hotez, P.J., et al., *Helminth infections: the great neglected tropical diseases.* J Clin Invest, 2008. **118**(4): p. 1311-21.

2. De Clercq, D., et al., *Failure of mebendazole in treatment of human hookworm infections in the southern region of Mali.* Am J Trop Med Hyg, 1997. **57**(1): p. 25-30.

3. Reynoldson, J.A., et al., *Failure of pyrantel in treatment of human hookworm infections (Ancylostoma duodenale) in the Kimberley region of north west Australia.* Acta Trop, 1997. **68**(3): p. 301-12.

4. Jia, T.W., et al., *Soil-transmitted helminth reinfection after drug treatment: a systematic review and meta-analysis.* PLoS Negl Trop Dis, 2012. **6**(5): p. e1621.

5. Speich, B., et al., *Efficacy and reinfection with soil-transmitted helminths 18-weeks post-treatment with albendazole-ivermectin, albendazole-mebendazole, albendazole-oxantel pamoate and mebendazole.* Parasit Vectors, 2016. **9**: p. 123.

6. Gause, W.C., T.A. Wynn, and J.E. Allen, *Type 2 immunity and wound healing: evolutionary refinement of adaptive immunity by helminths.* Nat Rev Immunol, 2013. **13**(8): p. 607-14.

7. Weatherhead, J.E., et al., *Host Immunity and Inflammation to Pulmonary Helminth Infections.* Front Immunol, 2020. **11**: p. 594520.

8. Marsland, B.J., et al., *Nippostrongylus brasiliensis infection leads to the development of emphysema associated with the induction of alternatively activated macrophages.* Eur J Immunol, 2008. **38**(2): p. 479-88.

9. Chen, F., et al., *Neutrophils prime a long-lived effector macrophage phenotype that mediates accelerated helminth expulsion.* Nat Immunol, 2014. **15**(10): p. 938-46.

10. Bouchery, T., et al., *Hookworms Evade Host Immunity by Secreting a Deoxyribonuclease to Degrade Neutrophil Extracellular Traps.* Cell Host Microbe, 2020. **27**(2): p. 277-289.e6.

11. Knott, M.L., et al., *Impaired resistance in early secondary Nippostrongylus brasiliensis infections in mice with defective eosinophilopoeisis.* Int J Parasitol, 2007. **37**(12): p. 1367-78.

12. Voehringer, D., et al., *Type 2 immunity is controlled by IL-4/IL-13 expression in hematopoietic non-eosinophil cells of the innate immune system.* J Exp Med, 2006. **203**(6): p. 1435-46.

13. Giacomin, P.R., et al., *The role of complement in innate, adaptive and eosinophil-dependent immunity to the nematode Nippostrongylus brasiliensis.* Mol Immunol, 2008. **45**(2): p. 446-55.

14. de Marcken, M., et al., *TLR7 and TLR8 activate distinct pathways in monocytes during RNA virus infection.* Sci Signal, 2019. **12**(605).

15. Serbina, N.V., et al., *Monocyte-mediated defense against microbial pathogens.* Annu Rev Immunol, 2008. **26**: p. 421-52.

16. Hohl, T.M., et al., *Inflammatory monocytes facilitate adaptive CD4 T cell responses during respiratory fungal infection.* Cell Host Microbe, 2009. **6**(5): p. 470-81.

17. Manta, C., et al., *CX(3)CR1(+) macrophages support IL-22 production by innate lymphoid cells during infection with Citrobacter rodentium.* Mucosal Immunol, 2013. **6**(1): p. 177-88.

18. Choi, J.Y., et al., *Indispensable Role of CX3CR1+ Dendritic Cells in Regulation of Virus-Induced Neuroinflammation Through Rapid Development of Antiviral Immunity in Peripheral Lymphoid Tissues.* Front Immunol, 2019. **10**: p. 1467.

19. Freria, C.M., et al., *Deletion of the Fractalkine Receptor, CX3CR1, Improves Endogenous Repair, Axon Sprouting, and Synaptogenesis after Spinal Cord Injury in Mice.* J Neurosci, 2017. **37**(13): p. 3568-3587.

20. Faustino, J., et al., *CX3CR1-CCR2-dependent monocyte-microglial signaling modulates neurovascular leakage and acute injury in a mouse model of childhood stroke.* J Cereb Blood Flow Metab, 2019. **39**(10): p. 1919-1935.

21. Ran, L., et al., *Cx3cr1 deficiency in mice attenuates hepatic granuloma formation during acute schistosomiasis by enhancing the M2-type polarization of macrophages.* Dis Model Mech, 2015. **8**(7): p. 691-700.

22. Cho, J.H., et al., *Human peptidoglycan recognition protein S is an effector of neutrophil-mediated innate immunity.* Blood, 2005. **106**(7): p. 2551-8.

23. Wang, J., et al., *Convergent and divergent development among M cell lineages in mouse mucosal epithelium.* J Immunol, 2011. **187**(10): p. 5277-85.

24. Langmead, B. and S.L. Salzberg, *Fast gapped-read alignment with Bowtie 2.* Nat Methods, 2012. **9**(4): p. 357-9.

25. Kim, D., et al., *TopHat2: accurate alignment of transcriptomes in the presence of insertions, deletions and gene fusions.* Genome Biol, 2013. **14**(4): p. R36.

26. Lawrence, M., et al., *Software for computing and annotating genomic ranges.* PLoS Comput Biol, 2013. **9**(8): p. e1003118.

27. Robinson, M.D., D.J. McCarthy, and G.K. Smyth, *edgeR: a Bioconductor package for differential expression analysis of digital gene expression data.* Bioinformatics, 2010. **26**(1): p. 139-40.

28. Mortazavi, A., et al., *Mapping and quantifying mammalian transcriptomes by RNA-Seq.* Nat Methods, 2008. **5**(7): p. 621-8.

29. Huang, d.W., B.T. Sherman, and R.A. Lempicki, *Bioinformatics enrichment tools: paths toward the comprehensive functional analysis of large gene lists.* Nucleic Acids Res, 2009. **37**(1): p. 1-13.

30. Batugedara, H.M., et al., *Hematopoietic cell-derived RELMα regulates hookworm immunity through effects on macrophages.* J Leukoc Biol, 2018.

31. Esser-von Bieren, J., et al., *Antibodies trap tissue migrating helminth larvae and prevent tissue damage by driving IL-4Rα-independent alternative differentiation of macrophages.* PLoS Pathog, 2013. **9**(11): p. e1003771.

32. Jung, S., et al., *Analysis of fractalkine receptor CX(3)CR1 function by targeted deletion and green fluorescent protein reporter gene insertion.* Mol Cell Biol, 2000. **20**(11): p. 4106-14.

33. Camberis, M., G. Le Gros, and J. Urban, *Animal model of Nippostrongylus brasiliensis and Heligmosomoides polygyrus.* Curr Protoc Immunol, 2003. **Chapter 19**: p. Unit 19.12.

34. Stein, M., et al., *Interleukin 4 potently enhances murine macrophage mannose receptor activity: a marker of alternative immunologic macrophage activation.* J Exp Med, 1992. **176**(1): p. 287-92.

35. Hussell, T. and T.J. Bell, *Alveolar macrophages: plasticity in a tissue-specific context.* Nat Rev Immunol, 2014. **14**(2): p. 81-93.

36. Aegerter, H., et al., *Influenza-induced monocyte-derived alveolar macrophages confer prolonged antibacterial protection.* Nat Immunol, 2020. **21**(2): p. 145-157.

37. Iyer, A.K., et al., *STAT3 promotes CD1d-mediated lipid antigen presentation by regulating a critical gene in glycosphingolipid biosynthesis.* Immunology, 2015. **146**(3): p. 444-55.

38. Marti, F., et al., *A transcription function for the T cell-specific adapter (TSAd) protein in T cells: critical role of the TSAd Src homology 2 domain.* J Exp Med, 2001. **193**(12): p. 1425-30.

39. Sagebiel, A.F., et al., *Tissue-resident Eomes+ NK cells are the major innate lymphoid cell population in human infant intestine.* Nat Commun, 2019. **10**(1): p. 975.

40. Rogers, M.L., et al., *ProNGF mediates death of Natural Killer cells through activation of the p75NTR-sortilin complex.* J Neuroimmunol, 2010. **226**(1-2): p. 93-103.

41. Salehi, A.H., S. Xanthoudakis, and P.A. Barker, *NRAGE, a p75 neurotrophin receptor-interacting protein, induces caspase activation and cell death through a JNK-dependent mitochondrial pathway.* J Biol Chem, 2002. **277**(50): p. 48043-50.

42. Zhan, Y., et al., *Ets-1 is a critical regulator of Ang II-mediated vascular inflammation and remodeling.* J Clin Invest, 2005. **115**(9): p. 2508-16.

43. Stamatovic, S.M., et al., *CCL2 regulates angiogenesis via activation of Ets-1 transcription factor.* J Immunol, 2006. **177**(4): p. 2651-61.

44. Frishberg, A., et al., *ImmQuant: a user-friendly tool for inferring immune cell-type composition from gene-expression data.* Bioinformatics, 2016. **32**(24): p. 3842-3843.

45. Yang, R., et al., *POU2F2 regulates glycolytic reprogramming and glioblastoma progression via PDPK1-dependent activation of PI3K/AKT/mTOR pathway.* Cell Death Dis, 2021. **12**(5): p. 433.

46. Coletta, S., et al., *The immune receptor CD300e negatively regulates T cell activation by impairing the STAT1-dependent antigen presentation.* Sci Rep, 2020. **10**(1): p. 16501.

47. Bernstein, K.E., et al., *Angiotensin-converting enzyme in innate and adaptive immunity.* Nat Rev Nephrol, 2018. **14**(5): p. 325-336.

48. Kang, D., et al., *A peptidoglycan recognition protein in innate immunity conserved from insects to humans.* Proc Natl Acad Sci U S A, 1998. **95**(17): p. 10078-82.

49. Tydell, C.C., et al., *Isolation, characterization, and antimicrobial properties of bovine oligosaccharide-binding protein. A microbicidal granule protein of eosinophils and neutrophils.* J Biol Chem, 2002. **277**(22): p. 19658-64.

50. Imai, T., et al., *Identification and molecular characterization of fractalkine receptor CX3CR1, which mediates both leukocyte migration and adhesion.* Cell, 1997. **91**(4): p. 521-30.

51. Charo, I.F., et al., *Molecular cloning and functional expression of two monocyte chemoattractant protein 1 receptors reveals alternative splicing of the carboxyl-terminal tails.* Proc Natl Acad Sci U S A, 1994. **91**(7): p. 2752-6.

52. Lee, J., et al., *CD11cHi monocyte-derived macrophages are a major cellular compartment infected by Mycobacterium tuberculosis.* PLoS Pathog, 2020. **16**(6): p. e1008621.

53. Shin, K.S., et al., *Monocyte-Derived Dendritic Cells Dictate the Memory Differentiation of CD8+ T cells During Acute Infection.* Front Immunol, 2019. **10**: p. 1887.

54. Bonduelle, O., et al., *Cutting edge: Protective effect of CX3CR1+ dendritic cells in a vaccinia virus pulmonary infection model.* J Immunol, 2012. **188**(3): p. 952-6.

55. Lin, K.L., et al., *CCR2+ monocyte-derived dendritic cells and exudate macrophages produce influenza-induced pulmonary immune pathology and mortality.* J Immunol, 2008. **180**(4): p. 2562-72.

56. Geissmann, F., S. Jung, and D.R. Littman, *Blood monocytes consist of two principal subsets with distinct migratory properties.* Immunity, 2003. **19**(1): p. 71-82.

57. Shi, C. and E.G. Pamer, *Monocyte recruitment during infection and inflammation.* Nat Rev Immunol, 2011. **11**(11): p. 762-74.

58. Francis, M., et al., *Editor's Highlight: CCR2 Regulates Inflammatory Cell Accumulation in the Lung and Tissue Injury following Ozone Exposure.* Toxicol Sci, 2017. **155**(2): p. 474-484.

59. Amsellem, V., et al., *Roles for the CX3CL1/CX3CR1 and CCL2/CCR2 Chemokine Systems in Hypoxic Pulmonary Hypertension.* Am J Respir Cell Mol Biol, 2017. **56**(5): p. 597-608.

60. Leonardi, I., et al., *CX3CR1+ mononuclear phagocytes control immunity to intestinal fungi.* Science, 2018. **359**(6372): p. 232-236.

61. Ishida, Y., et al., *Essential involvement of the CX3CL1-CX3CR1 axis in bleomycin-induced pulmonary fibrosis via regulation of fibrocyte and M2 macrophage migration.* Sci Rep, 2017. **7**(1): p. 16833.

62. Beresford, P.J., et al., *Granzyme A activates an endoplasmic reticulum-associated caspase-independent nuclease to induce single-stranded DNA nicks.* J Biol Chem, 2001. **276**(46): p. 43285-93.

63. Fan, Z., et al., *Tumor suppressor NM23-H1 is a granzyme A-activated DNase during CTL-mediated apoptosis, and the nucleosome assembly protein SET is its inhibitor.* Cell, 2003. **112**(5): p. 659-72.

64. Fan, Z., et al., *Cleaving the oxidative repair protein Ape1 enhances cell death mediated by granzyme A.* Nat Immunol, 2003. **4**(2): p. 145-53.

65. Martinvalet, D., P. Zhu, and J. Lieberman, *Granzyme A induces caspase-independent mitochondrial damage, a required first step for apoptosis.* Immunity, 2005. **22**(3): p. 355-70.

66. Zhang, D., et al., *Induction of rapid histone degradation by the cytotoxic T lymphocyte protease Granzyme A.* J Biol Chem, 2001. **276**(5): p. 3683-90.

67. Elavazhagan, S., et al., *Granzyme B expression is enhanced in human monocytes by TLR8 agonists and contributes to antibody-dependent cellular cytotoxicity.* J Immunol, 2015. **194**(6): p. 2786-95.

68. Zhang, M., et al., *Serine protease inhibitor 6 protects cytotoxic T cells from self-inflicted injury by ensuring the integrity of cytotoxic granules.* Immunity, 2006. **24**(4): p. 451-61.

69. Fujiwara, A., et al., *Villus epithelial injury induced by infection with the nematode Nippostrongylus brasiliensis is associated with upregulation of granzyme B.* J Parasitol, 2004. **90**(5): p. 1019-26.

70. Hartmann, W., et al., *A novel and divergent role of granzyme A and B in resistance to helminth infection.* J Immunol, 2011. **186**(4): p. 2472-81.

Chapter Six – Conclusion

Summary

RELMα induces resolution of inflammatory granulomatous tissue by downregulating *Serpine1*.

The regulatory function of RELMα in Th2 immune responses during mouse hookworm infection is well characterized in the lung. However, helminth infections in humans are mostly chronic within the intestine. We took advantage of mouse chronic helminth infection model, *H. polygyrus* and *Retnla*$^{tdT/tdT}$ knockout mice, to investigate the function of RELMα in chronic intestinal helminth infections. RELMα downregulated the size of the granulomas and expedited resolution and closure of the wounds. By utilizing Nanostring technology, we found that there was increased migration of monocyte-derived macrophages in WT granulomas, which might be the source of RELMα. Moreover, the anti-wound healing gene, *Serpine1*, was downregulated in WT granulomas, and it was highly expressed in the center of KO granulomas. Collectively, these results suggest that RELMα derived from monocyte-derived macrophages is required for limiting inflammation and host damage caused by macroparasite infection.

Choline metabolism is required for M2 macrophage polarization and RELMα expression during helminth infection.

Previous studies demonstrated that choline uptake and metabolism are crucial for M1 polarization and activation of macrophages such as cytokine production. We found that choline metabolism is also required for M2 macrophage polarization and RELMα

expression during *H. polygyrus* infection by using pharmacological choline kinase α inhibitor. Upon *H. polygyrus* infection, choline kinase α, RSM-932A decreased recruitment of macrophages, B-1cells, eosinophils, but increased monocytes and neutrophils in the peritoneal cavity. RSM-932A injection also downregulated M2 polarization of macrophages and optimal immune response to *H.polygyrus*, increasing egg burden. These data demonstrated that appropriate metabolism of dietary nutrient play an important role in activation of immune response to helminth infection.

Epithelial cell-derived RELMα facilitates infection of epithelial cells with Influenza A Virus.

While RELMα function in helminth and bacterial infections has been investigated, it has never been studied in viral infection. We employed influenza A/California/04/2009 (H1N1) strain (IAV) and *Retnla*$^{tdT/tdT}$ KO mice to investigate the role of RELMα during influenza infection. Unlike helminth infections, IAV infection induced RELMα expression specifically in lung epithelial cells. *Retnla*$^{tdT/tdT}$ KO mice had significantly lower viral burden compared to WT mice, and RELMα directly increased IAV infection of lung epithelial cells *in vitro* and *in vivo*. This study implicates a pathogenic function of RELMα in promoting IAV infection of the epithelial cell.

CX3CR1 dampens lung inflammation by downregulating host-helminth interaction, proinflammatory cytokines, and cytotoxic molecules. CX3CR1 is a chemokine receptor, which is important for recruitment of myeloid cells in inflammatory environments. We found that CX3CR1-expressing cells are recruited to the lung during *Nippostrongylus brasiliensis* infection by using CX3CR1 knock out/GFP knock in mice. In addition to chemotactic function, CX3CR1 inhibited binding of monocytes to worms and proinflammatory cytokine production by monocytes. RNA-sequencing data demonstrated that CX3CR1 decreased expression of cytotoxic molecules including granzymes A and B. These results suggest that CX3CR1 intrinsically regulates response to helminths and production of inflammatory molecules in addition to its canonical chemotactic function.

Future Directions

What is the receptor of RELMα?

Even if the function of RELMα on diverse cell types in different contexts are well characterized, the surface receptor of RELMα has not been identified yet. Since RELMα is secreted, RELMα may bind to a surface receptor and be translocated into the cytoplasm through transporter or endocytosis to activate downstream signaling pathways. In chapter 4, recombinant RELMα increased infection of MLE-12 cells with IAV *in vitro*, indicating that there is a putative RELMα receptor or transporter in epithelial cells. However, other studies showed that RELMα also alters gene expression, proliferation, and migration of immune cells such as macrophages and CD4 T cells, suggesting the presence of a RELMα binding partner on the surface of immune cells. To identify the surface receptor of RELMα, membrane proteins interacting with RELMα should be immunoprecipitated and analyzed by mass spectrometry. After identification, future studies with inhibitors or gene silencing would be needed to validate RELMα functions through theses candidate proteins.

What is the mechanism by which RELMα activates IAV infection in lung epithelial cells?

We showed that RELMα directly upregulates IAV infection of lung epithelial cells with no striking effects on the immune response, suggesting that RELMα alters condition of epithelial cells for increased viral uptake or replication. It is possible that RELMα expedites IAV infection of lung epithelial cells by upregulating its receptor sialic

acid or required activating signaling pathways. Both RELMα and IAV infection activates PI3K/Akt pathway, which induce viral uptake. To determine RELMα synergically activates PI3K/AKT pathway with IAV infection, the pathway should be inhibited by its inhibitor wortmannin upon RELMα treatment and viral burden should be measured in mouse lung epithelial cells. Furthermore, future studies should employ RNA-sequencing to identify signaling pathways activated by RELMα during IAV infection. CC10 Cre/*Retnla*$^{flox/flox}$ mice should also be used to specifically remove RELMα expression in lung epithelial cells.

Conclusion

In this dissertation, we investigated the function of the secreted protein RELMα and the chemokine receptor CX3CR1 in murine infections with soil-transmitted helminths and influenza A virus (Figure 24). First, we examined whether RELMα affects immune responses and tissue repair in the small intestine during chronic helminth infection. RELMα had no significant effects in regulating Th2 immune responses and parasite burdens in the intestine. However, we demonstrated that RELMα is highly expressed in inflammatory granulomatous tissue in the intestine and induces resolution of infection in these tissues. Mechanistically, RELMα downregulates the anti-wound healing gene, *Serpine1*, in granulomatous tissue, leading to expedited closure of opened lesions. Thus, RELMα function is more skewed toward tissue repair rather than immune regulation in the intestine. Next, we demonstrated that M2 macrophage polarization and RELMα expression following chronic helminth infection are regulated by choline metabolism. Impaired choline metabolism may affect mitochondrial oxidative phosphorylation, which is crucial for M2 macrophage polarization, and its role needs to be clarified. The function of RELMα is well characterized in the type 2 immune response, but not in the type 1 immune response. Recently, a pleiotropic function of RELMα was revealed in different infection contexts, and the novel function of RELMα in Influenza infection was discovered in this dissertation. RELMα directly facilitates infection of lung epithelial cells with influenza viruses without the intervention of immune cells, and downstream signaling in epithelial cells should be identified. Lastly, in addition to functioning as a chemokine receptor, we demonstrated a cell-intrinsic

immunomodulatory function for CX3CR1 in mouse lung hookworm infection. CX3CR1-expressing cells are recruited to the site of infection by CX3CR1, but CX3CR1 signaling balances activation of these cells to limit excessive inflammatory response and tissue damage in the lung. This dissertation suggests a versatile function of host proteins, RELMα and CX3CR1, in balancing the immune response and tissue repair during mucosal infection.

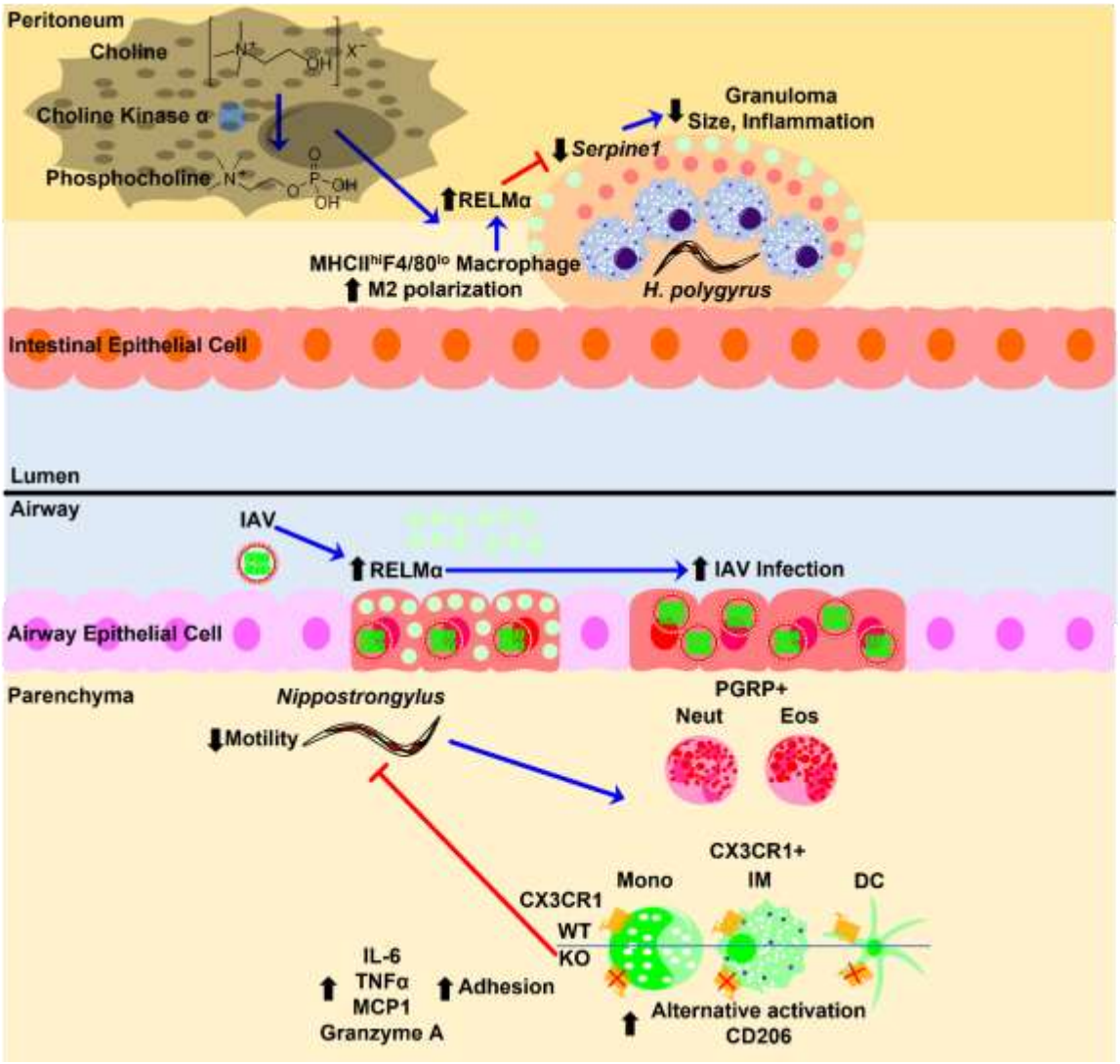

Figure 24. Immunomodulatory function of RELMα and CX3CR1 in mucosal infection.